Quantum electromechanics

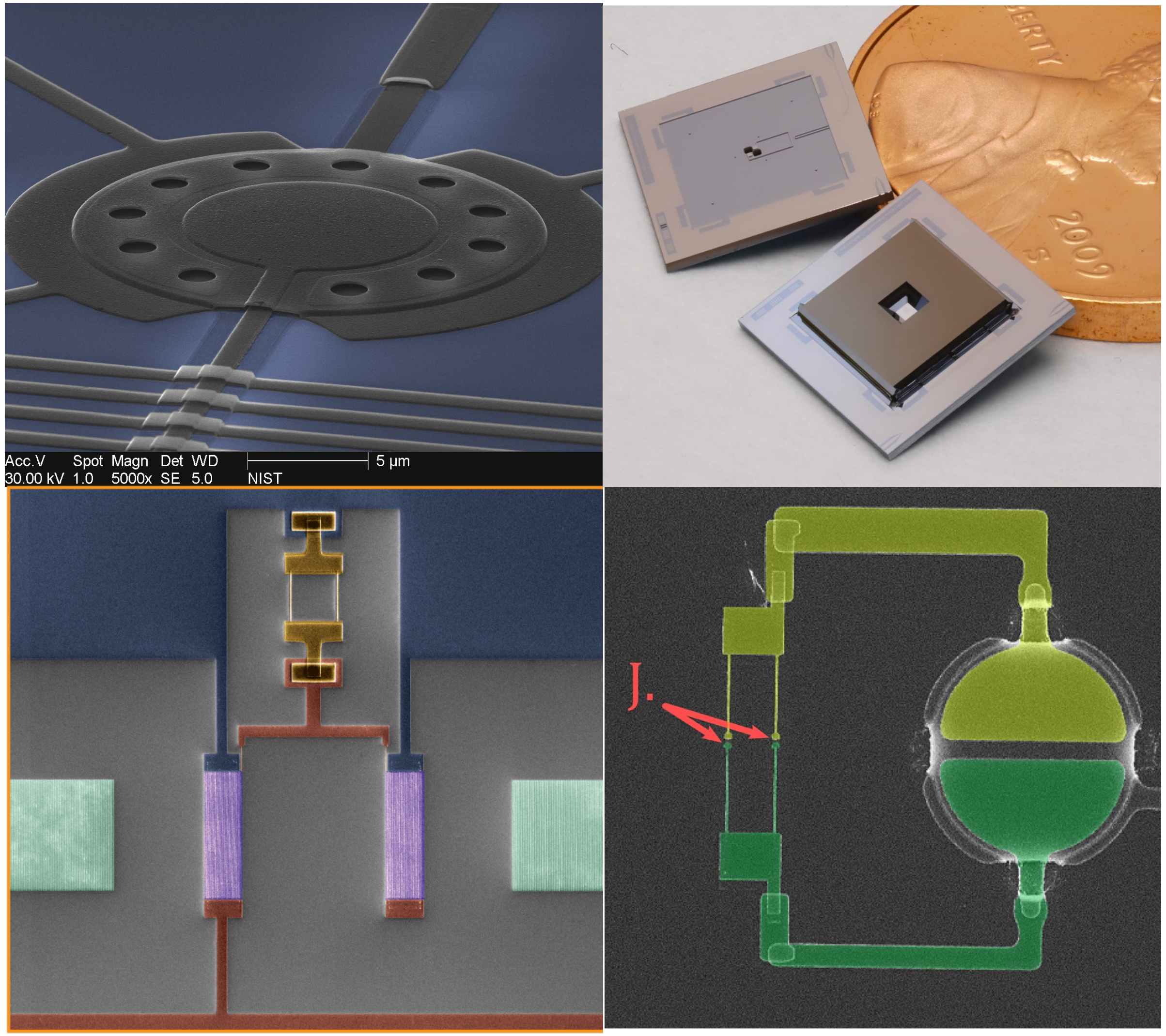

from linear quantum acoustics to quantum phononics

JILA
CU Boulder and NIST

Quantum superposition of macroscopically distinguishable states

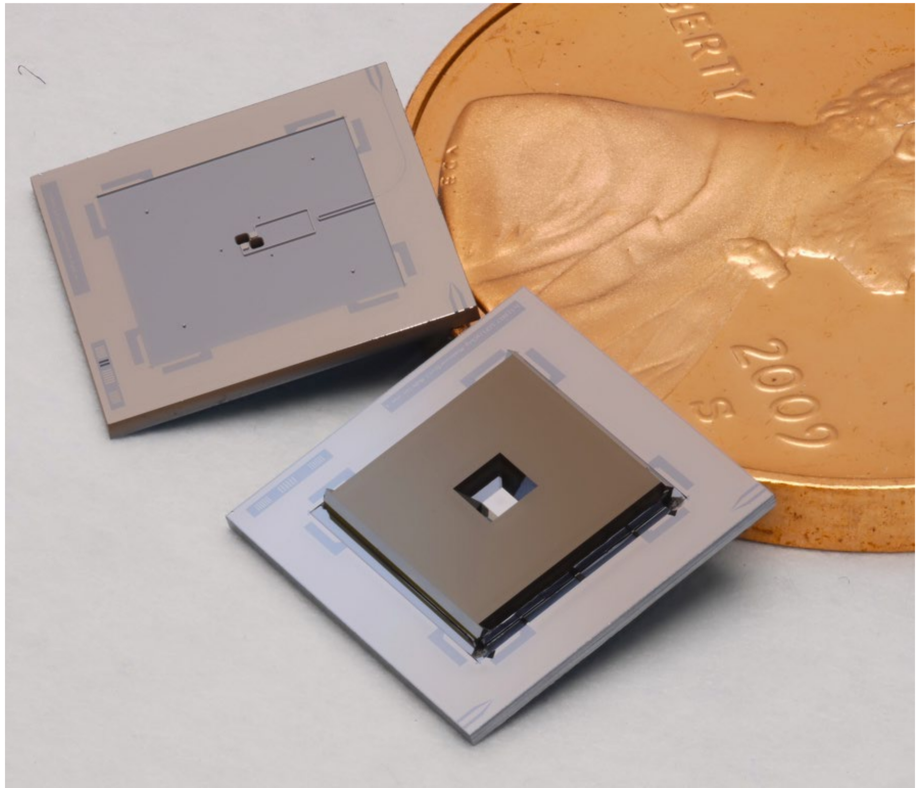

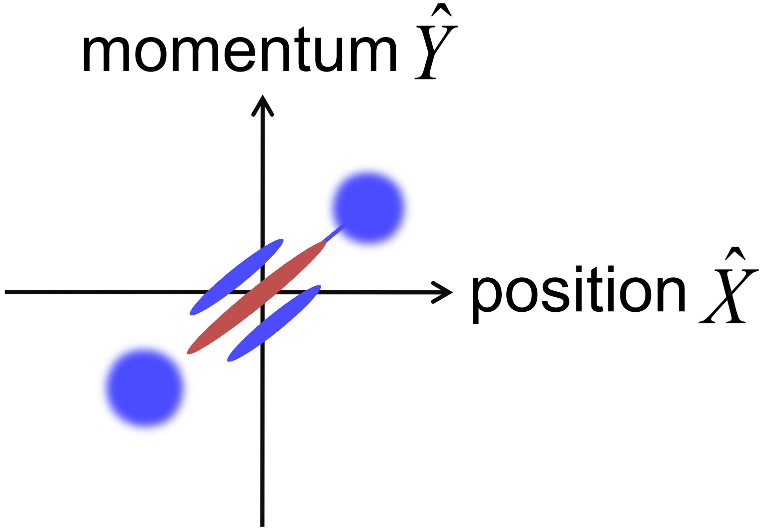

mechanical coherent state

classical amplitude and phase

quantum uncertainty blob

mechanical “Schrödinger cat” state

Wigner function negativity

Quantum measurement of macroscopic mechanical oscillators

standard quantum limit (SQL)

quantum non-demolition measurements (QND)

back action evasion (BAE)

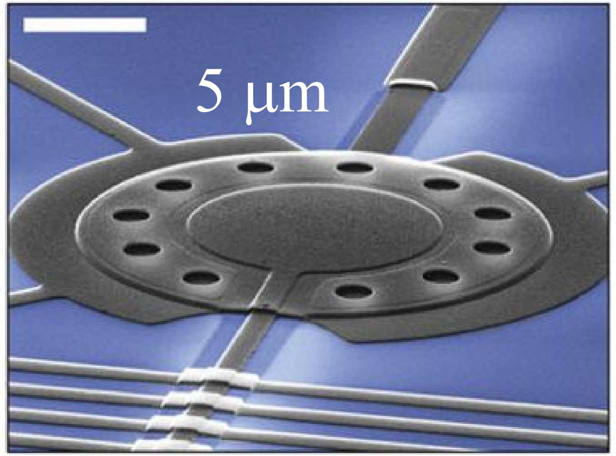

On the measurement of a weak classical force coupled to a quantum-mechanical oscillator. I. Issues of principle

Carlton M. Caves, Kip S. Thorne, Ronald W. P. Drever, Vernon D. Sandberg, and Mark Zimmermann
Rev. Mod. Phys. **52**, 341 – Published 1 April 1980

Measurement of Motion beyond the Quantum Limit by Transient Amplification
R. D. Delaney, A. P. Reed, R. W. Andrews, and K. W. Lehnert
Phys. Rev. Lett. 123, 183603 (2019)

JILA
CU Boulder and NIST

Universal transducers/sensors in the quantum regime

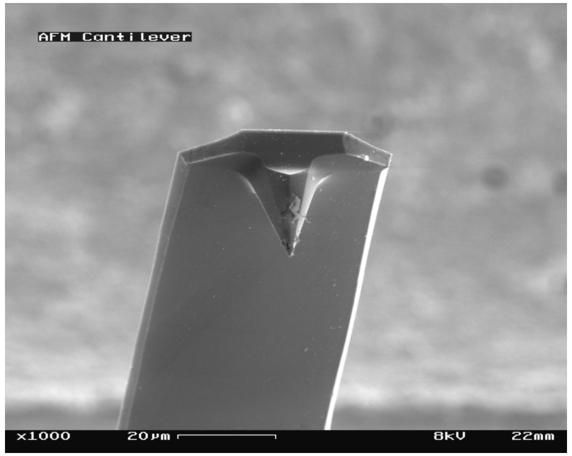

Atomic Force Microscope (AFM)

map atom scale surface forces to laser intensity

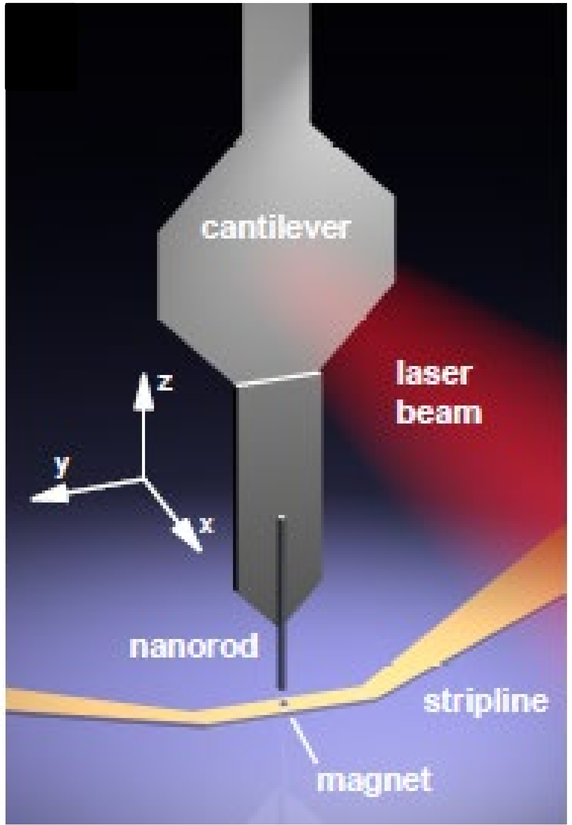

Magnetic Resonance Force Microscopy (MRFM)

image 3D nuclear spin density

Degen group: ETHZ

JILA
CU Boulder and NIST

Acoustical information processing in the quantum regime?

sound waves: slow and small

$v_s = c/100{,}000$

"micro"- waves

timing

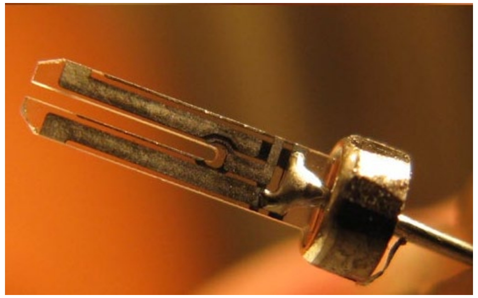

delay

filtering

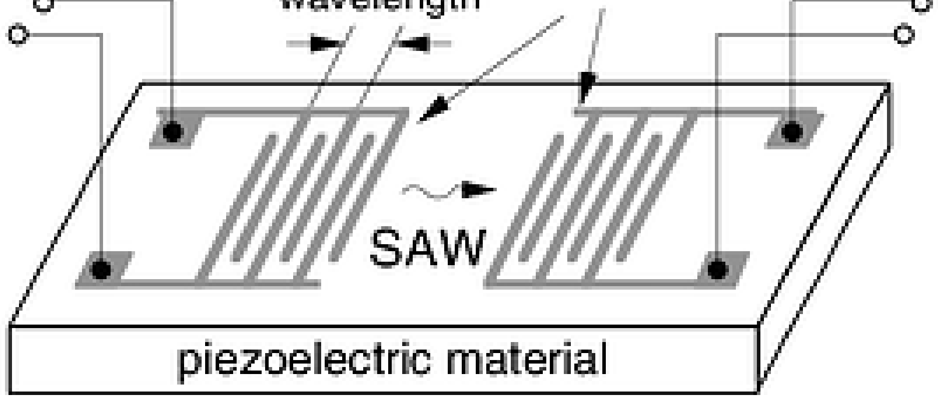

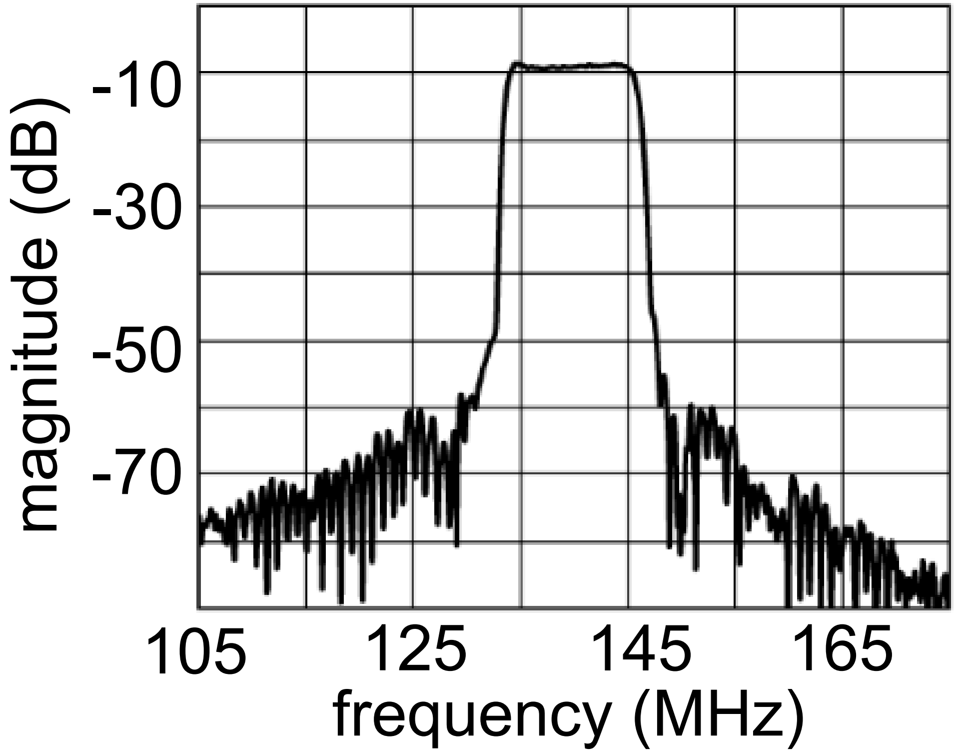

JILA CU Boulder and NIST

quantum electromechanics and optomechanics

Optical fields precisely control and measure macroscopic motion (optomechanics)

motion of mechanical oscillator

control with radiation force

infer through optical phase

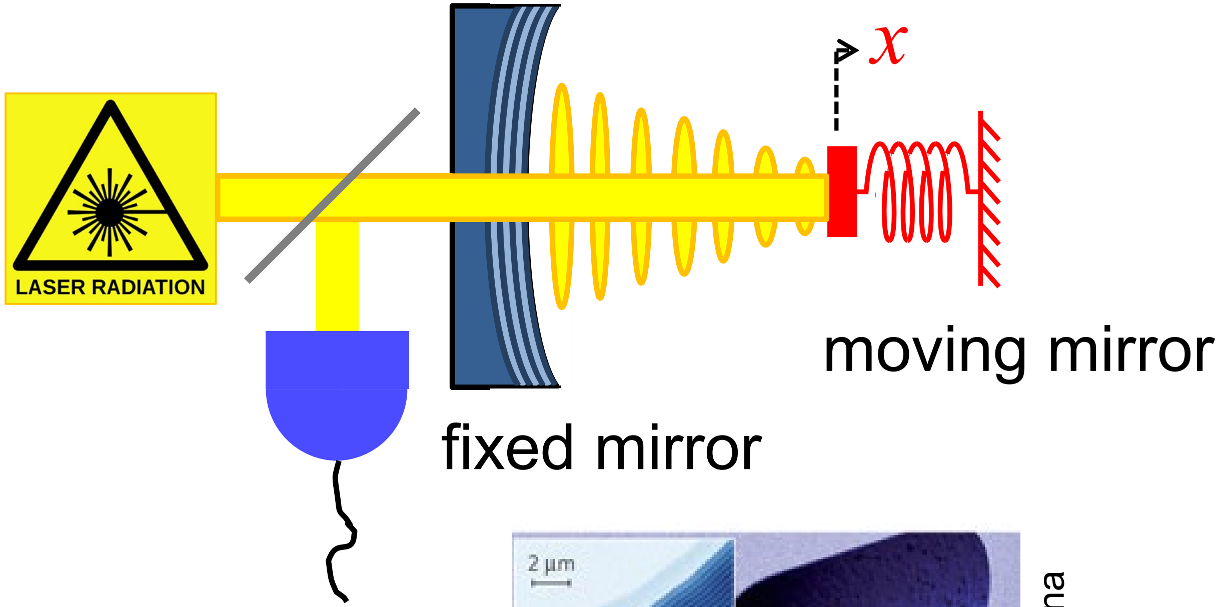

LIGO: Hanford

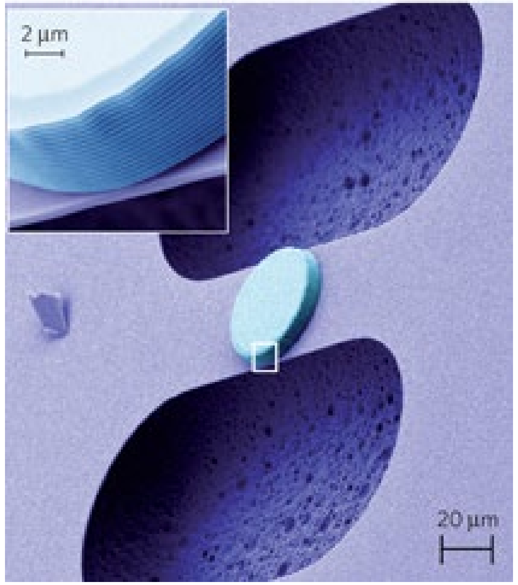

Aspelmeyer lab, IOQOI, Vienna

Quantum electromechanics: control and measure motion with electrical circuits

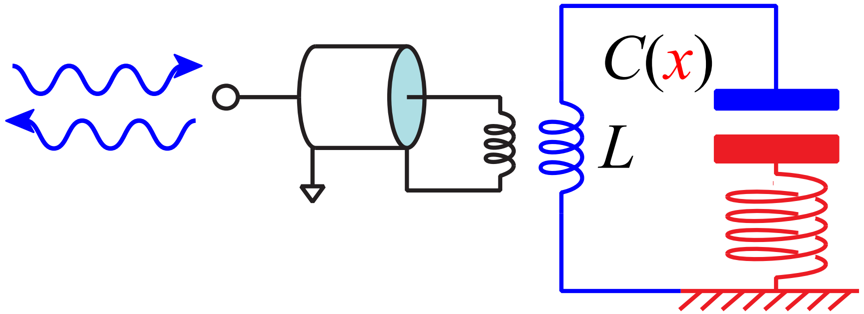

motion of compliant LC circuit

control with electrostatic force

infer through electrical phase

microwave frequency electrical circuits

quantum operation at $T_{\mathrm{env}} \ll 1\ \mathrm{K}$

interface with superconducting qubits

transmon qubit
in cavity

JILA CU Boulder and NIST

Vibrating membrane electromechanics

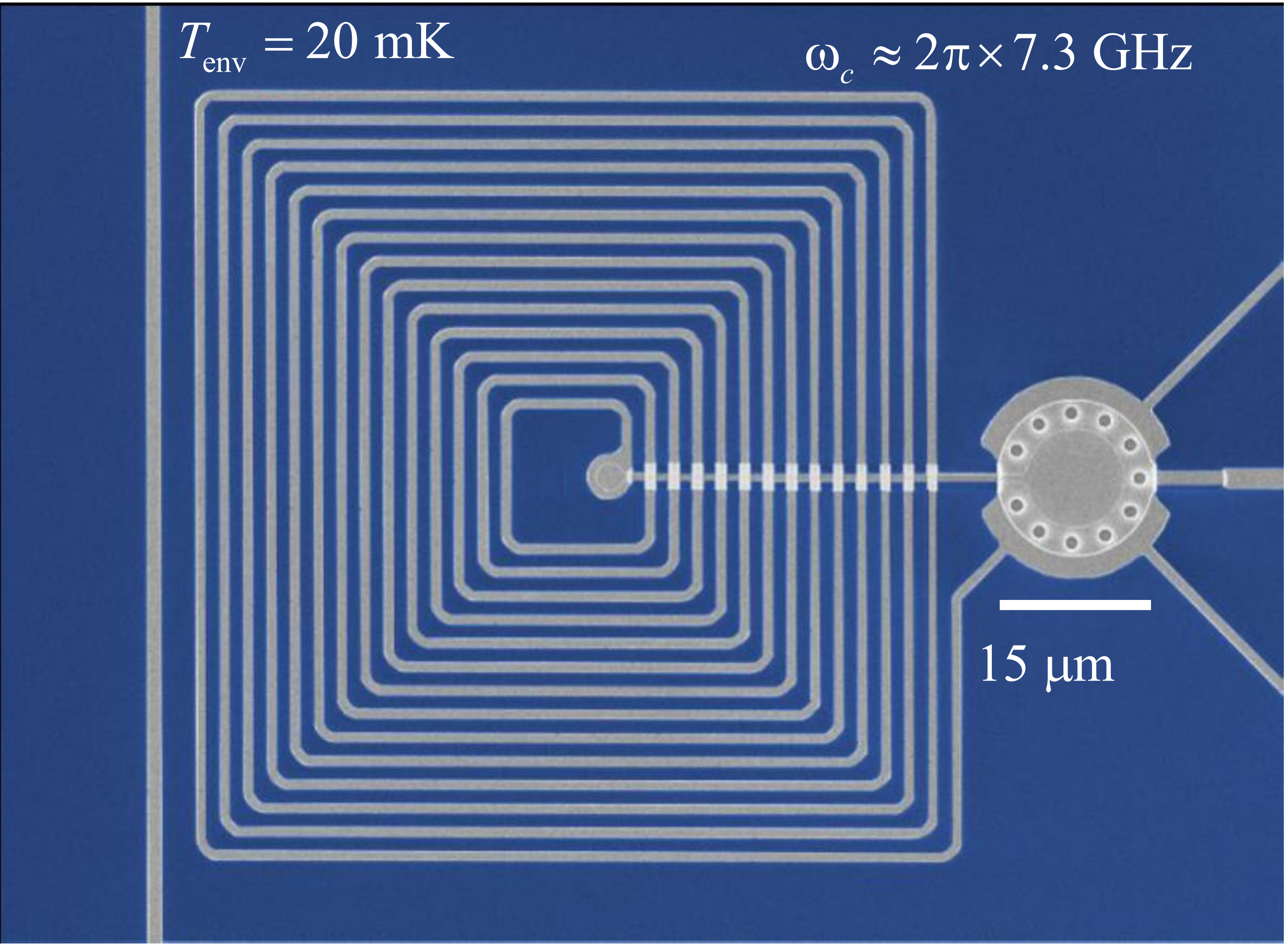

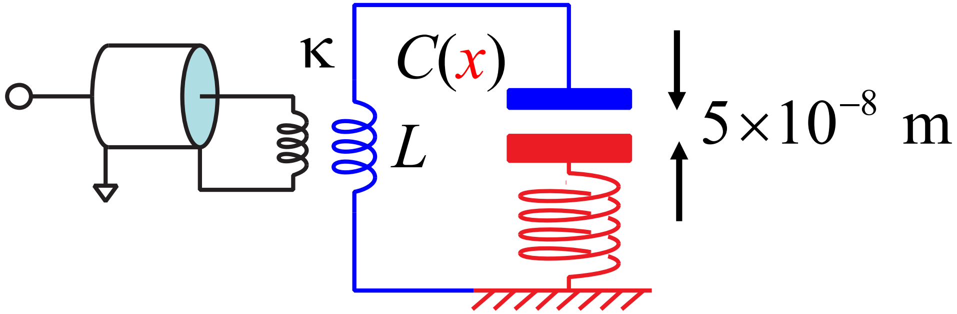

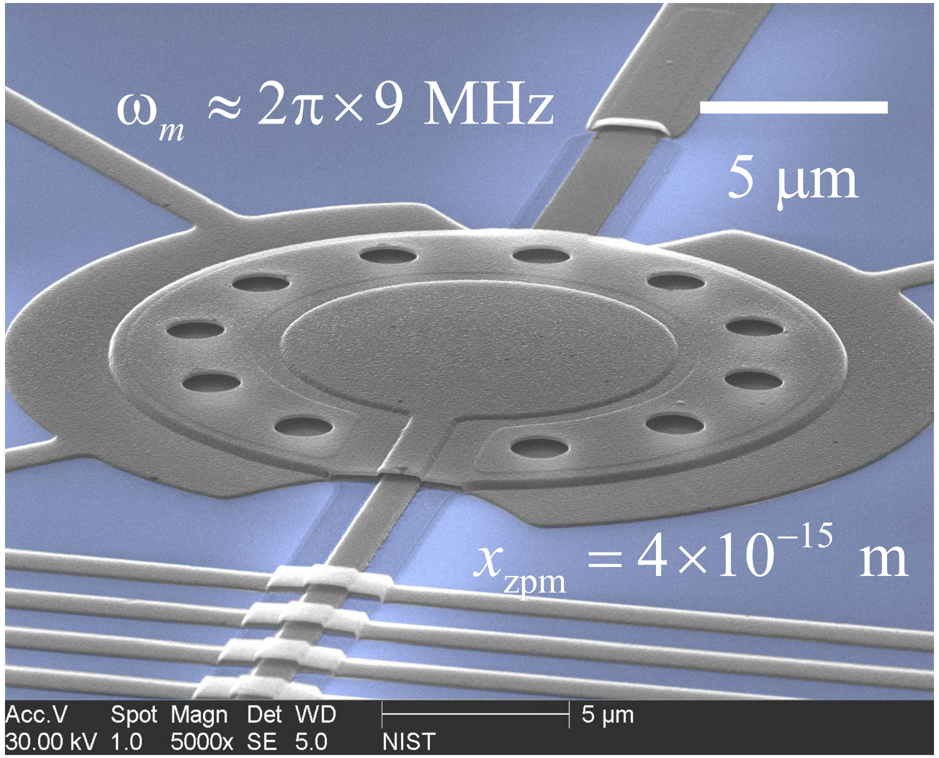

$g_0 = 2\pi \times 200$ Hz

J. D. Teufel, et al. *Nature* **471**, 204–208 (2011).

JILA CU Boulder and NIST

Pump creates parametric, linear coupling

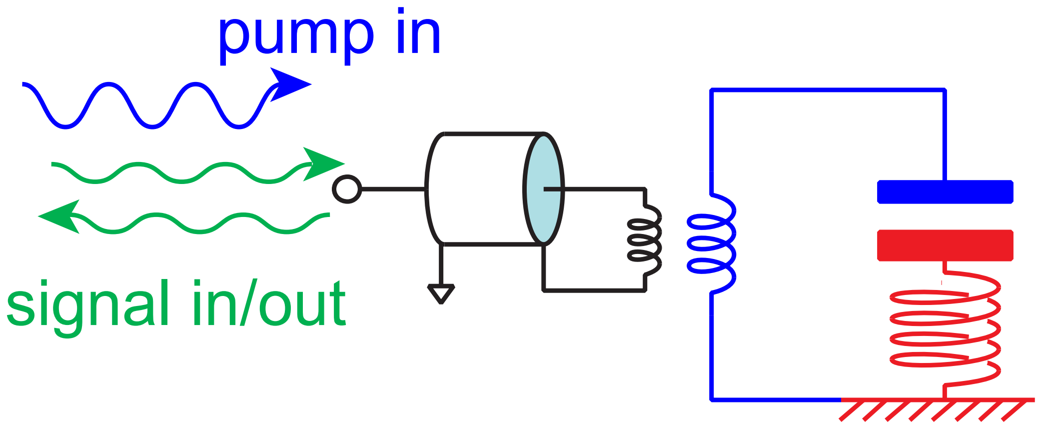

swap phonons and photons

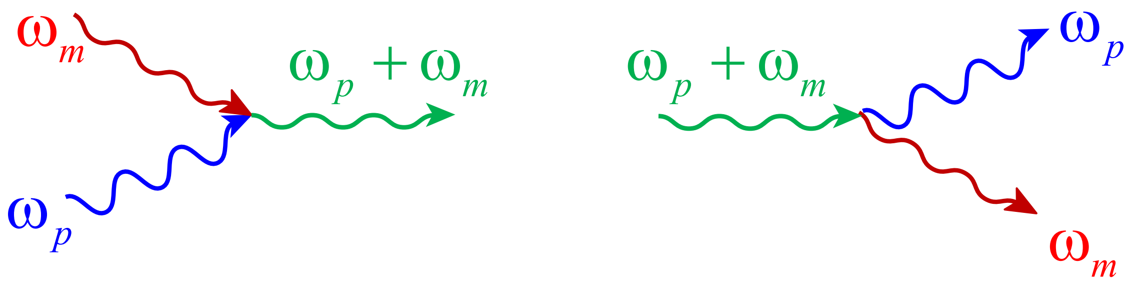

$$H_I = g_0 \alpha \left(a^\dagger b + b^\dagger a \right)$$

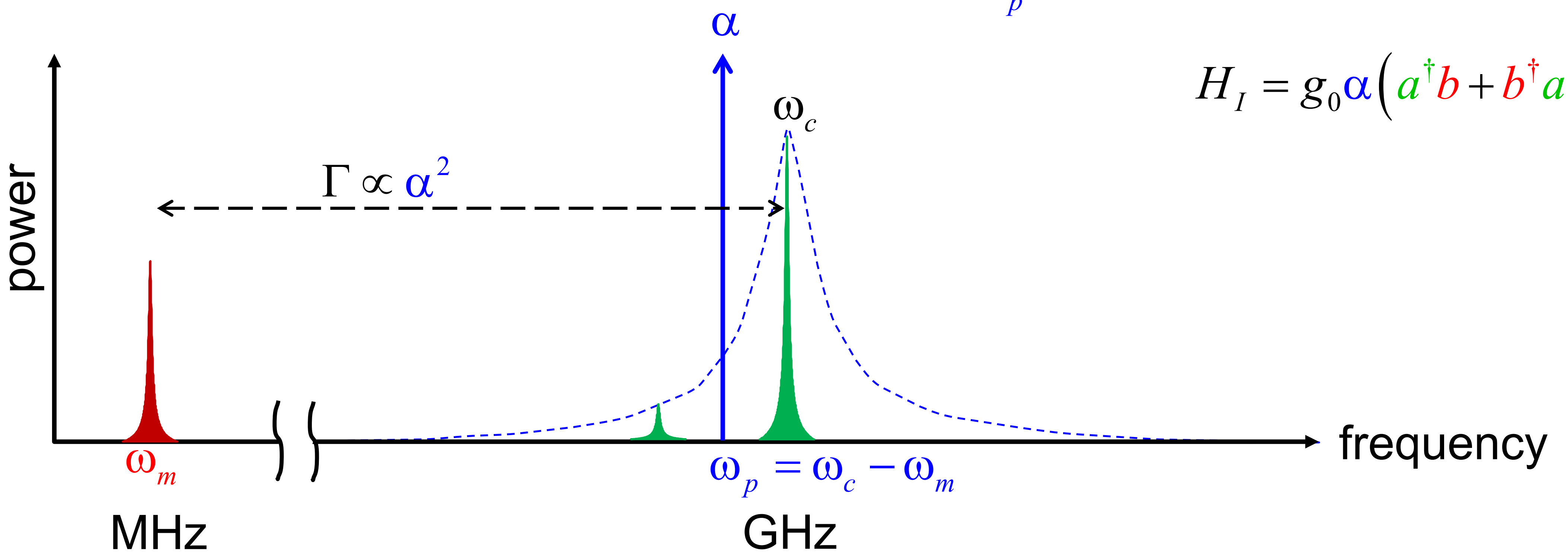

JILA
CU Boulder and NIST

Coherent conversion of microwave to optical fields

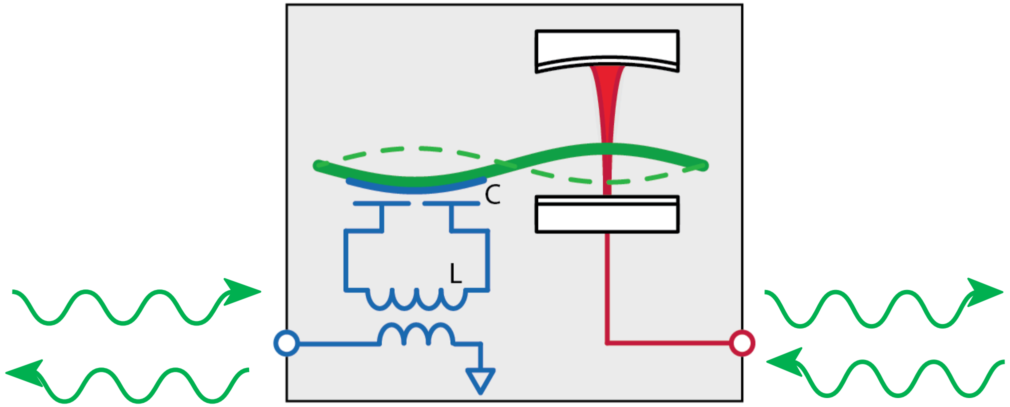

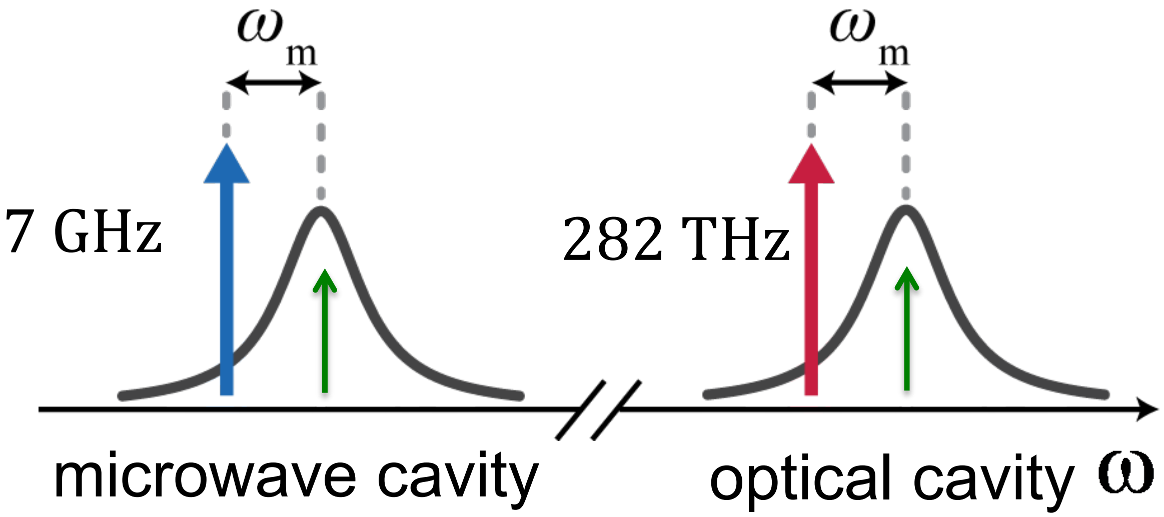

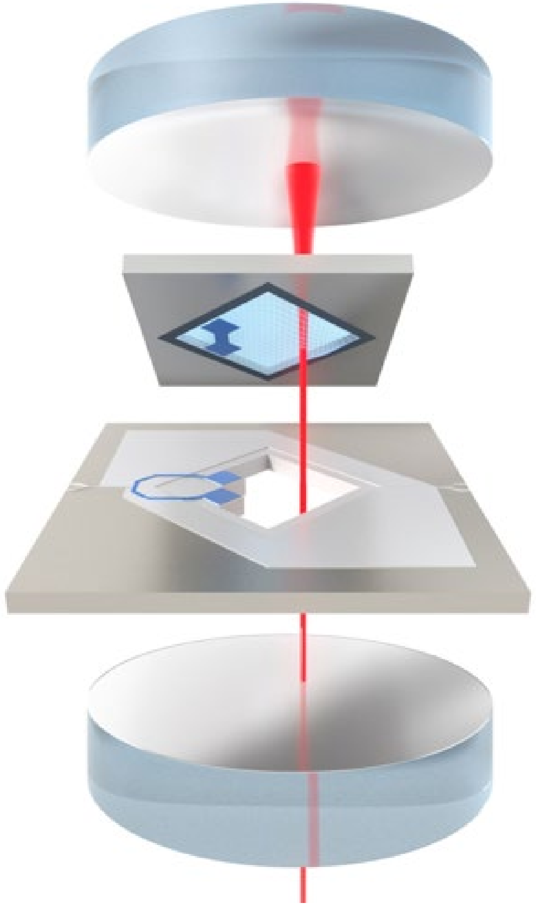

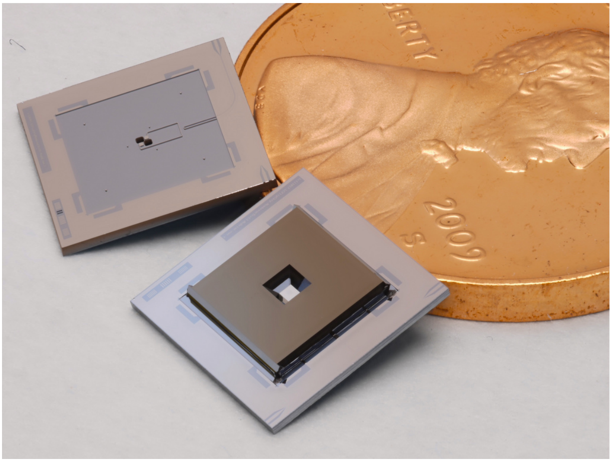

Quantum link between superconducting qubits and light enables a quantum communication network

quantum network

- secure communication
- processing power exponential in nodes

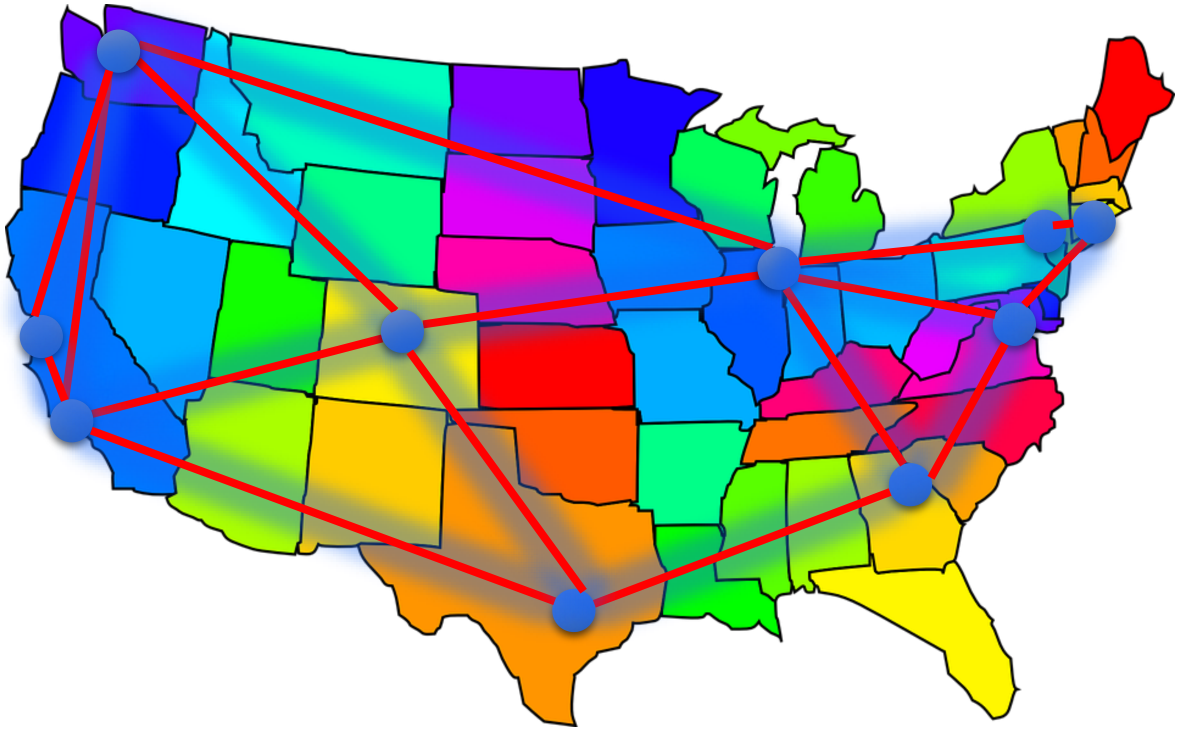

nodes

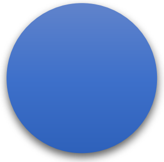

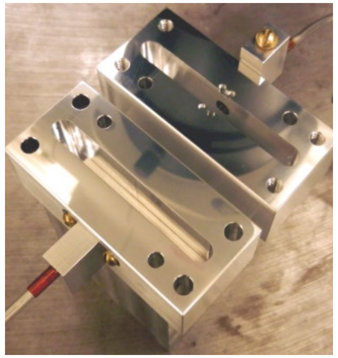

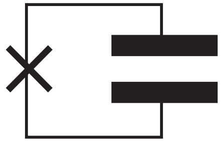

superconducting qubits
(process and store information)

links

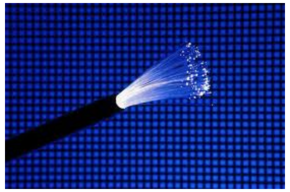

optics (transmit)

JILA
CU Boulder and NIST

Microwave signal processing in the quantum regime

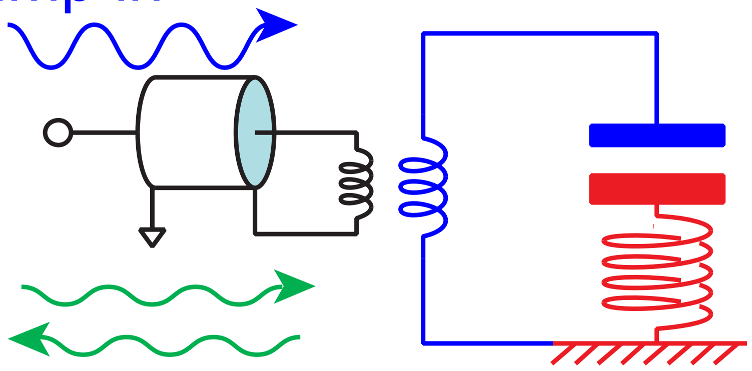

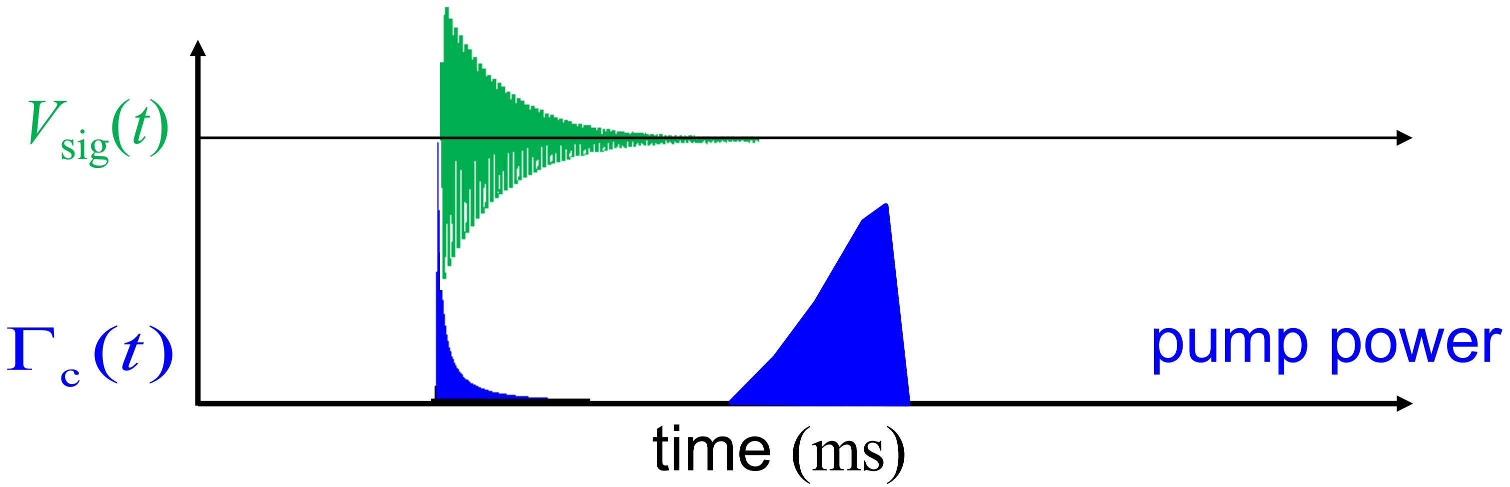

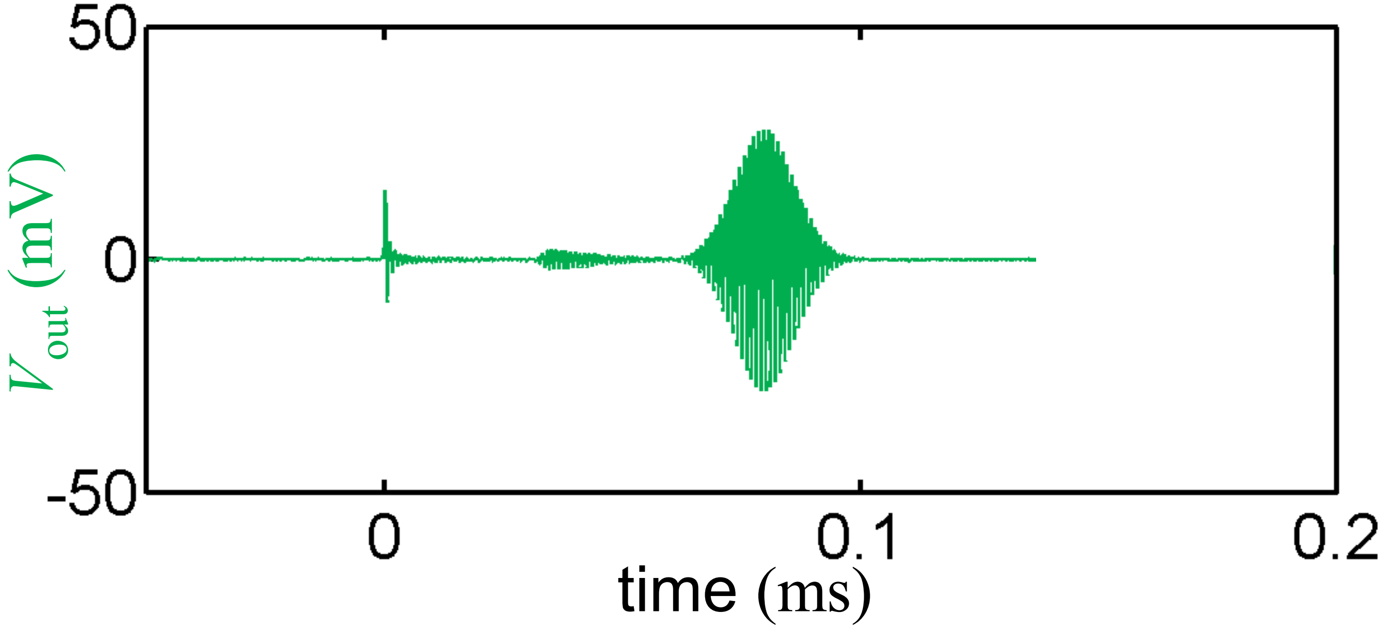

storage/delay
frequency conversion
temporal mode filtering
entanglement
amplification

quantum phononics

Is a single phonon detectable?

the quantum harmonic oscillator

$$\hat{H} = \hbar\omega_{\mathrm{m}}\left(\hat{b}^{\dagger}\hat{b} + \frac{1}{2}\right)$$

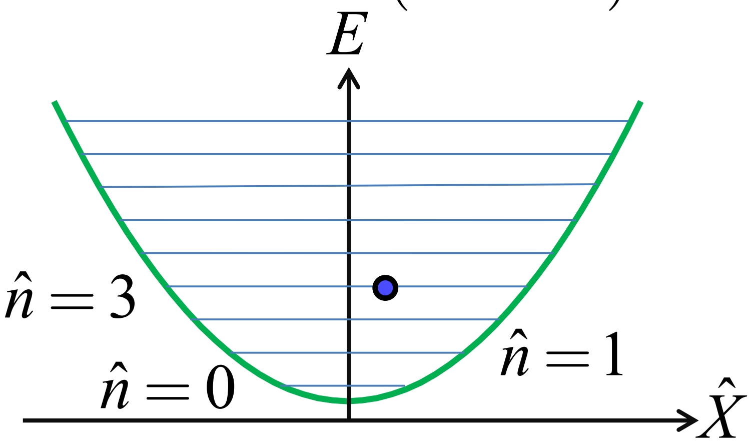

$$[\hat{n}, \hat{H}] = 0$$

student’s preference

$$\hat{H} = \frac{1}{2}\hbar\omega_{\mathrm{m}}\left(\hat{X}^2 + \hat{Y}^2\right)$$

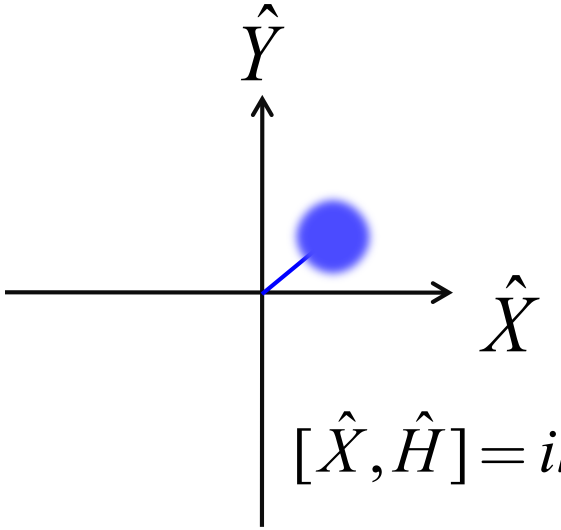

$$[\hat{X}, \hat{H}] = i\hbar\omega_{\mathrm{m}}\hat{Y}$$

nature’s preference

single phonons: require strong non-linearity

Vacuum electromechanical coupling is nonlinear but weak

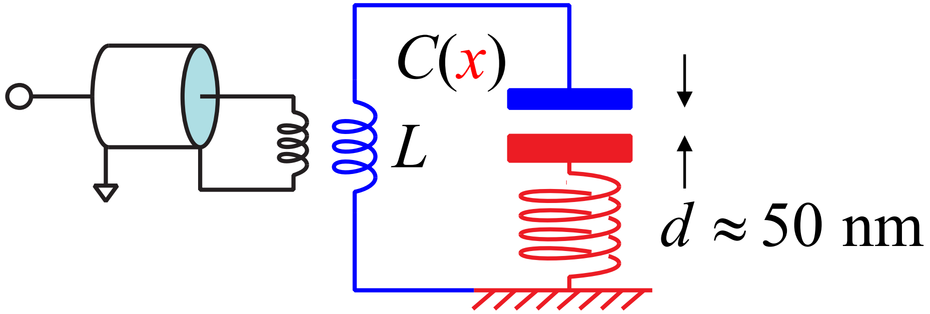

$$H_I = F_{\mathrm{el}} \cdot x = \frac{1}{2} V^2 \frac{\partial C}{\partial x} \cdot x$$

$$H_I = \frac{1}{4} \hbar\omega_{\mathrm{e}} \cdot \frac{x_{\mathrm{zpm}}}{d} a^\dagger a \left(b + b^\dagger\right)$$

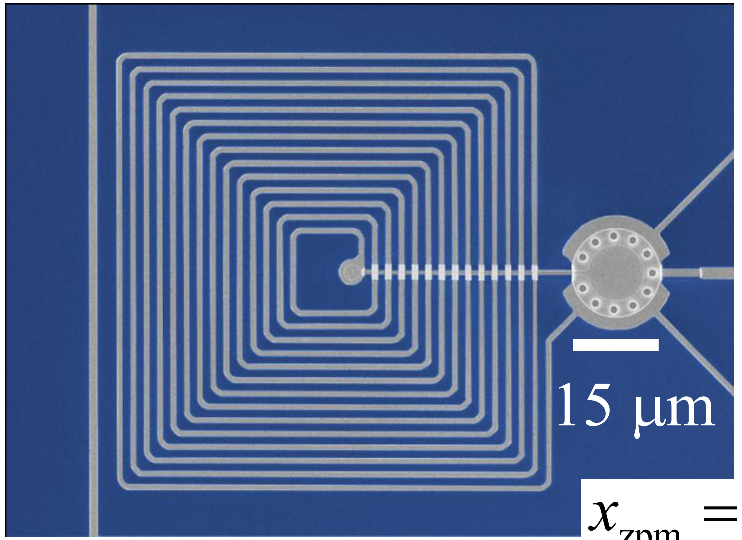

$x_{\mathrm{zpm}} = 4$ fm

$$\hbar g_0 = \frac{1}{4} \hbar\omega_{\mathrm{e}} \cdot \frac{x_{\mathrm{zpm}}}{d} \approx 2\pi\hbar \times 200 \text{ Hz}$$

$\omega_{\mathrm{e}} = 2\pi \times 7$ GHz

JILA
CU Boulder and NIST

Overcoming small vacuum electromechanical coupling

apply static voltage

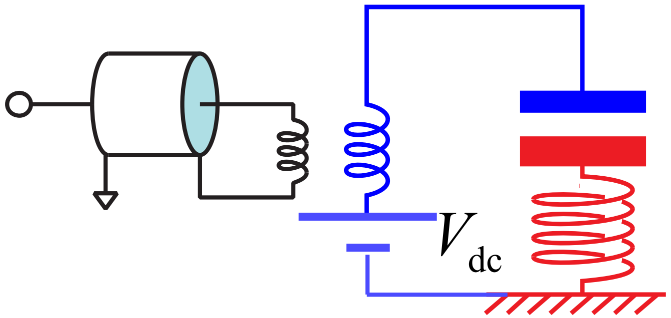

or use piezo-electric coupling

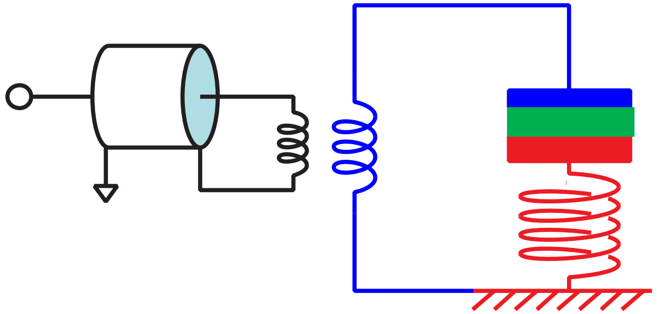

$$H_I = g_0\left(a + a^\dagger\right)\left(b + b^\dagger\right)$$

$$g_0 \approx 2\pi \times 10\ \mathrm{MHz}$$

add electrical non-linearity

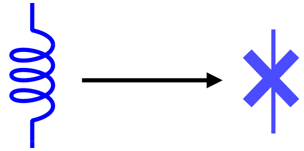

superconducting qubit
coupled mechanics

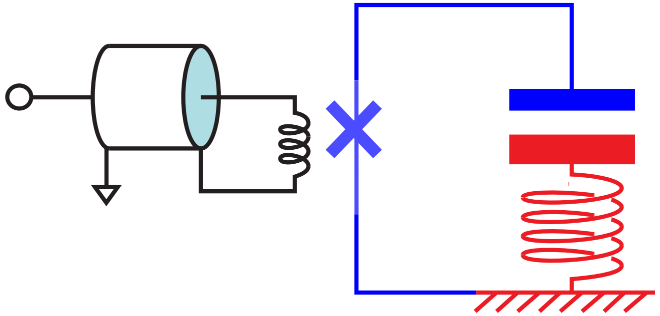

$$H_I = g_0 \sigma_x \left(b + b^\dagger\right)$$

Outline

mechanical oscillator coupled to a charge qubit: a particle in a quantum potential

energy sensitive detector of mechanical oscillator

stabilizing a non-classical state of motion

electromechanical device as an artificial molecule mechanical oscillator coupled to a charge qubit

Mechanics: vibrating aluminum membrane

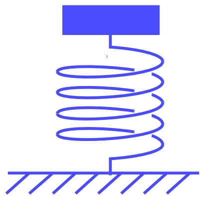

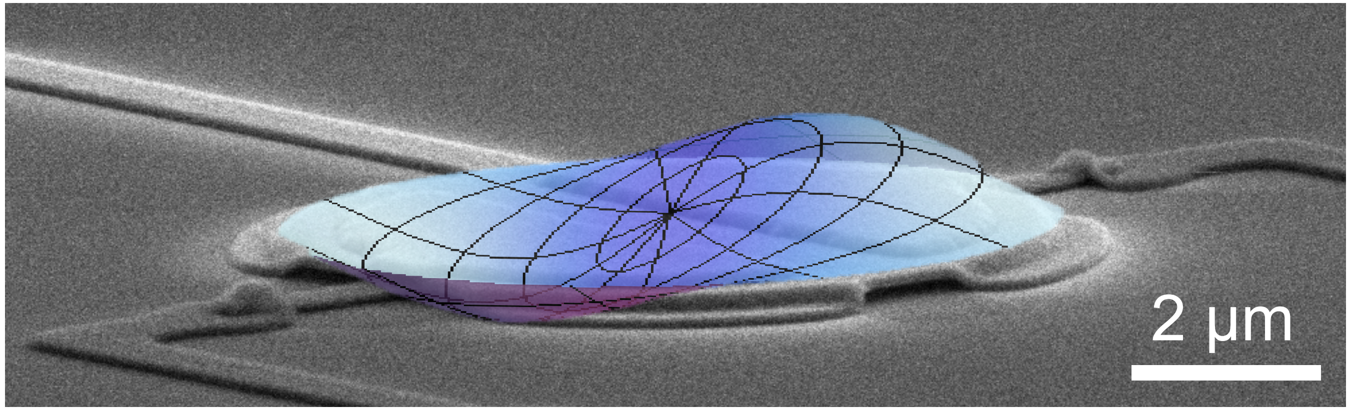

$$\omega_m = 2\pi \times 25 \text{ MHz}$$

antisymmetric 2:1 mode

Coupling an Al drum oscillator to a Cooper pair box qubit

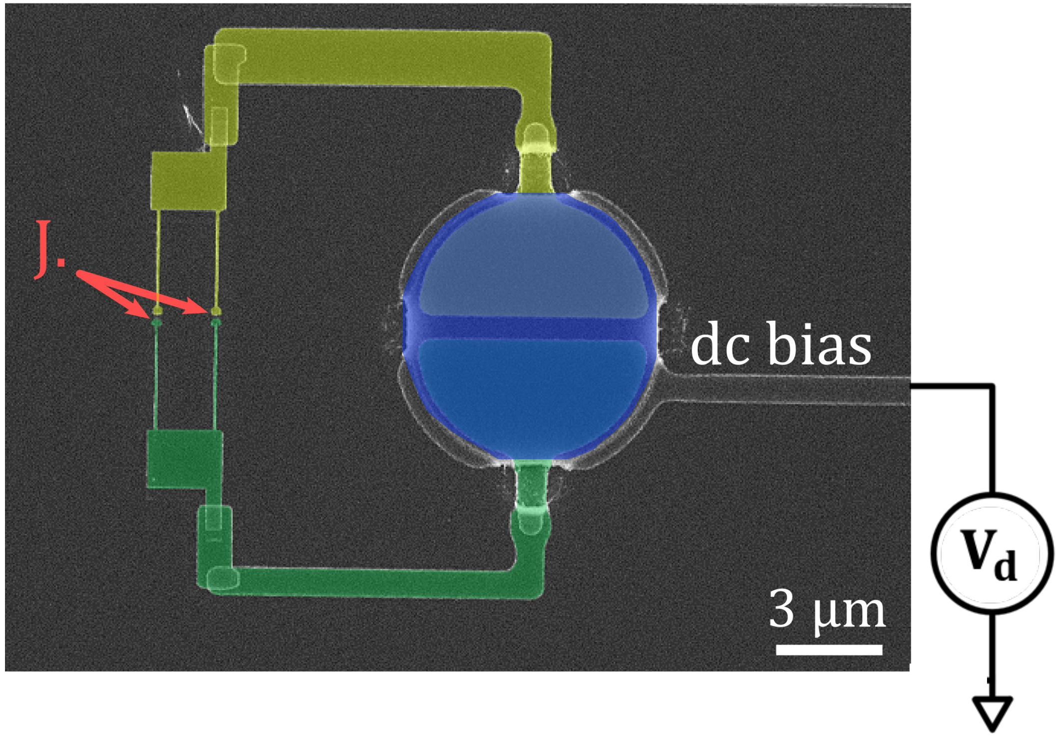

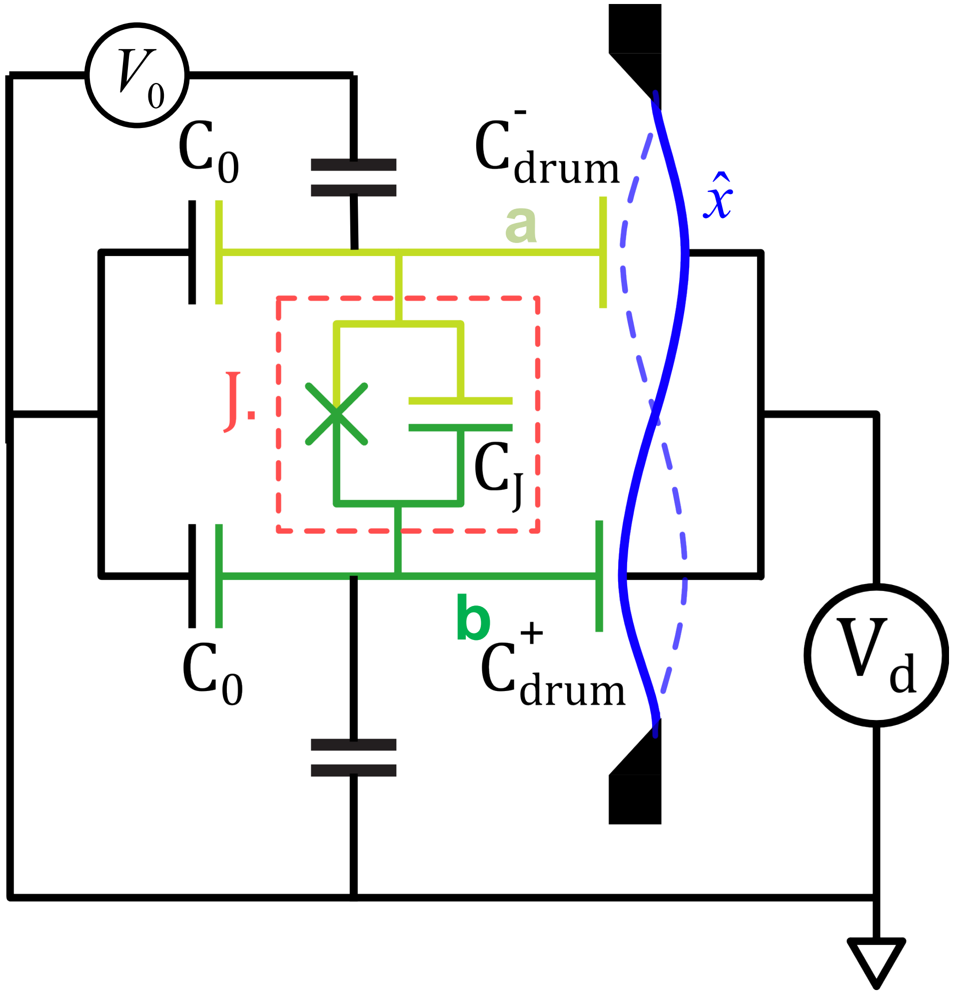

Thevenin equivalent

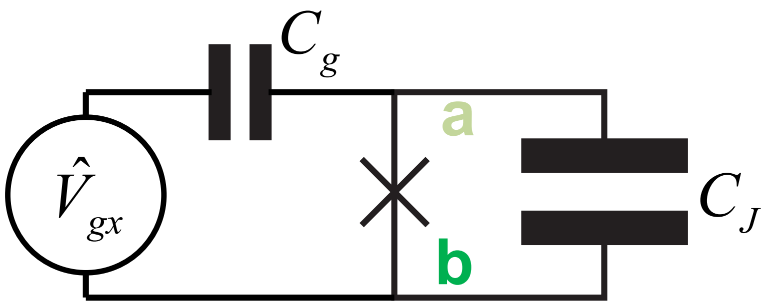

$$\hat{V}_{gx} = (\partial_x V_g)\hat{x}$$

gate voltage *is* oscillator coordinate

Mechanical oscillator moving in a qubit potential

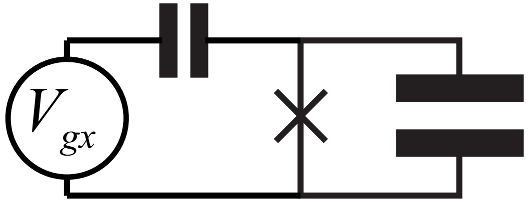

$$V_{gx} = V_0 + \partial_x V_g \hat{x}$$

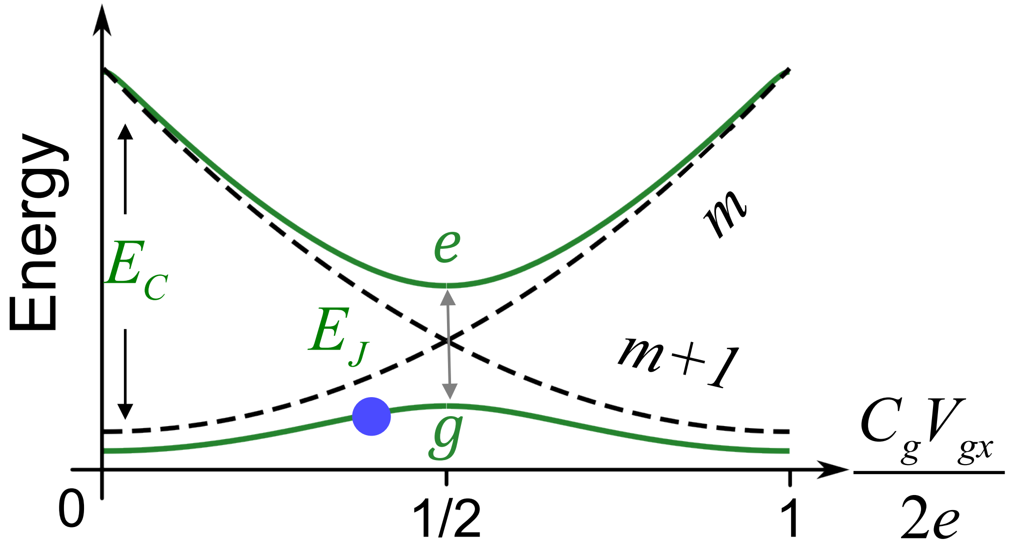

oscillator particle in qubit potential

$$\omega_m \ll \omega_q$$

$$\frac{C_g V_0}{2e} \neq \frac{1}{2}$$ qubit dependent force

$$\hat{H}_I \propto \hat{\sigma}_z \hat{x} = \hat{\sigma}_z (b^\dagger + b)$$

$$\frac{C_g V_0}{2e} = \frac{1}{2}$$ qubit dependent spring constant

$$\hat{H} = \frac{1}{2}\left(\hbar\omega_q \hat{\sigma}_z + \hat{p}^2 / m + k\hat{x}^2\right) + \frac{1}{2} k_q \hat{x}^2 \hat{\sigma}_z$$

JILA
CU Boulder and NIST

Ultrastrong coupling, dispersive limit of Rabi Hamiltonian

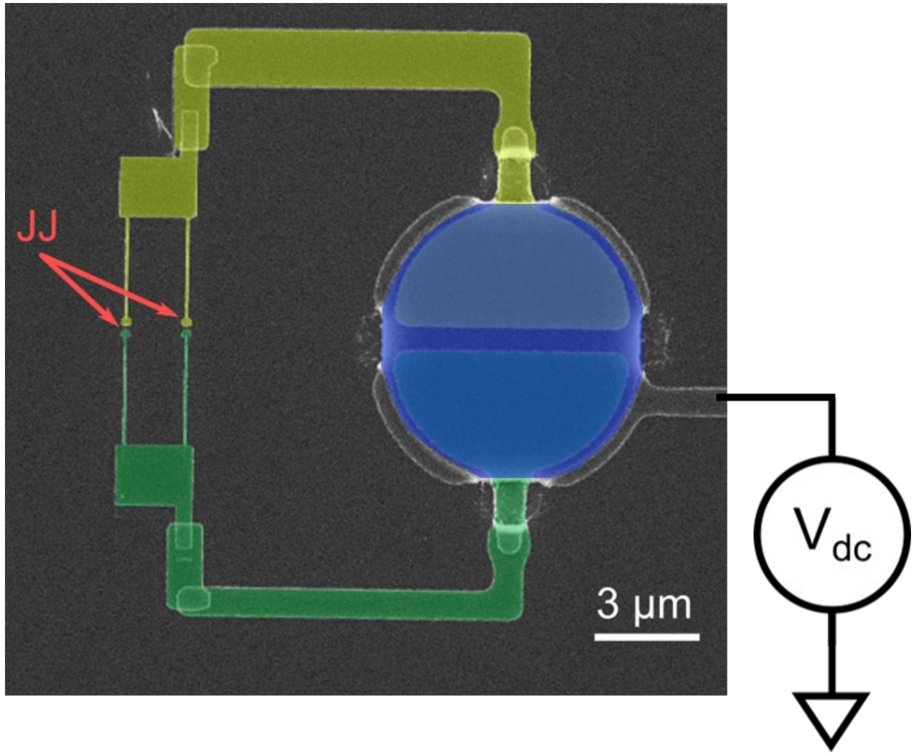

at charge degeneracy

$$H_{\text{Rabi}}/\hbar = \frac{1}{2}\omega_q\sigma_z + \omega_m b^\dagger b + \frac{1}{2}g_0\sigma_x\left(b+b^\dagger\right)$$

$$g_0 \propto V_{\text{dc}}$$

$$V_{\text{dc}} = 6\text{ V} \Rightarrow \text{g}_0 \approx 2\pi\times 22\text{ MHz}$$

$$\text{g}_0 \sim \omega_m$$

$$\omega_q + \omega_m \approx \omega_q - \omega_m$$

$$\chi_m = \frac{2g_0{}^2}{\omega_m} \approx 2\pi\times 260\text{ kHz}$$

$$\hat{H}_I = \chi_m\hat{\sigma}_z\hat{x}^2 = \boxed{\chi_m\hat{\sigma}_z b^\dagger b} + \boxed{\frac{1}{2}\chi_m\hat{\sigma}_z(b^{\dagger 2}+b^2)}$$

Stark shift + sidebands

JILA CU Boulder and NIST

energy sensitive detector of mechanical oscillator

Motional dispersion of qubit emulated with classical drive

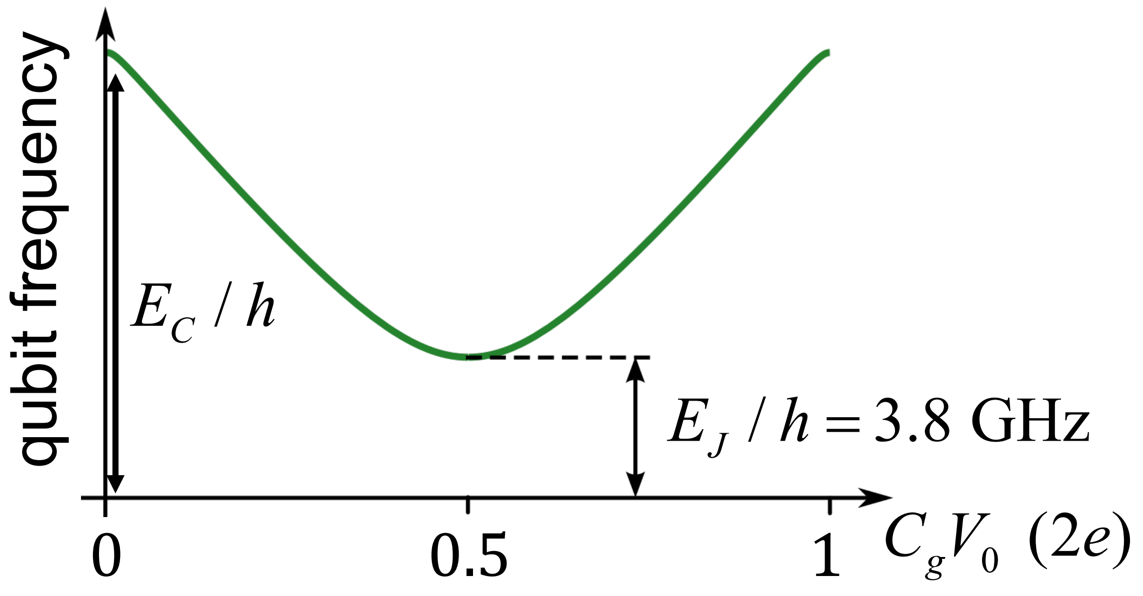

$$V_{\mathrm{dc}} = 0;\ \partial_x V_g = 0$$

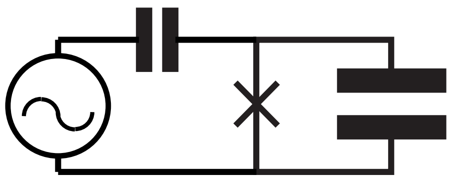

$$\frac{C_g V_0}{2e} = \frac{1}{2} + \lambda \cos(\omega_m t)$$

$$\hbar\omega_q(t) = \sqrt{E_J{}^2 + \left[E_C \lambda \cos(\omega_m t)\right]^2}$$

$$\hbar\omega_q(t) = E_J + \underbrace{\frac{E_C{}^2}{E_J}\lambda^2}_{\text{Stark shift}} + \underbrace{\frac{E_C{}^2}{E_J}\lambda^2 \cos(2\omega_m t)}_{\text{sidebands}} + O(\lambda^4)$$

Motional modulation of qubit emulated with classical drive

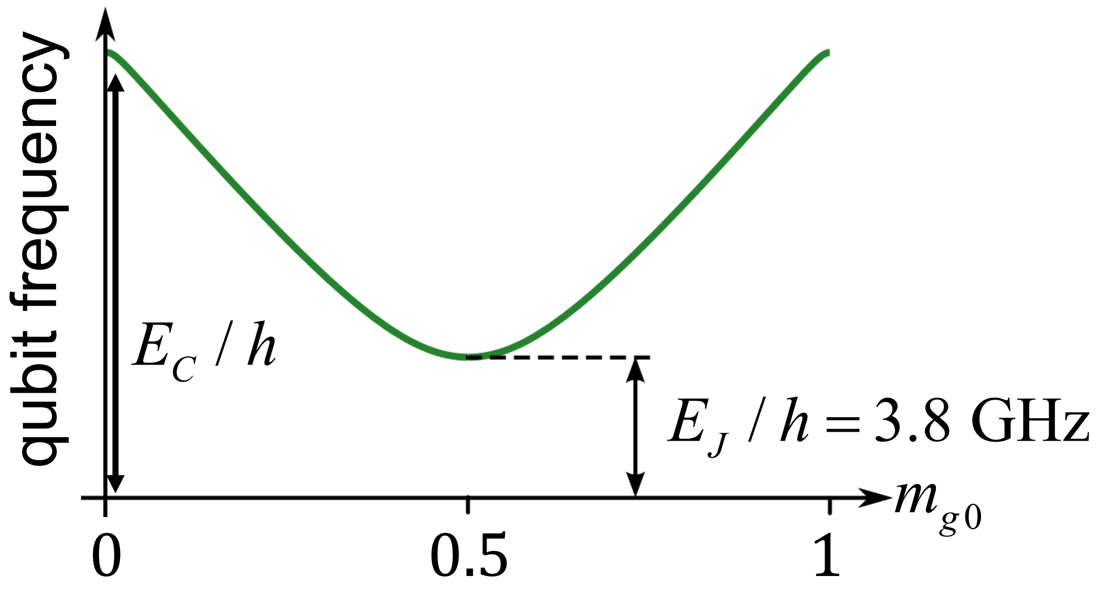

$$\hbar\omega_q(t) = \sqrt{E_J^2 + \left[E_C \lambda \cos(\omega_m t)\right]^2}$$

$$\hbar\omega_q(t) = E_J + \underbrace{\frac{E_C^2}{E_J}\lambda^2}_{\text{Stark shift}} + \underbrace{\frac{E_C^2}{E_J}\lambda^2 \cos(2\omega_m t)}_{\text{sidebands}} + O(\lambda^4)$$

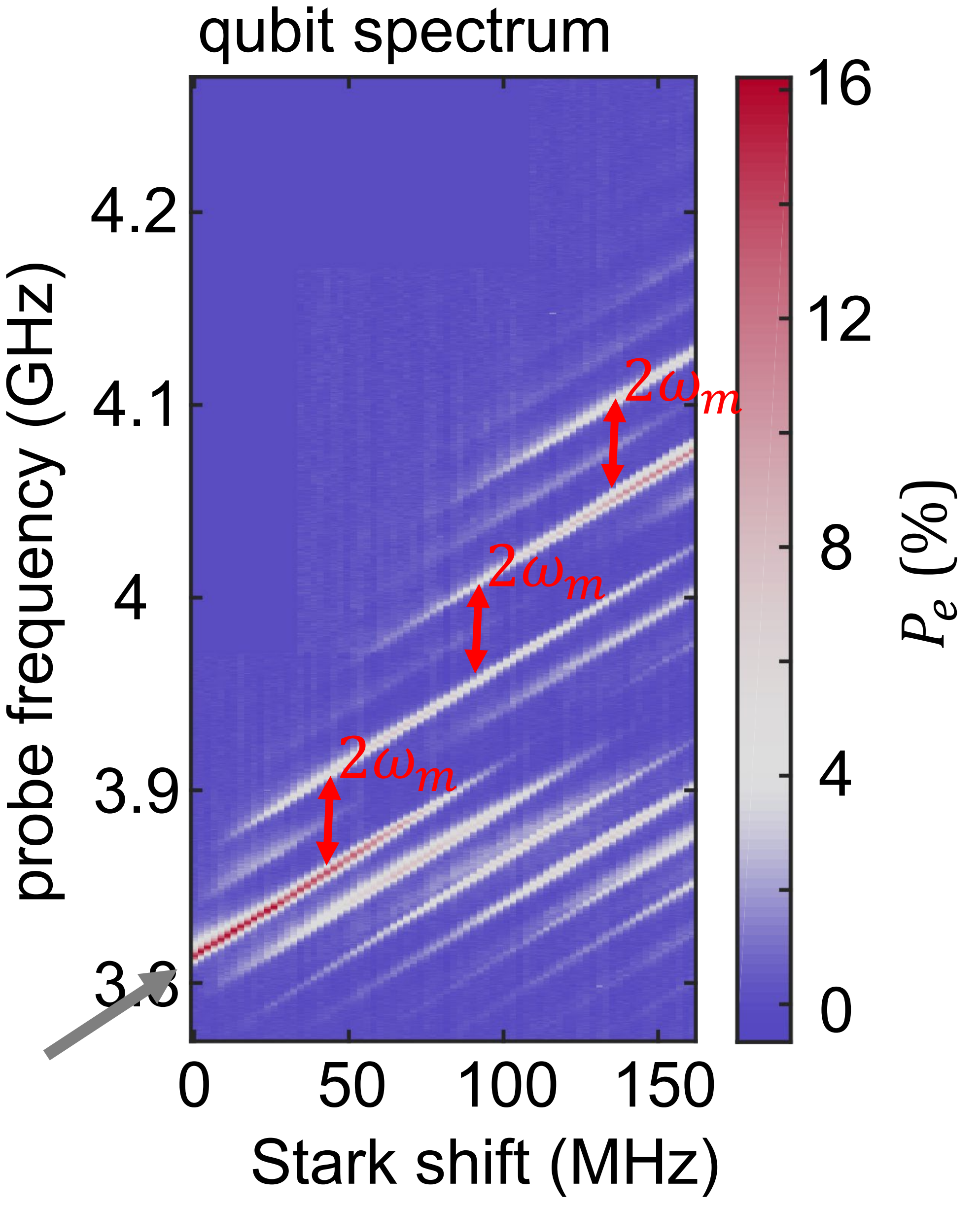

JILA
CU Boulder and NIST

Qubit spectrum encodes phonon number distribution

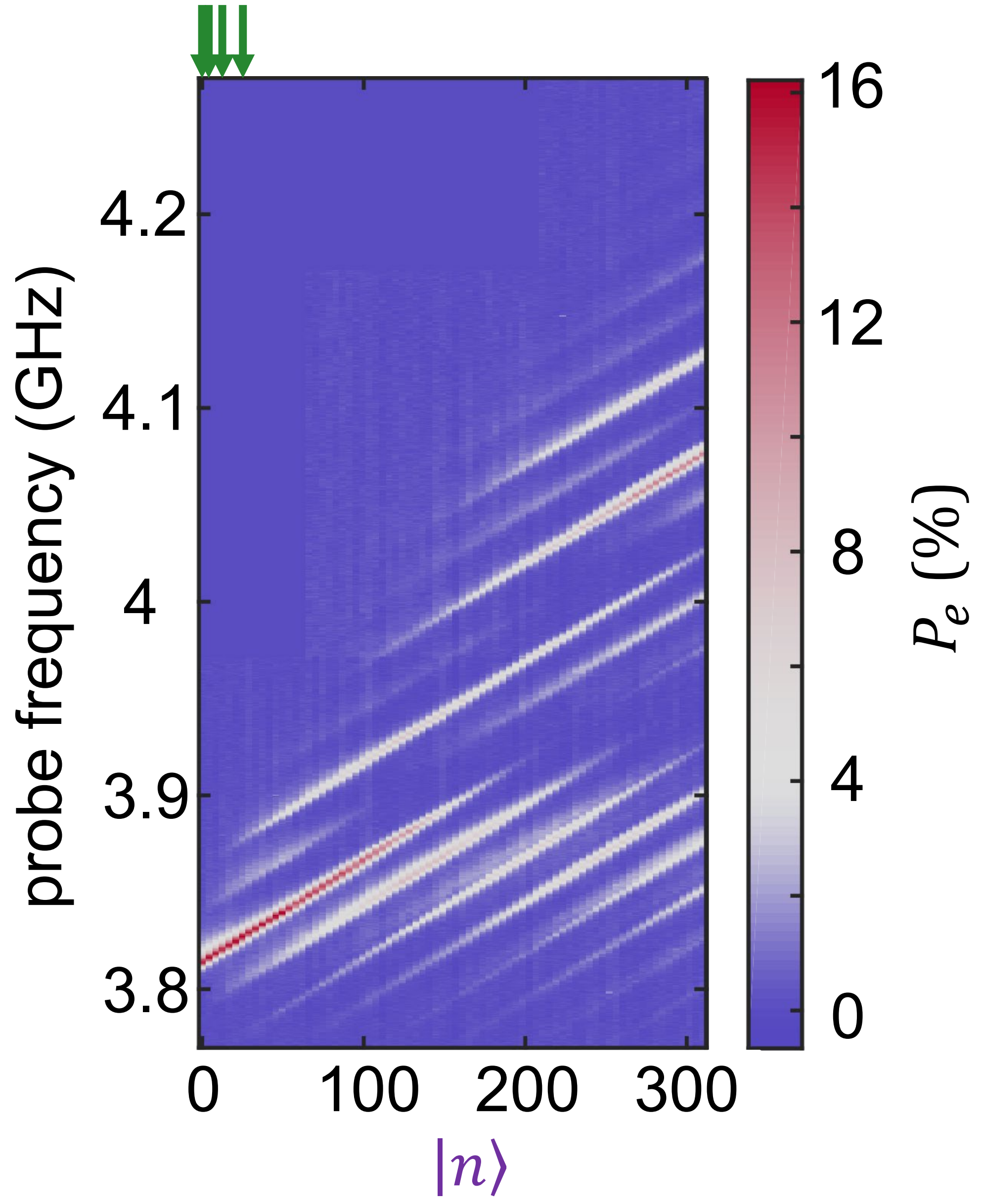

$2\chi_m = 2\pi \times 0.52$ MHz
$\Gamma_2^* = 2\pi \times 3.7$ MHz

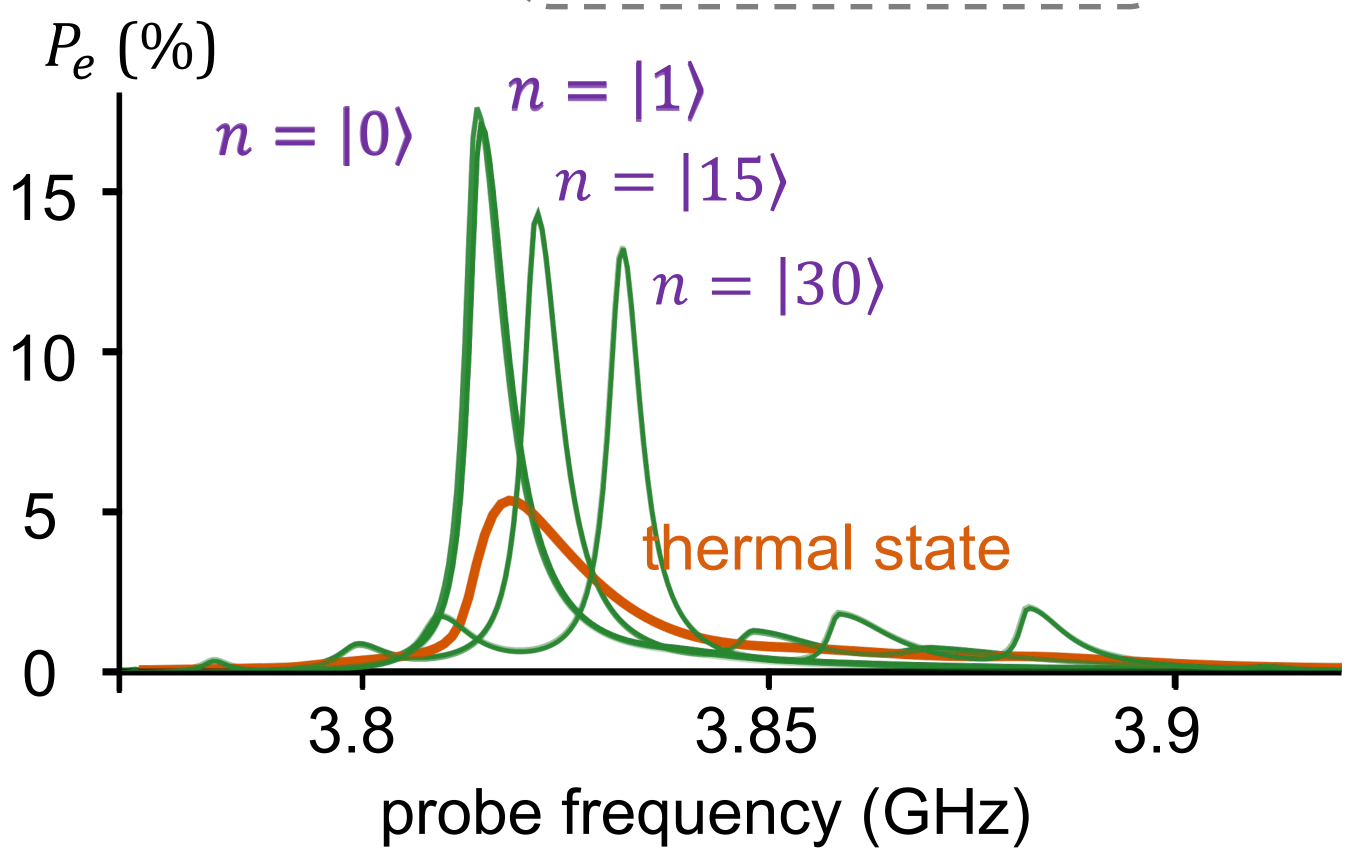

De-convolution reveals phonon statistics

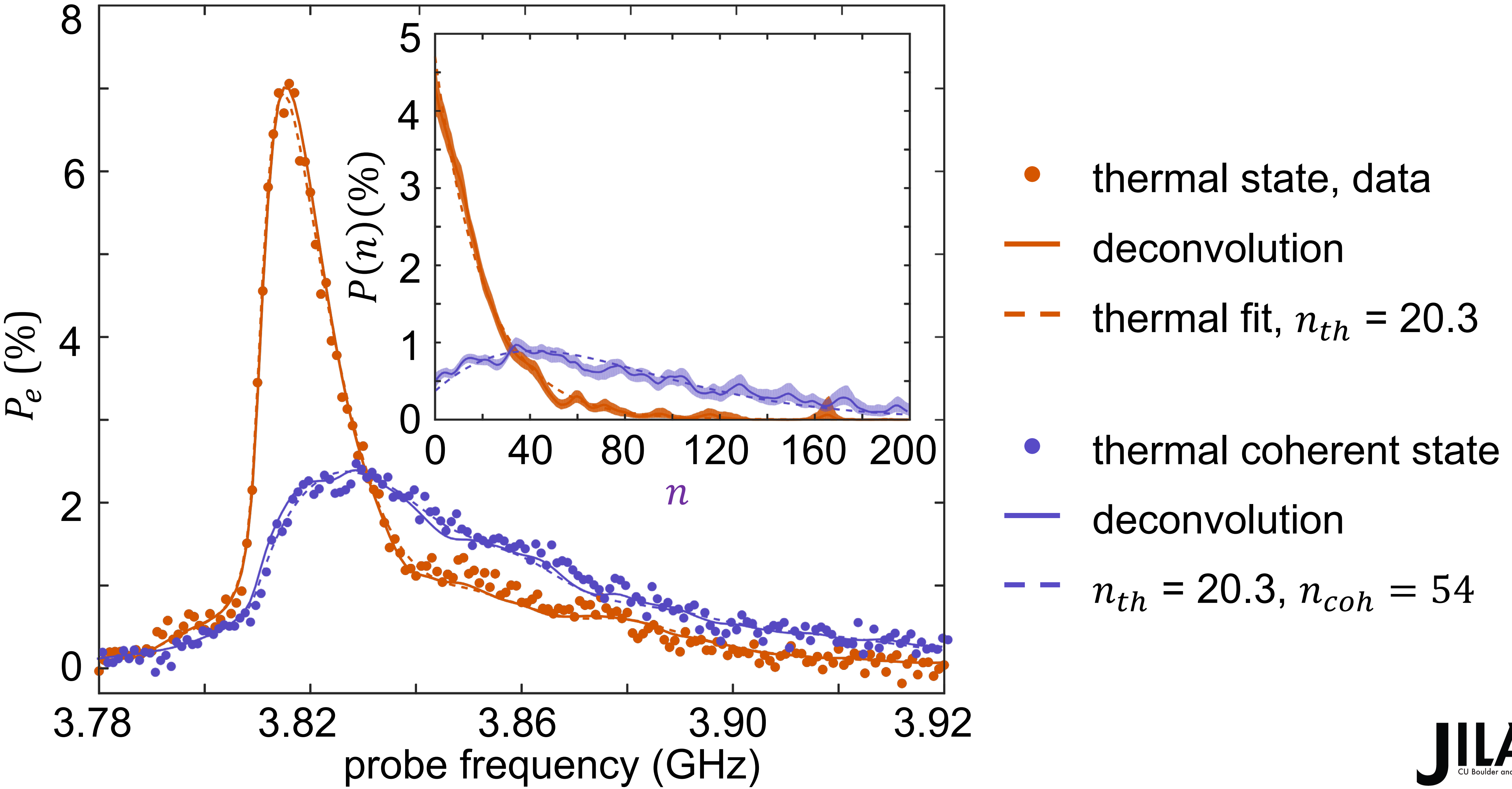

JILA
CU Boulder and NIST

stabilizing a phonon number squeezed state

Number sensitive sideband transitions

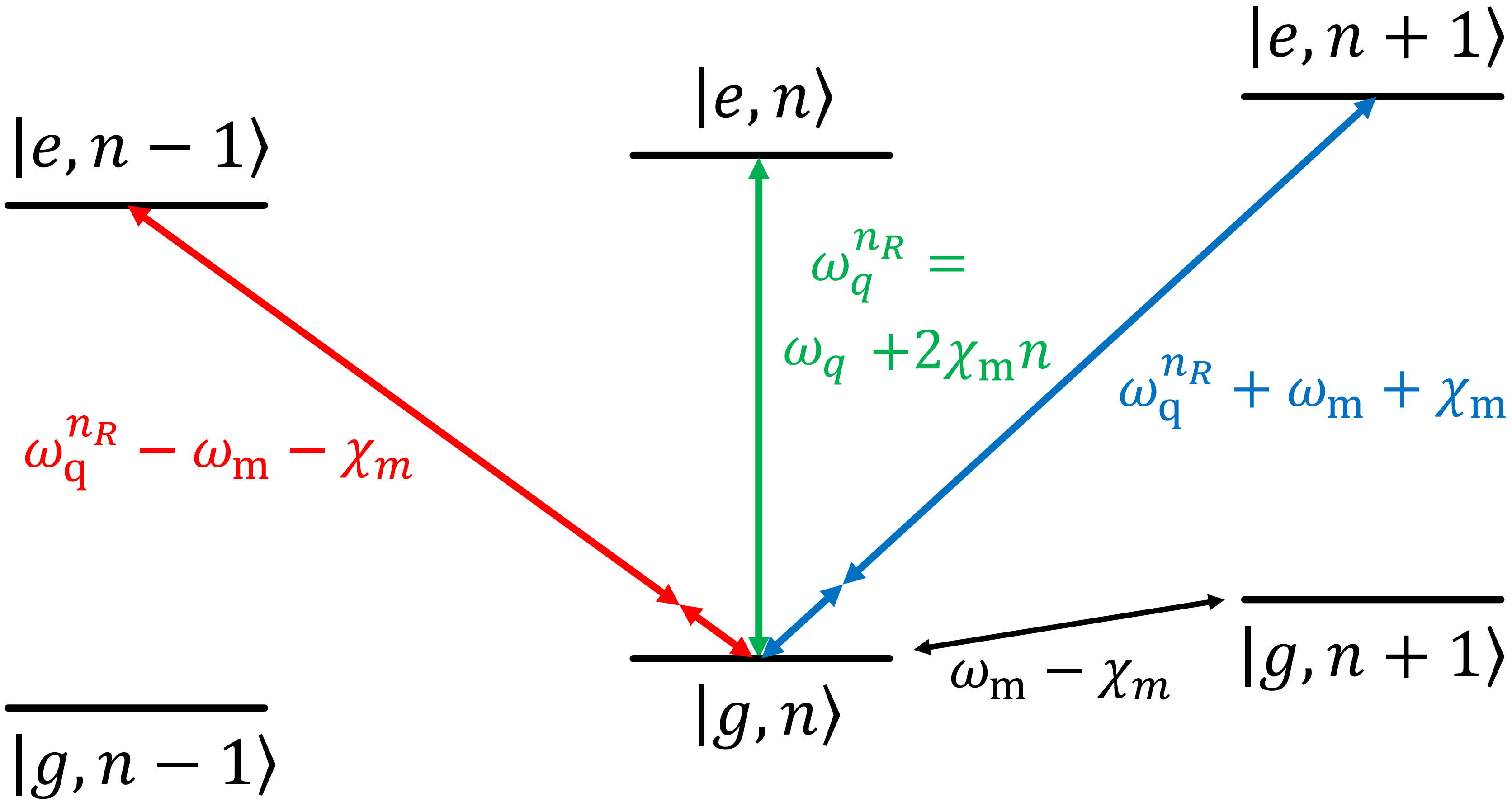

JILA
CU Boulder and NIST

Sideband drive moves population selectively

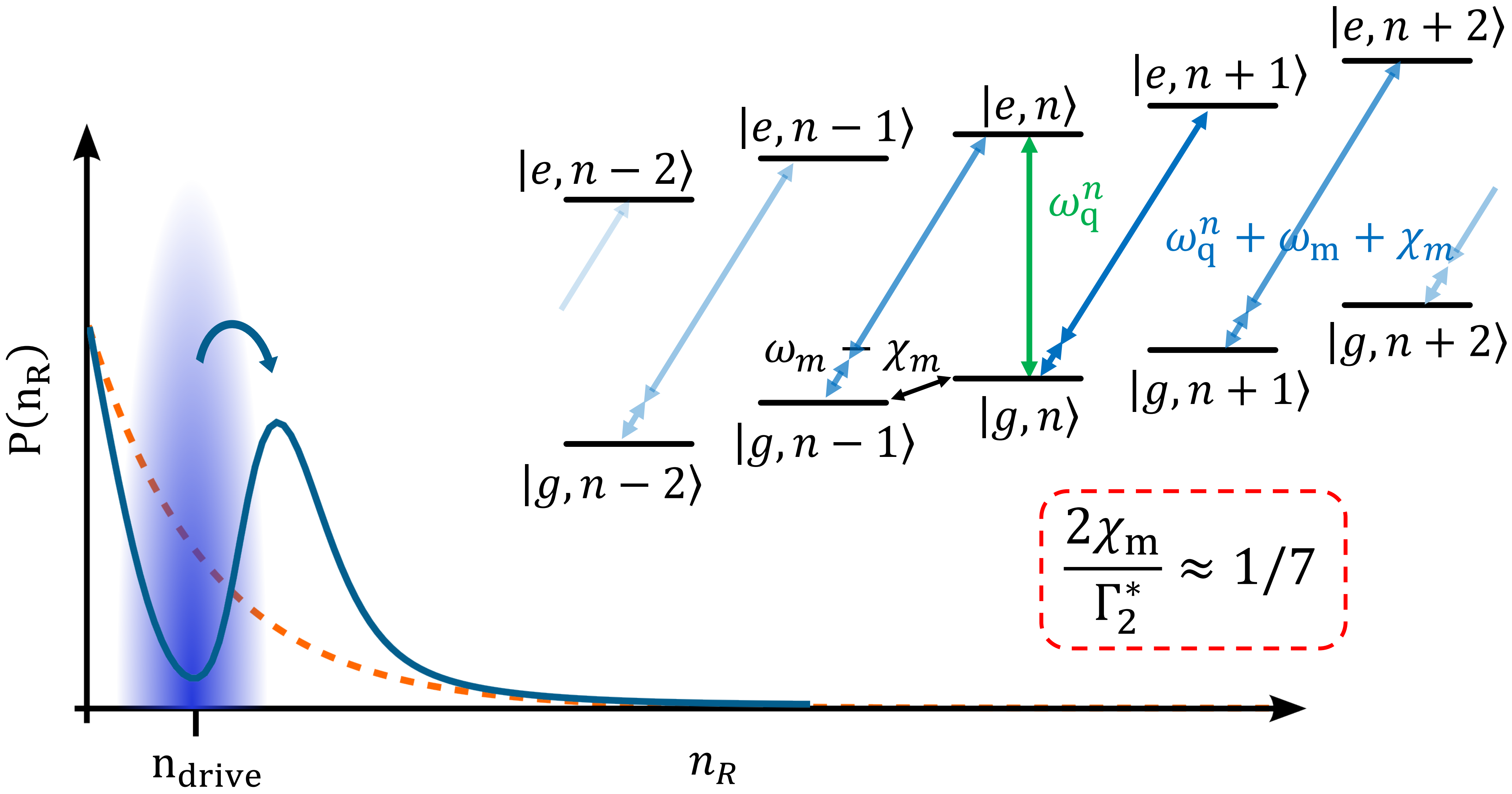

J.J. Viennot, X. Ma, and K.W. Lehnert, PRL (2018)

Number sensitive blue sideband

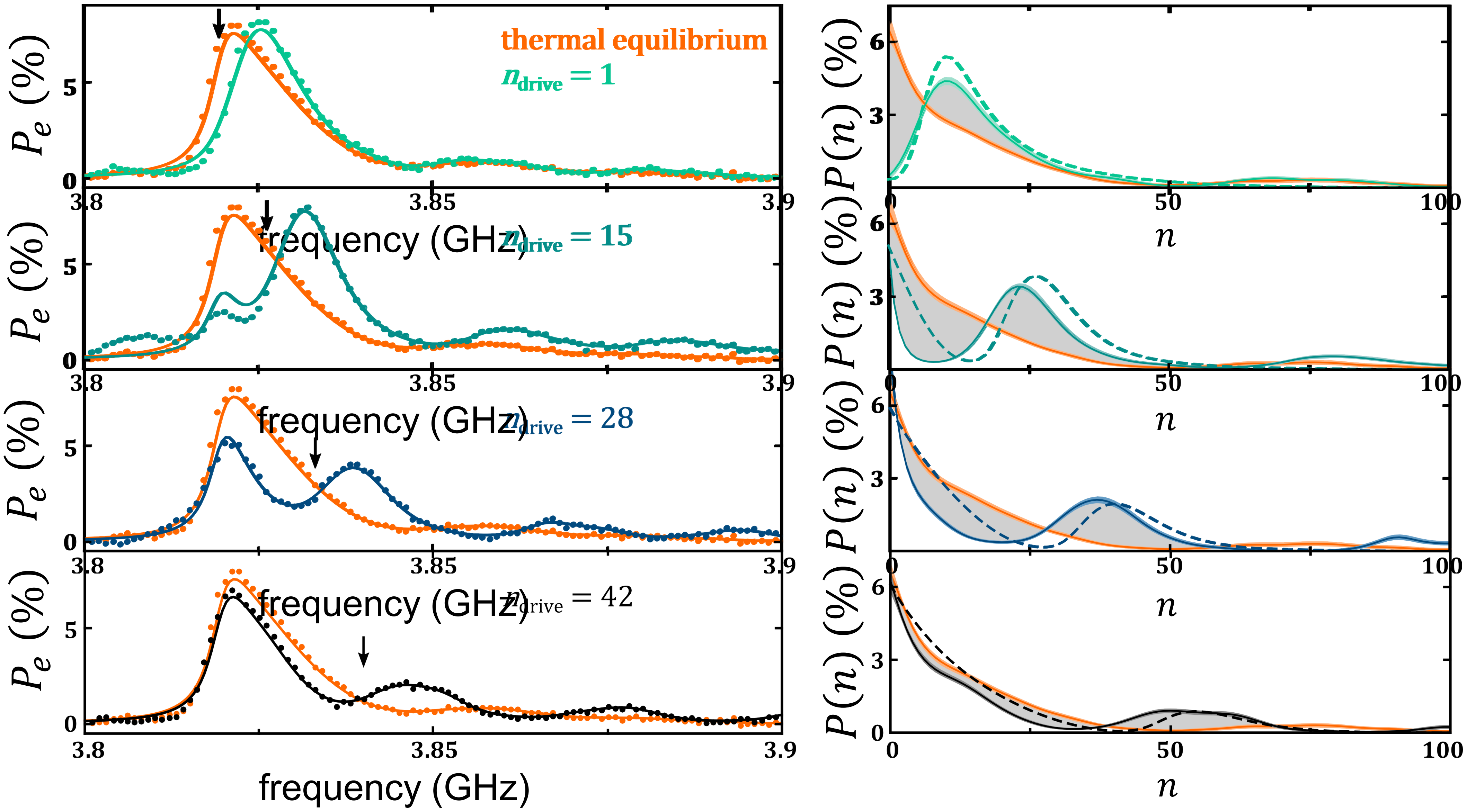

JILA
CU Boulder and NIST

Sideband drive moves population selectively

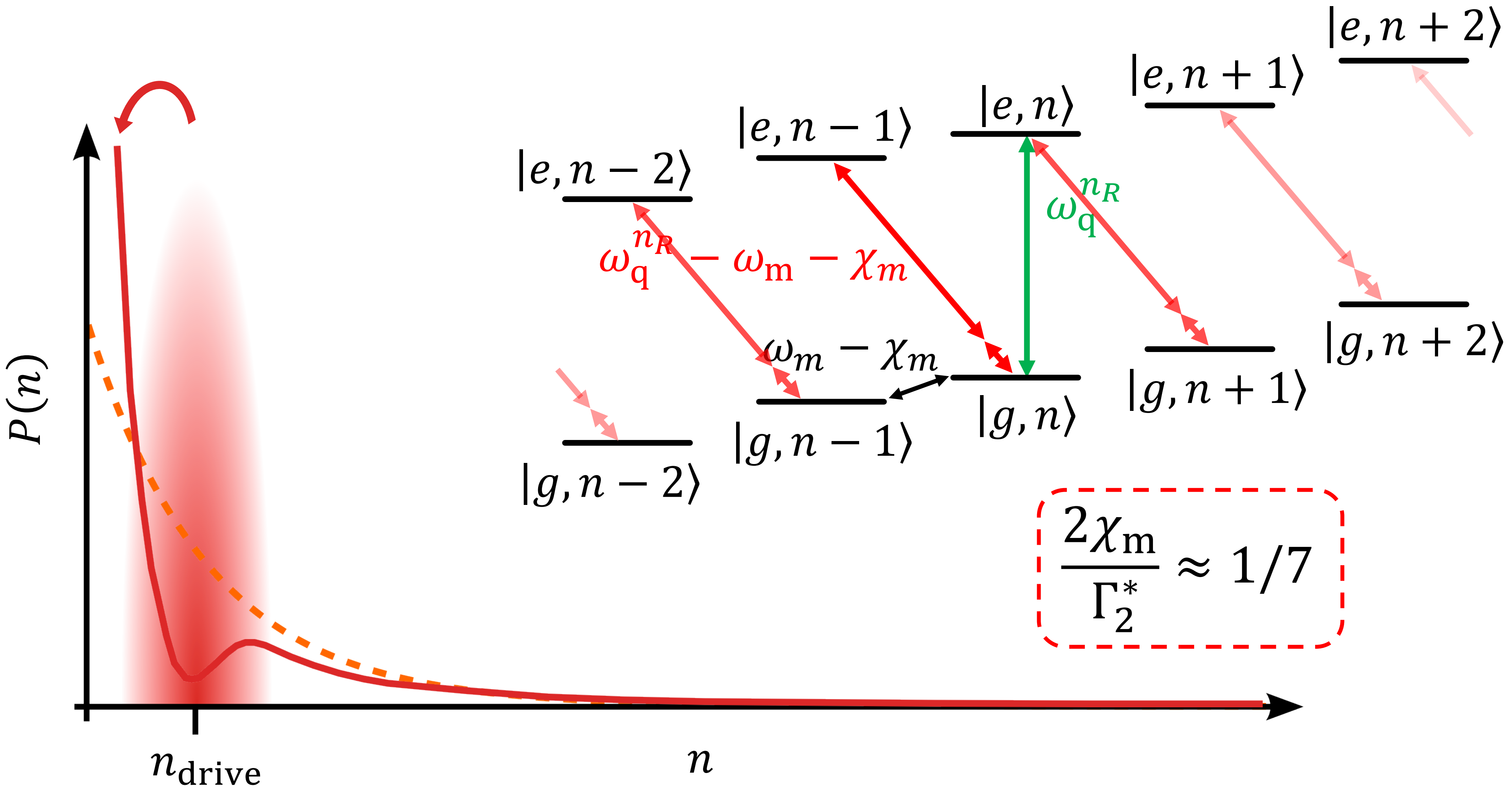

$$\frac{2\chi_m}{\Gamma_2^*} \approx 1/7$$

Number sensitive red sideband : cooling a mechanical oscillator with a two level system

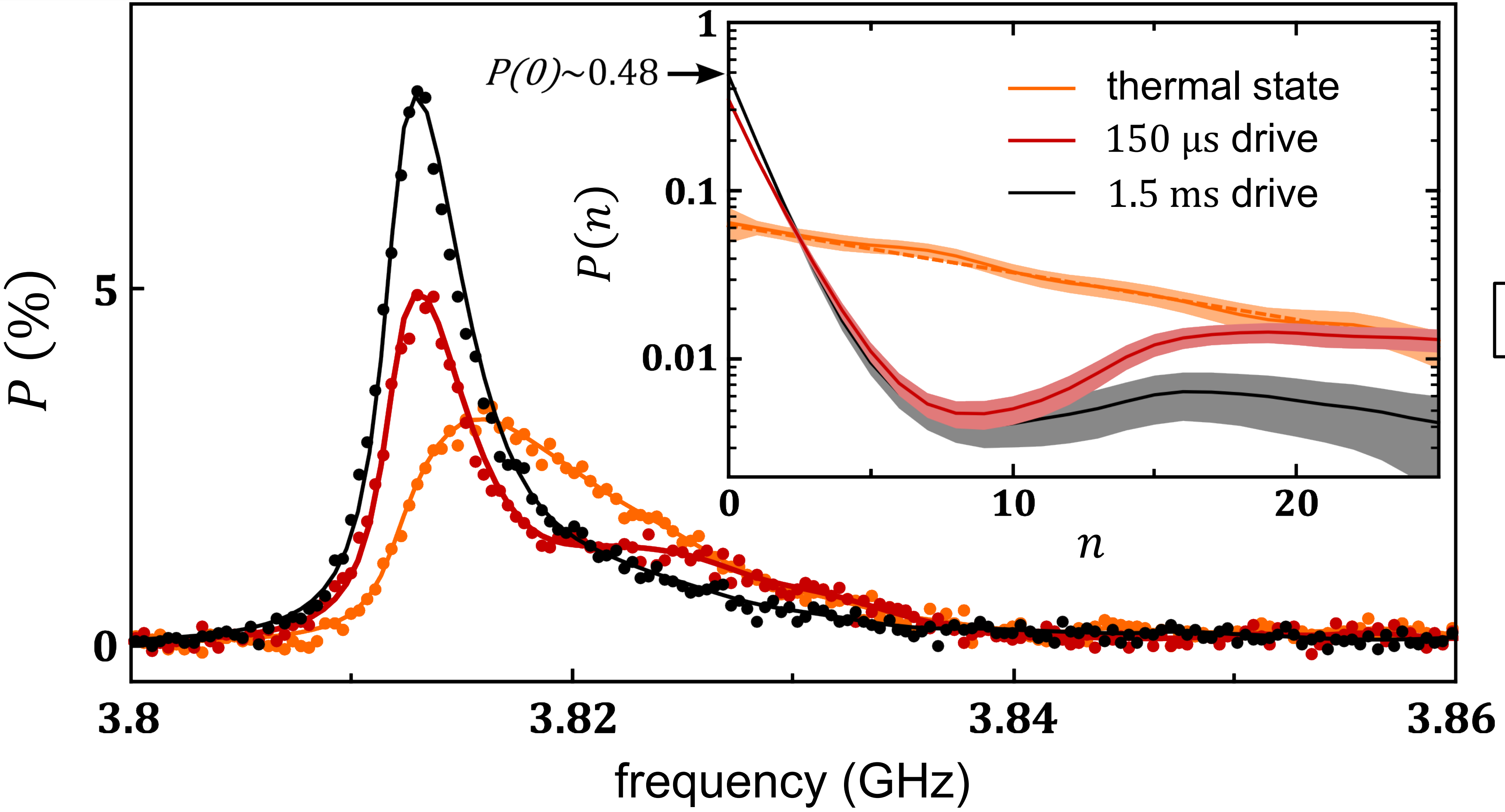

$n_{\mathrm{drive}} \approx 8$

J.J. Viennot, X. Ma, and K.W. Lehnert, PRL (2018)

JILA CU Boulder and NIST

Chirped blue sideband displace thermal distribution

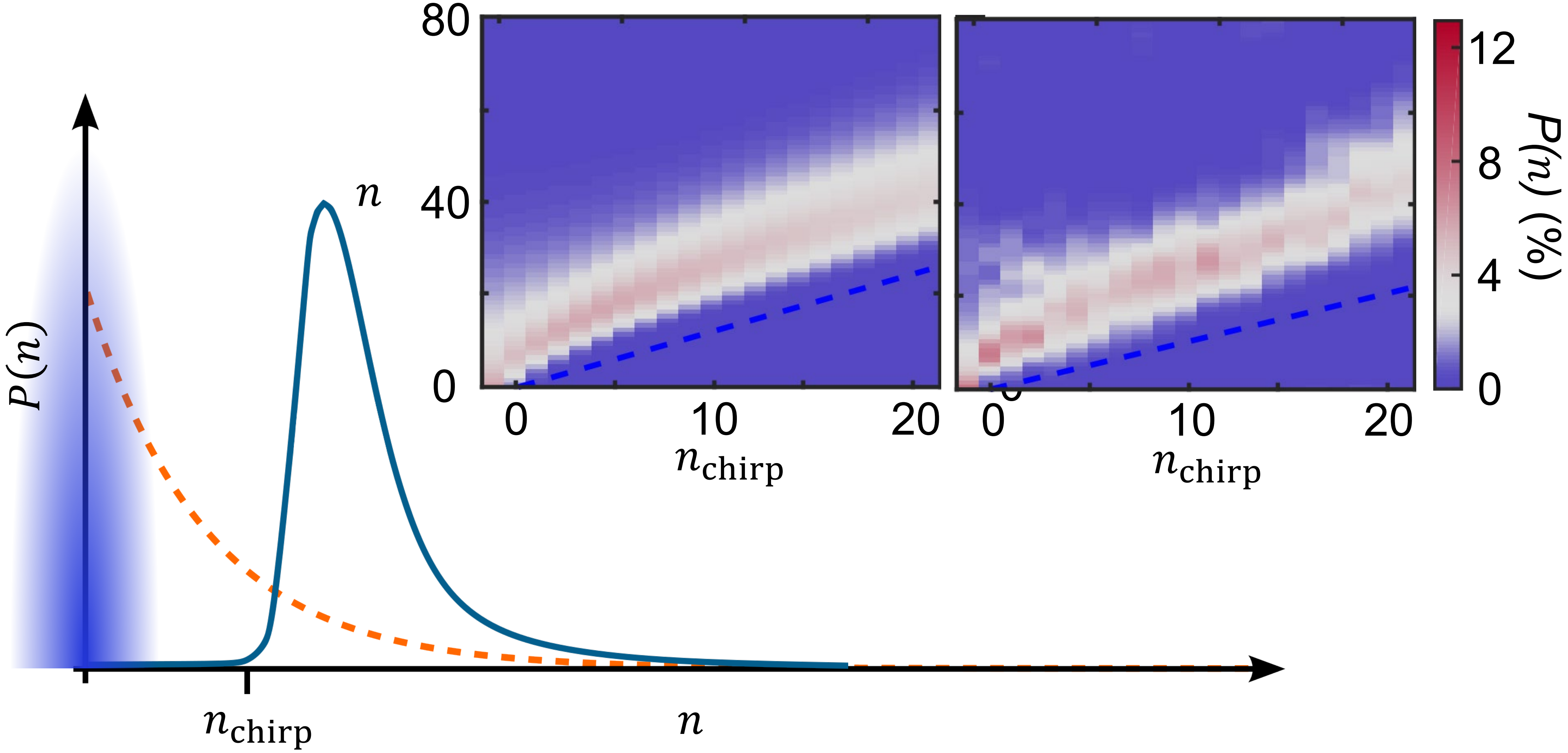

Squeezing the number distribution with sideband drives

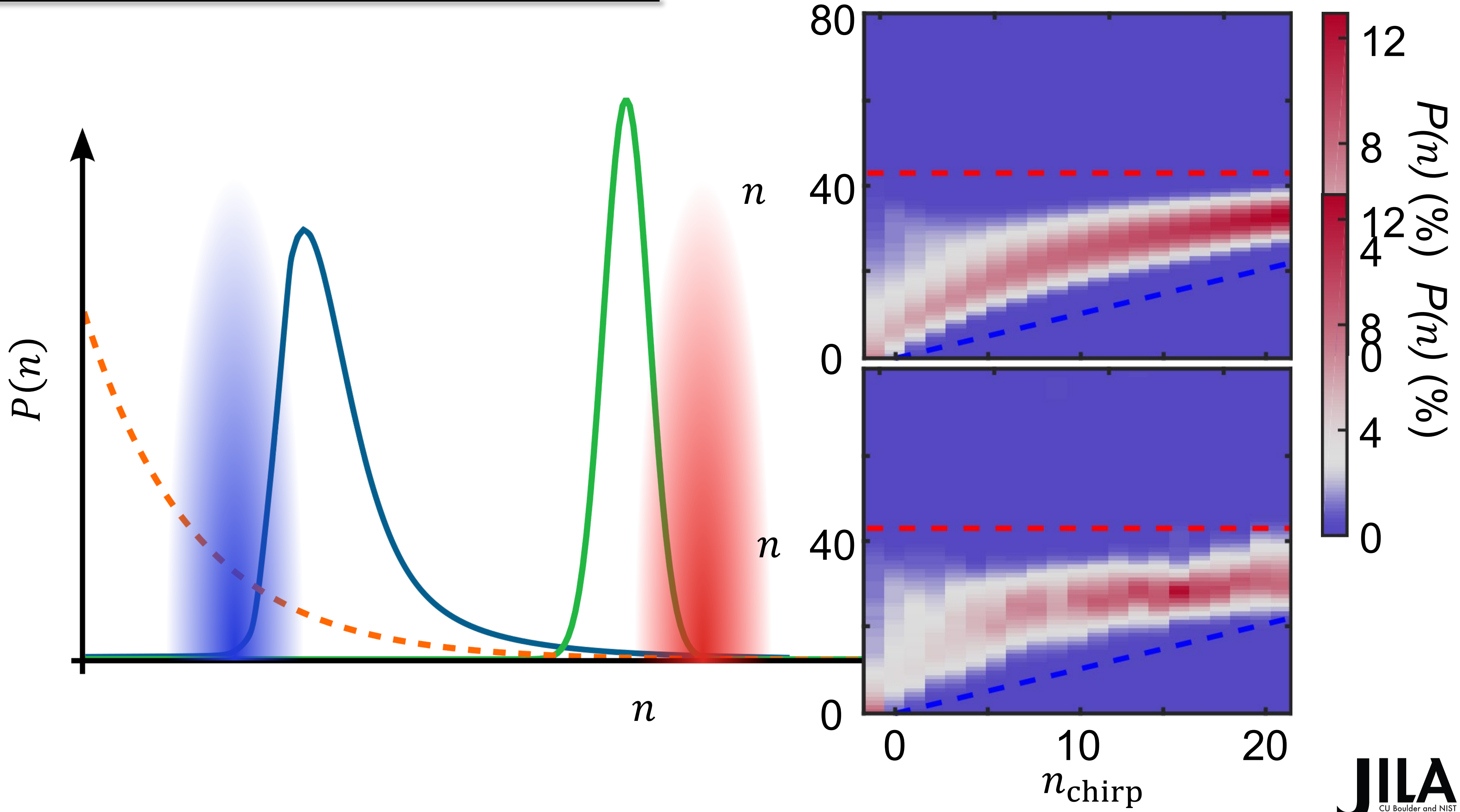

JILA
CU Boulder and NIST

Number squeezed state, dissipatively stabilized

Fano factor $F = \frac{\mathrm{var}(n)}{\langle n \rangle}$

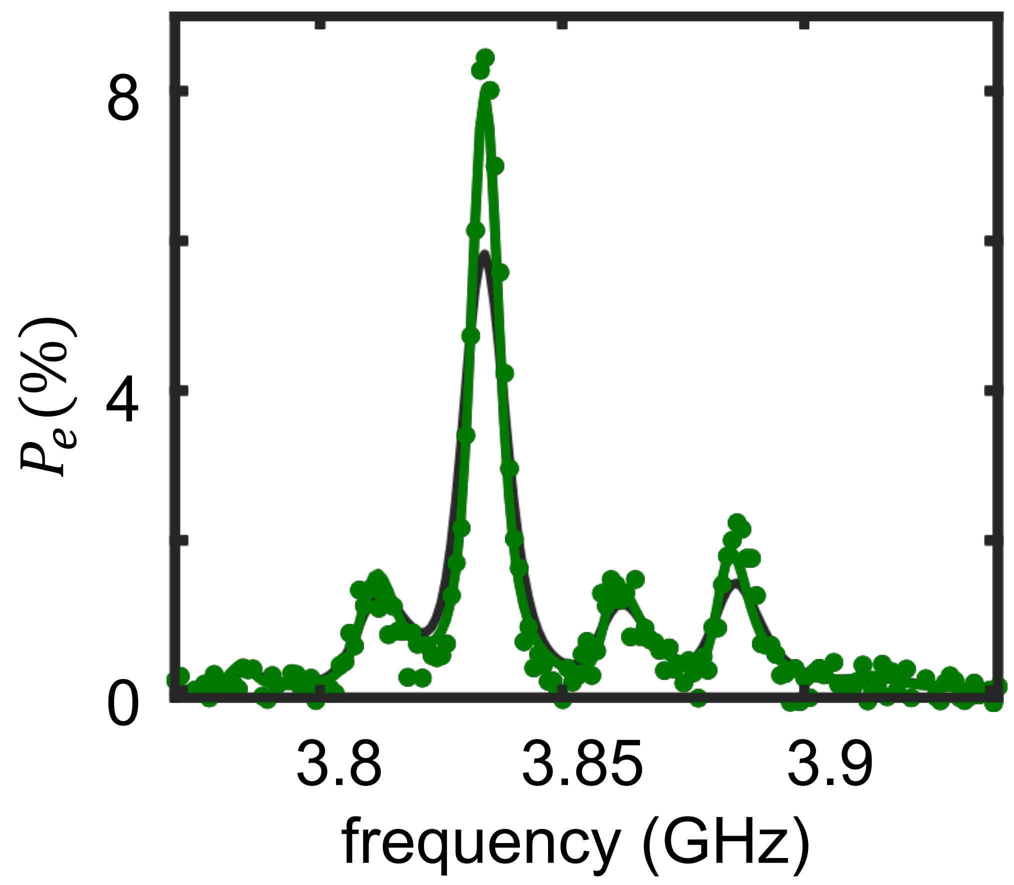

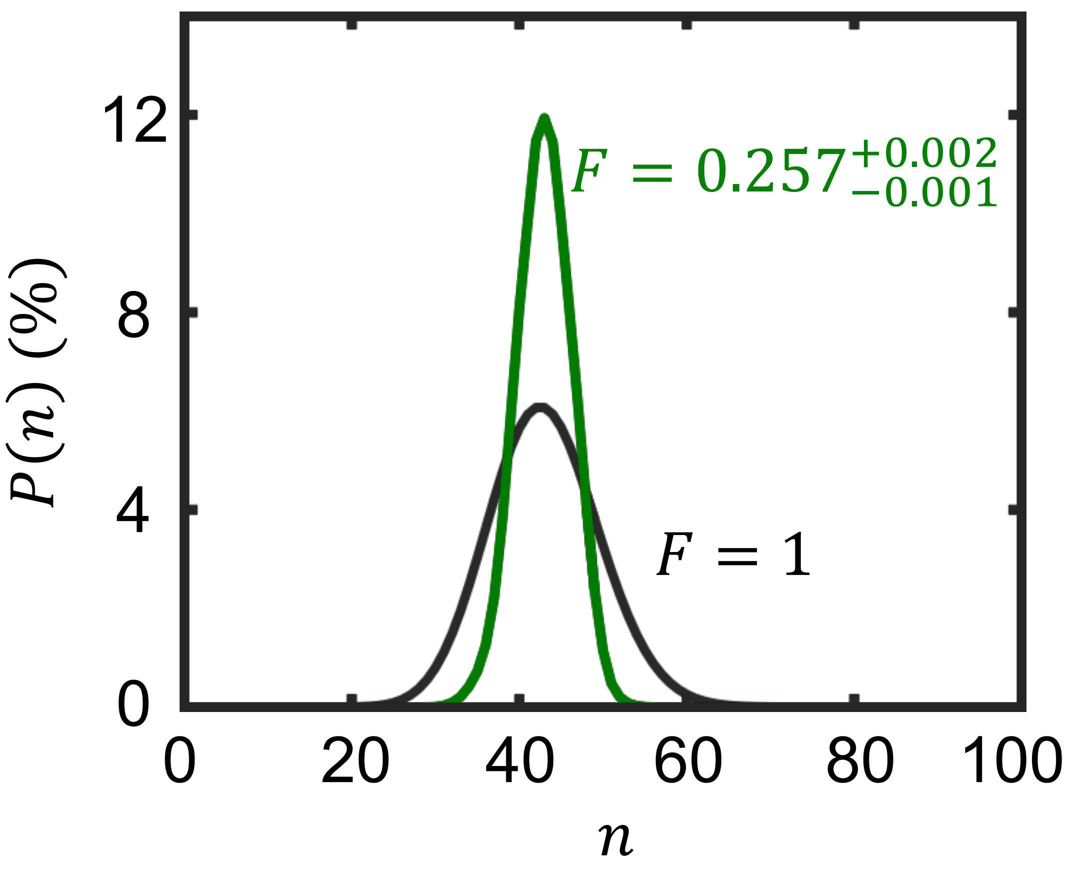

vibronic transitions in electromechanics

Qubit response to quantized motion

$$\omega_m(\sigma_z) = \sqrt{k(\sigma_z)/m} \approx \omega_m^0 + \sigma_z \chi_m$$

$$H_{\mathrm{eff}} = \frac{1}{2}\omega_{\mathrm{q}}\sigma_z + \frac{\hat{p}^2}{2m} + \frac{1}{2}k\hat{x}^2 + \frac{1}{2}k\left(\frac{2\chi_m}{\omega_m}\right)\sigma_z\hat{x}^2$$

$$\chi_m = 2\frac{g^2}{\omega_q} \approx 2\pi \times 260\ \mathrm{kHz}$$

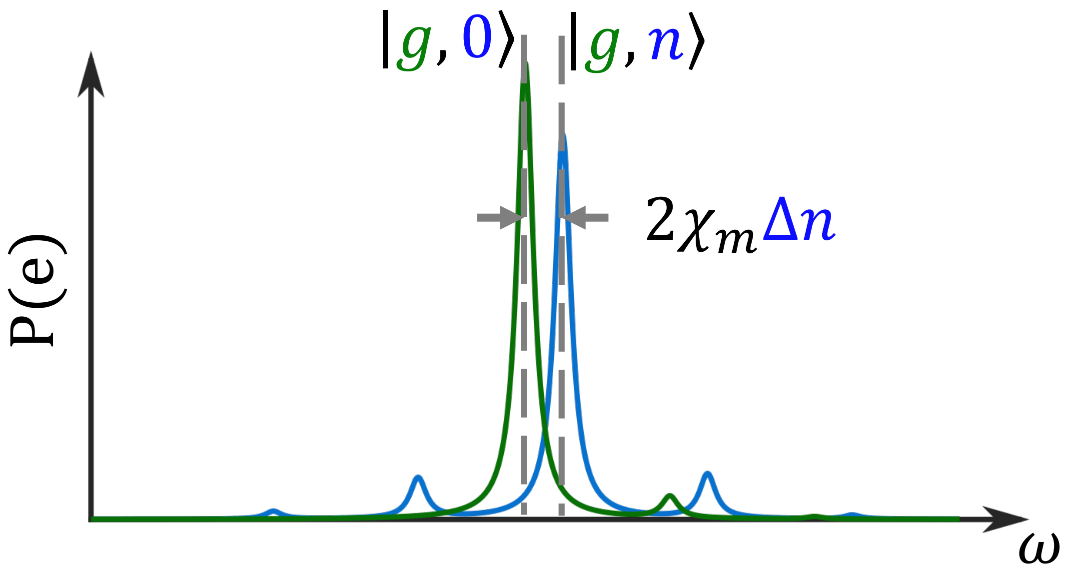

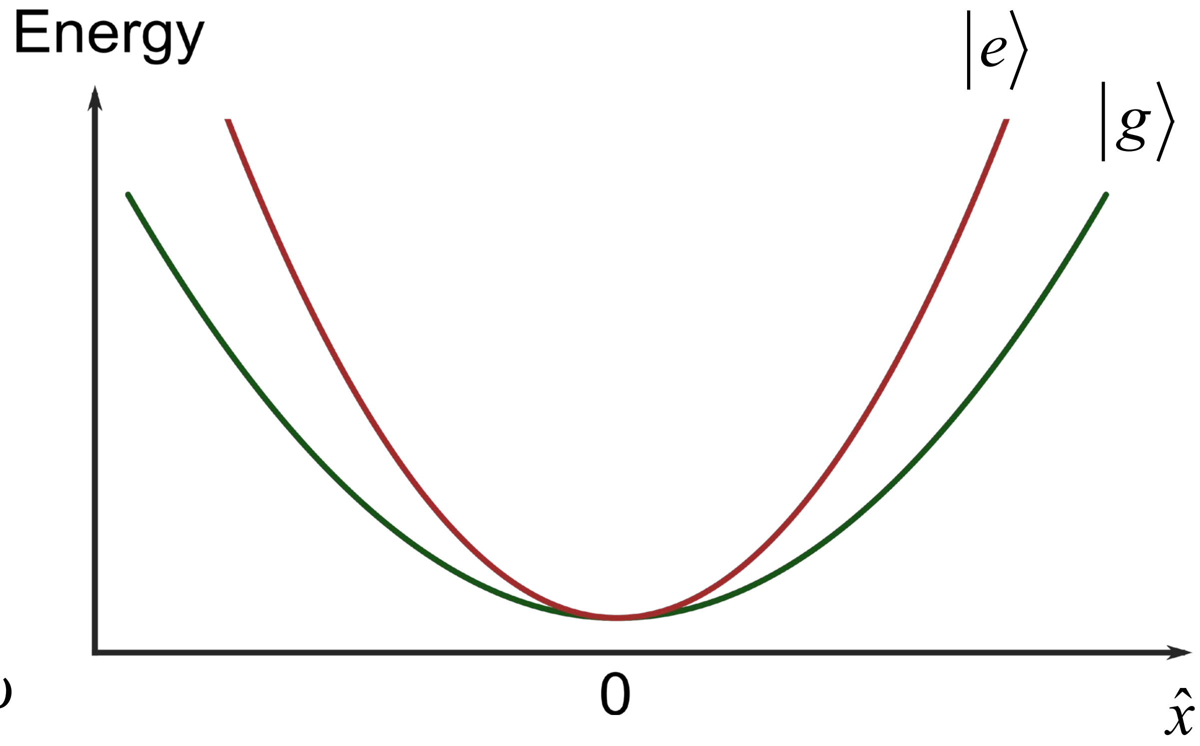

Qubit response to quantized motion

$$H_{\mathrm{eff}} = \frac{1}{2}\omega_{\mathrm{q}}\sigma_z + \frac{\hat{P}^2}{2m} + \frac{1}{2}k\hat{X}^2 + \frac{1}{2}k\left(\frac{2\chi_m}{\omega_m}\right)\sigma_z\hat{X}^2$$

$$\chi_m = 2\frac{g^2}{\omega_q} \approx 2\pi \times 260\ \mathrm{kHz}$$

$$\omega_m(\sigma_z) = \sqrt{k(\sigma_z)/m} \approx \omega_m^0 + \sigma_z\chi_m$$

$$Z_m(\sigma_z) = \sqrt{k(\sigma_z) \times m} = p_{zpf}/x_{zpf}$$

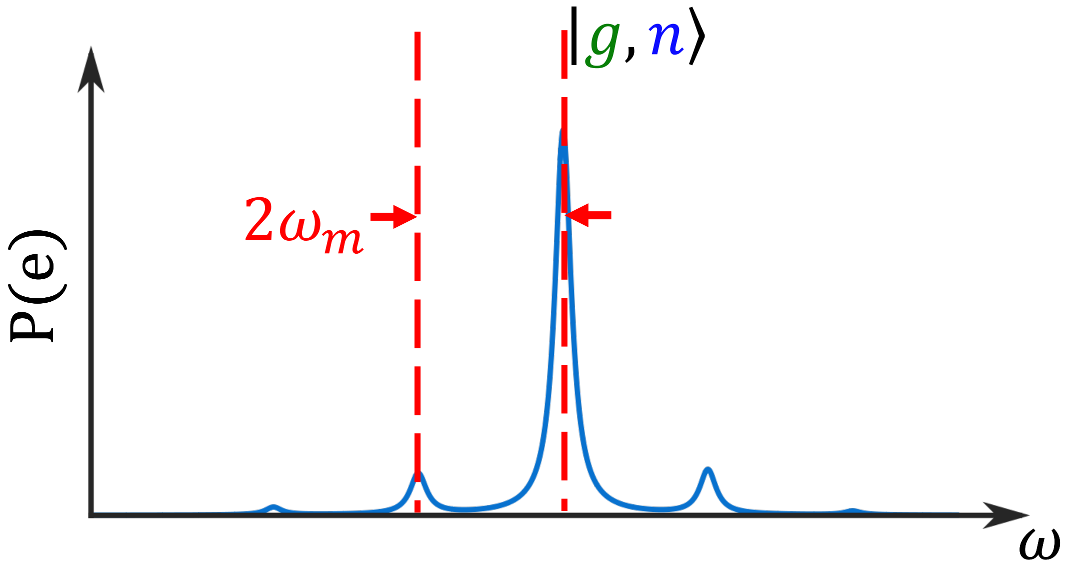

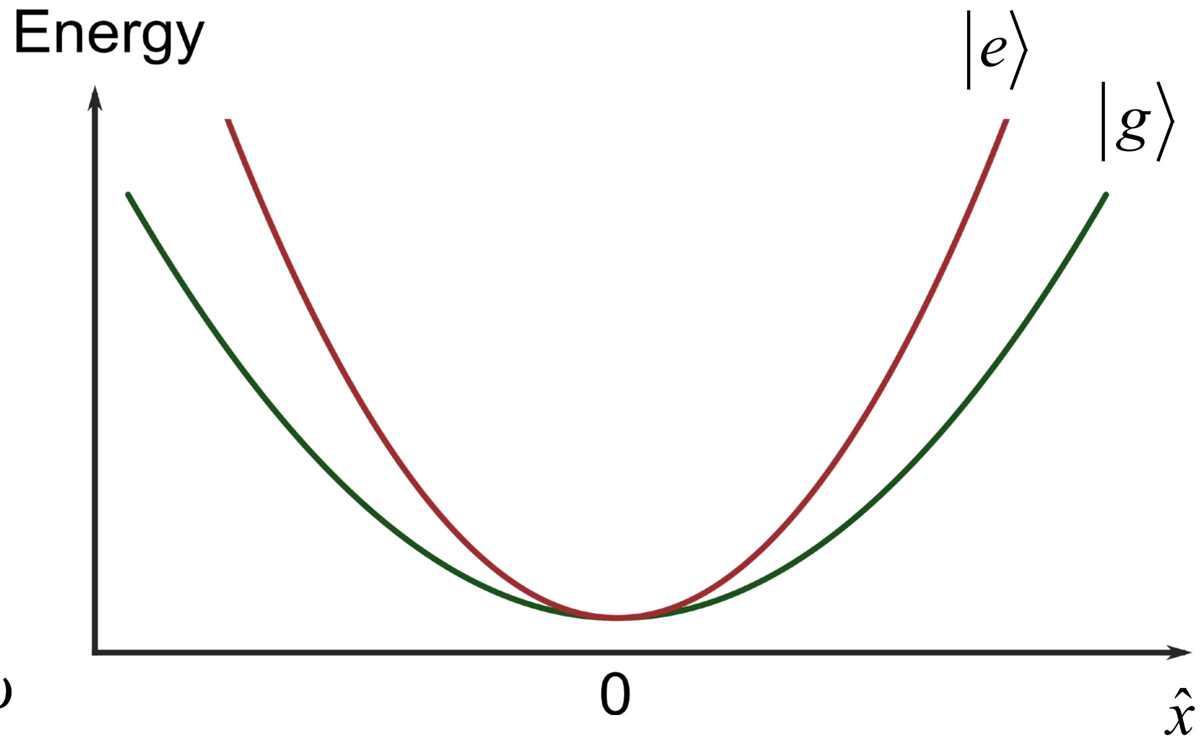

Qubit response to quantized motion

$$H_{\text{eff}} = \frac{1}{2}\omega_q\sigma_z + \frac{\hat{p}^2}{2m} + \frac{1}{2}k\hat{x}^2 + \frac{1}{2}k\left(\frac{2\chi_m}{\omega_m}\right)\sigma_z\hat{x}^2$$

$$\omega_m(\sigma_z) = \sqrt{k(\sigma_z)/m} \approx \omega_m^0 + \sigma_z\chi_m$$

$$Z_m(\sigma_z) = \sqrt{k(\sigma_z)\times m} = p_{zpf}/x_{zpf}$$

$$\chi_m = 2\frac{g^2}{\omega_q} \approx 2\pi \times 260\ \text{kHz}$$

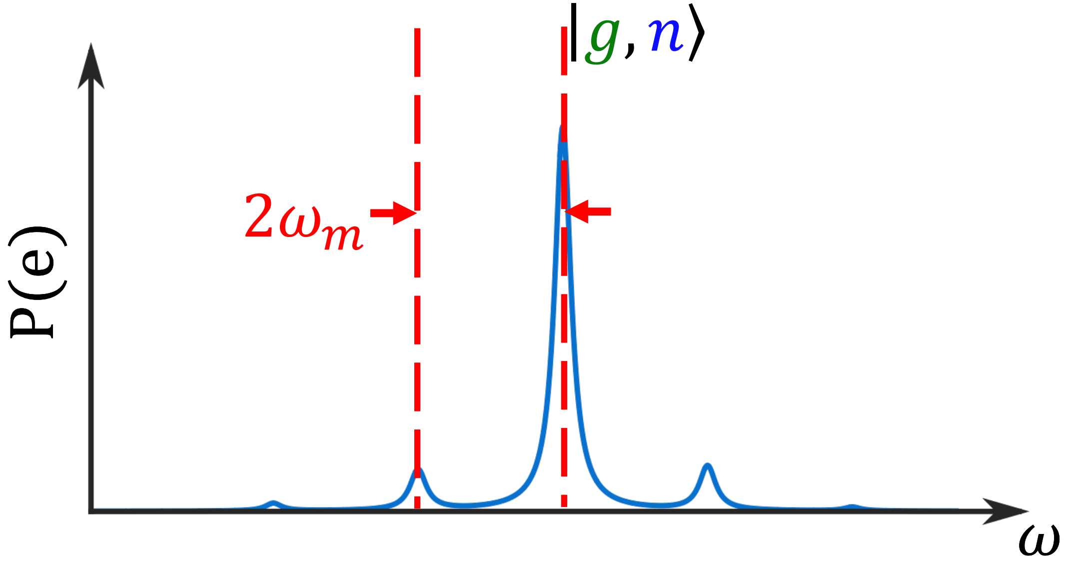

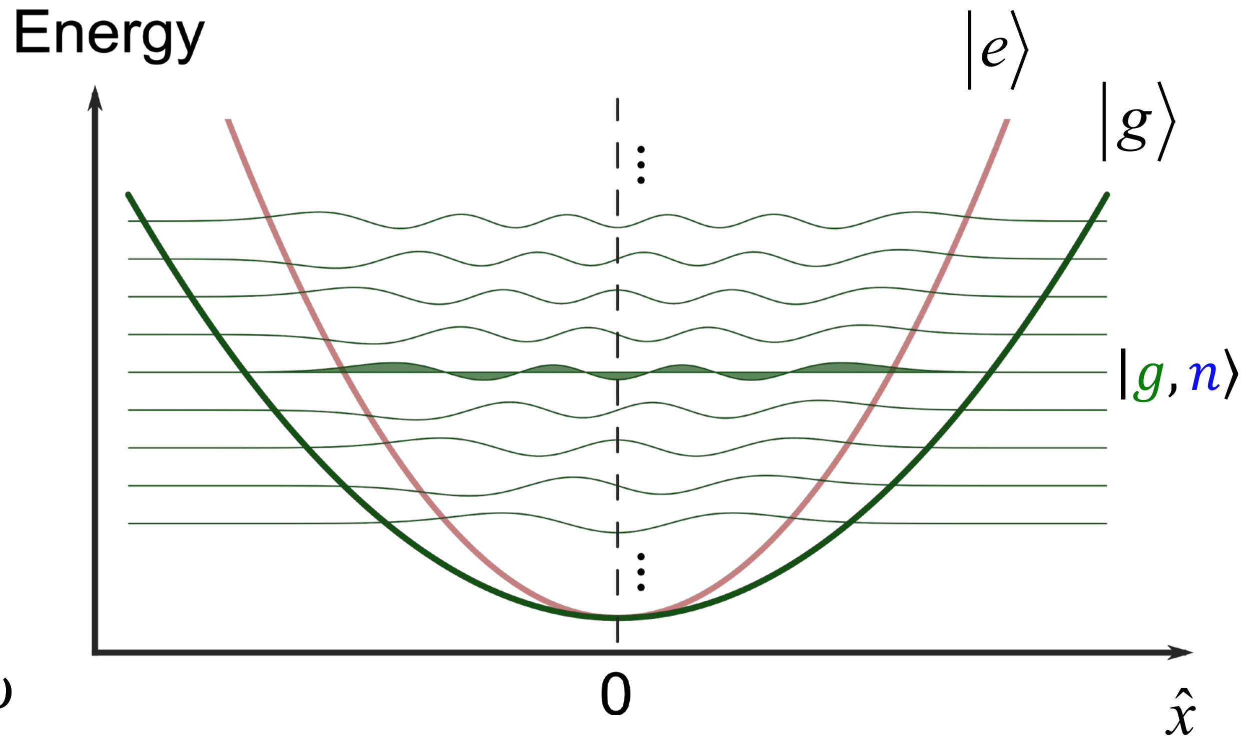

Qubit response to quantized motion

$$H_{\text{eff}} = \frac{1}{2}\omega_q\sigma_z + \frac{\hat{p}^2}{2m} + \frac{1}{2}k\hat{x}^2 + \frac{1}{2}k\left(\frac{2\chi_m}{\omega_m}\right)\sigma_z\hat{x}^2$$

$$\chi_m = 2\frac{g^2}{\omega_q} \approx 2\pi \times 260\ \text{kHz}$$

$$\omega_m(\sigma_z) = \sqrt{k(\sigma_z)/m} \approx \omega_m^0 + \sigma_z\chi_m$$

$$Z_m(\sigma_z) = \sqrt{k(\sigma_z) \times m} = p_{zpf}/x_{zpf}$$

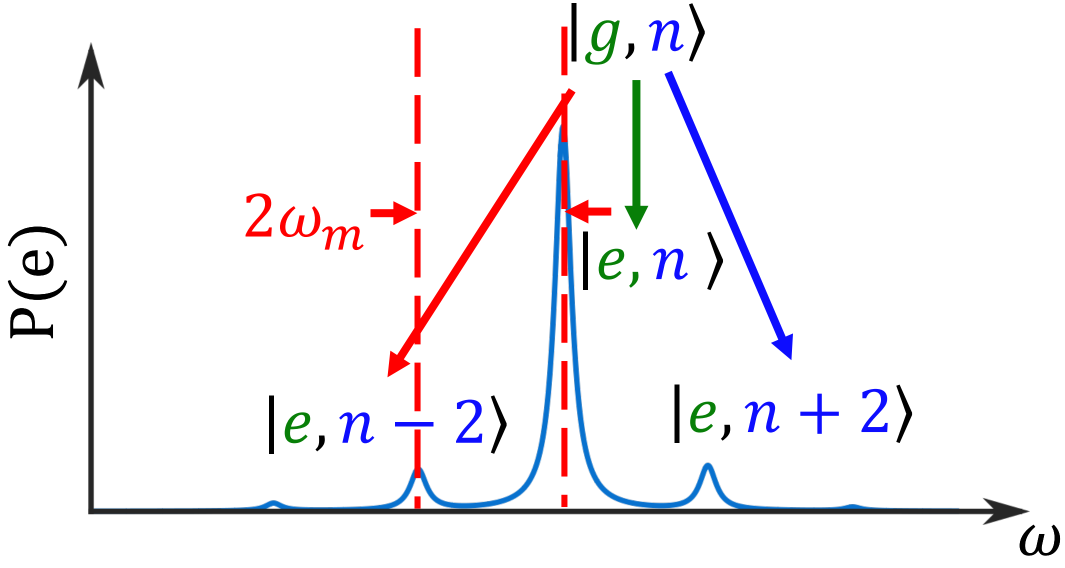

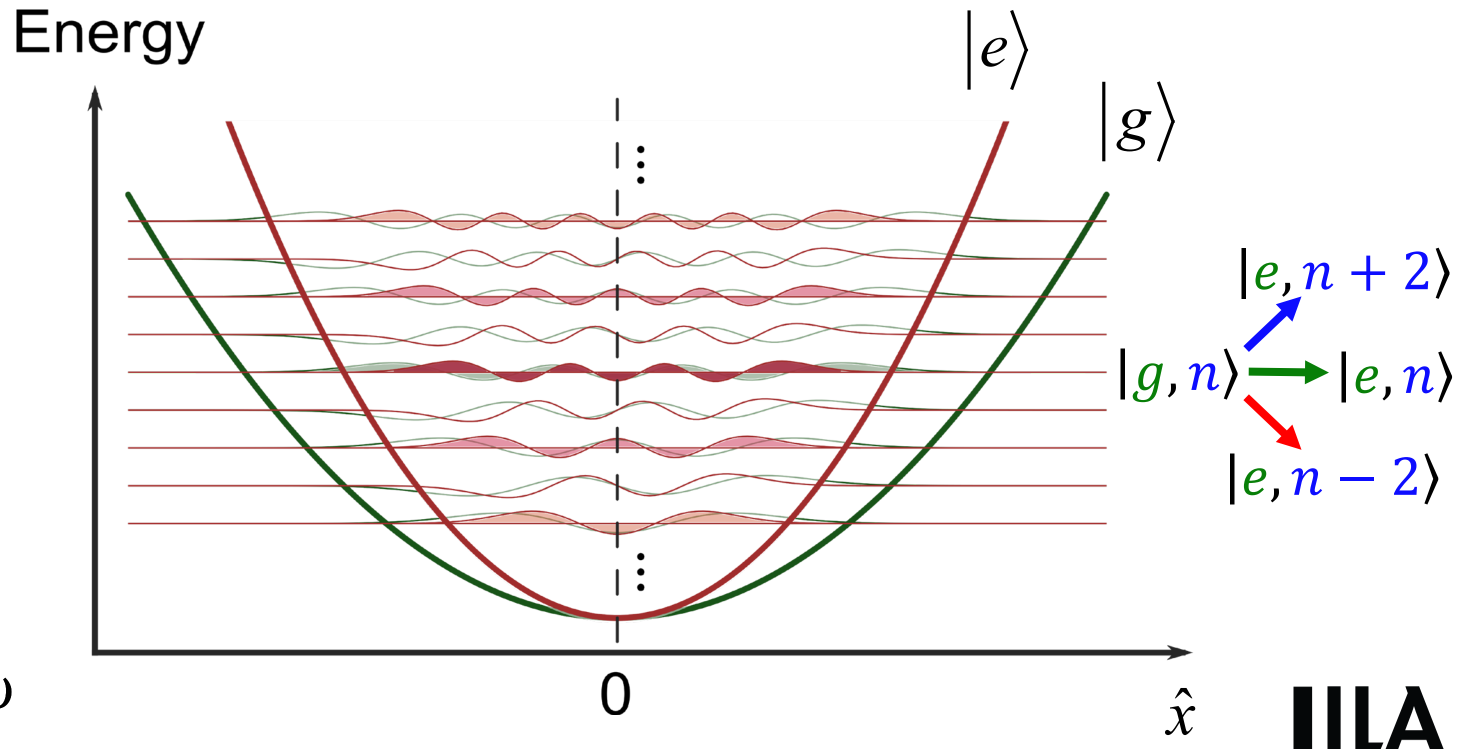

Qubit spectrum acquires vibronic sidebands

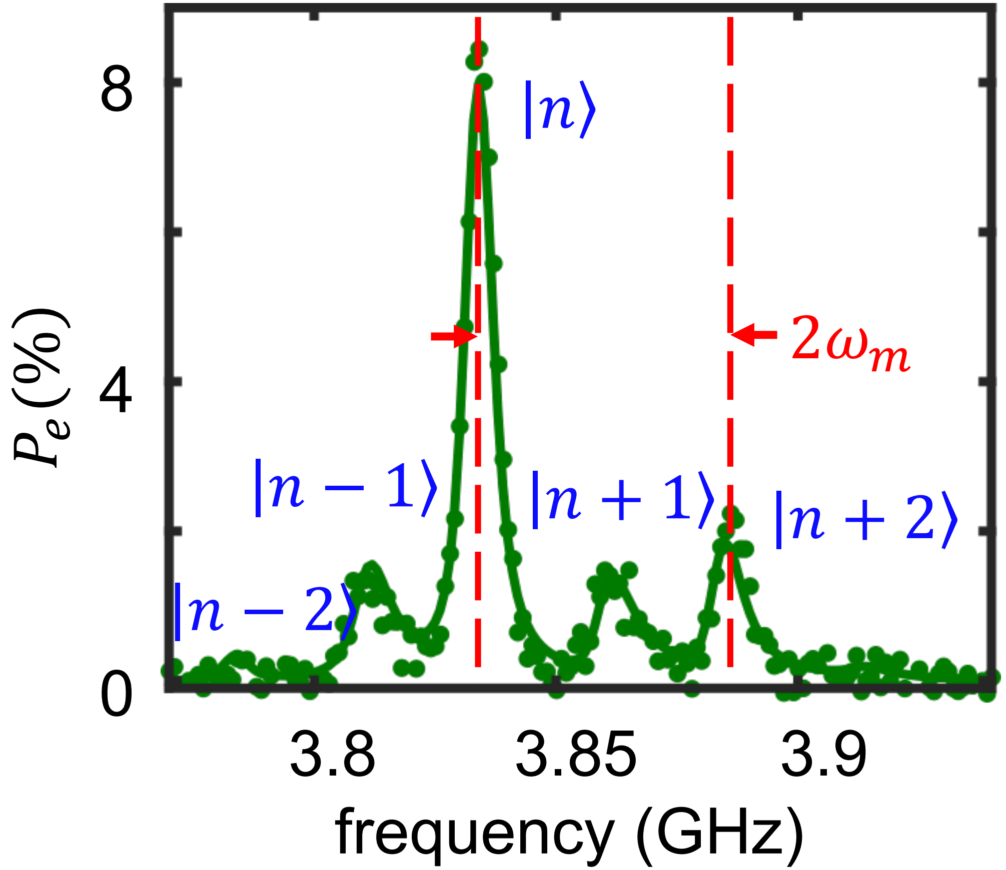

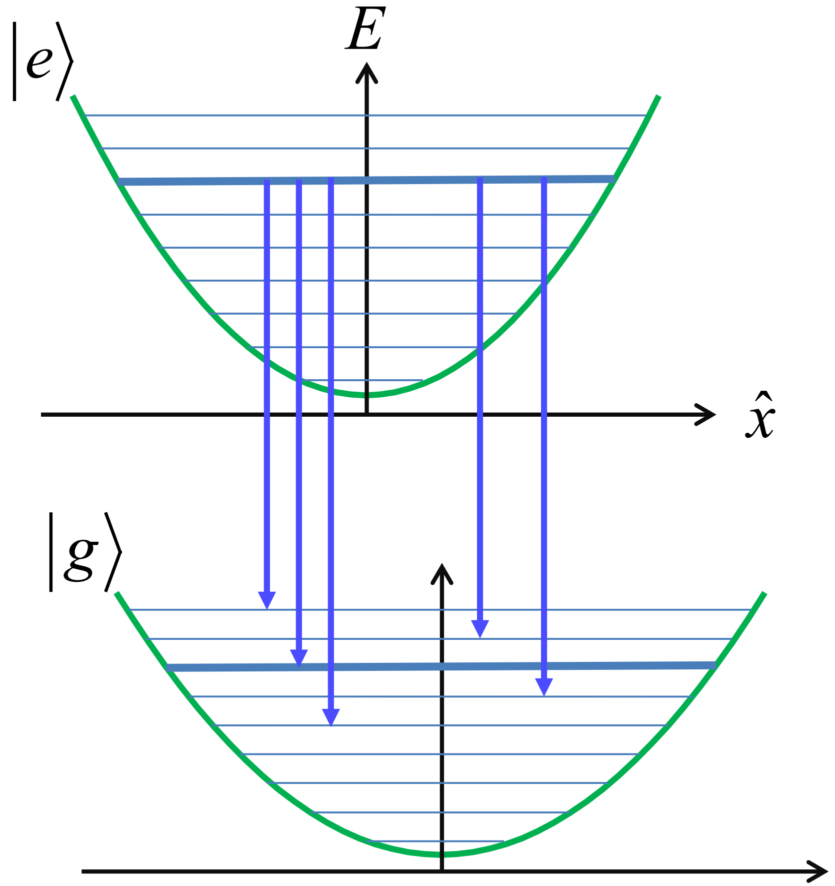

resolving the mechanical recoil of a qubit transition: Franck – Condon physics

from artificial atoms to artificial molecules

Overcoming small vacuum electromechanical coupling

apply static voltage

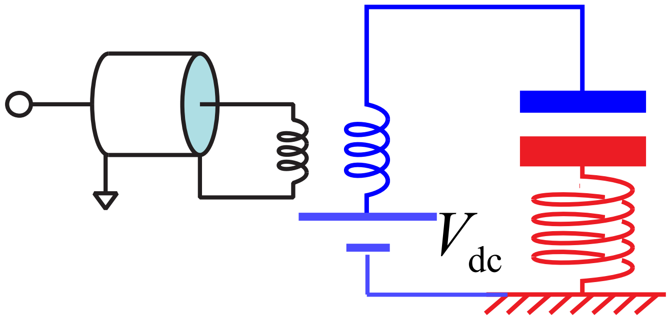

or

use piezo-electric coupling

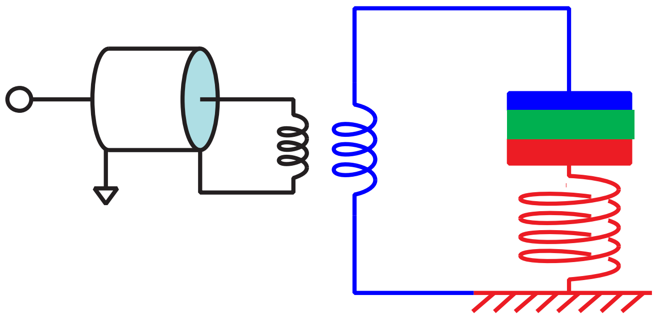

$$H_I = g_0\left(a + a^\dagger\right)\left(b + b^\dagger\right)$$

$$g_0 \approx 2\pi \times 10\ \mathrm{MHz}$$

add electrical non-linearity

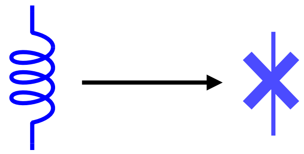

superconducting qubit
coupled mechanics

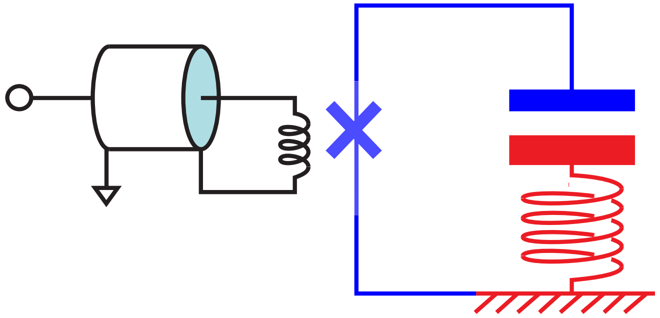

$$H_I = g_0 \sigma_x \left(b + b^\dagger\right)$$

JILA CU Boulder and NIST

accessing single phonons with piezomechanics

Transmon qubit: a strongly nonlinear LC circuit

$$H = \frac{\Phi^2}{2L} + \frac{Q^2}{2C}$$

$$H = \frac{E_J}{2}\left(1 - \cos\left(2\pi\frac{\Phi}{\Phi_0}\right)\right) + \frac{Q^2}{2C}$$

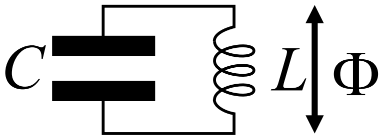

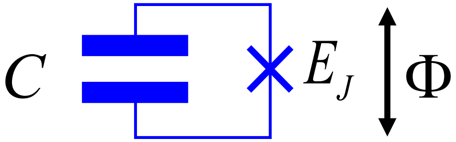

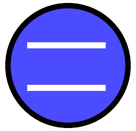

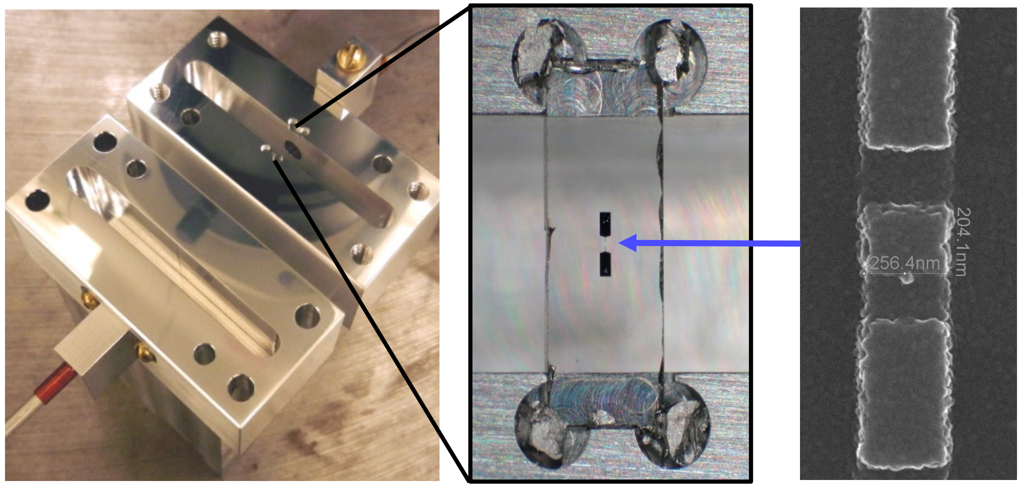

Al cavity

Al antenna
on sapphire

Al/AlOx/Al
Josephson junction

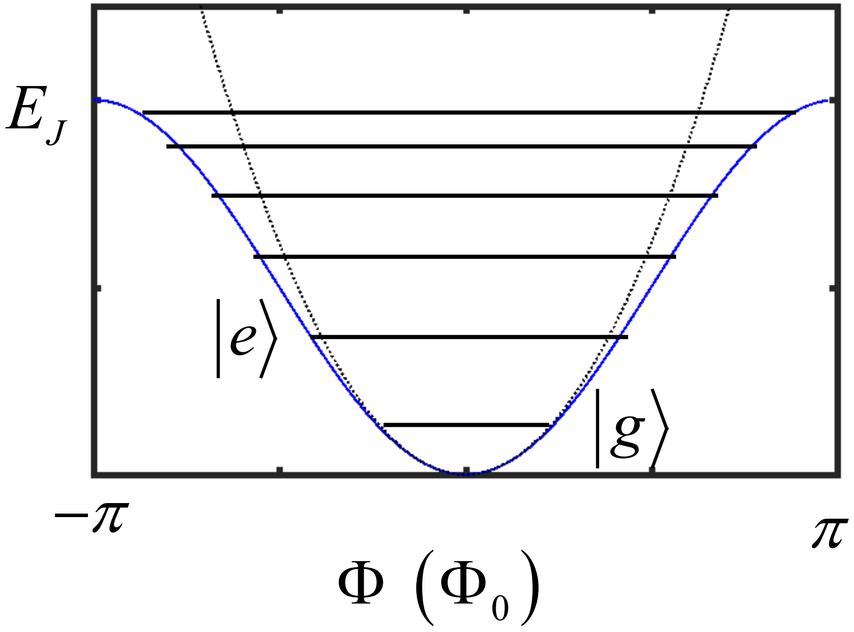

JILA
CU Boulder and NIST

Circuit quantum acoustodynamics (CQAD): Superconducting qubits and piezo-electric materials

strong resonant coupling (qutons and phonbits) $g_0 > \max[\kappa, \gamma]$

bulk waves

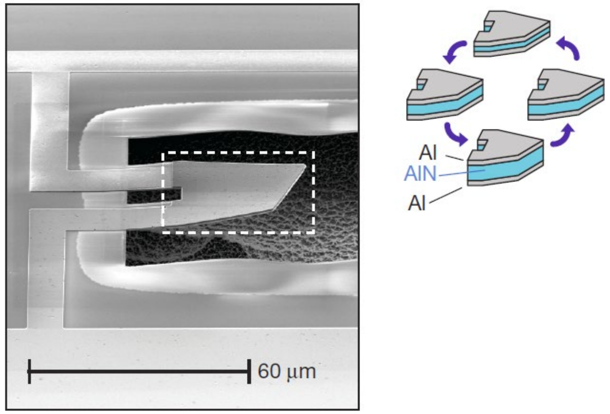

A. O'Connell, A. Cleland
UCSB, 2011

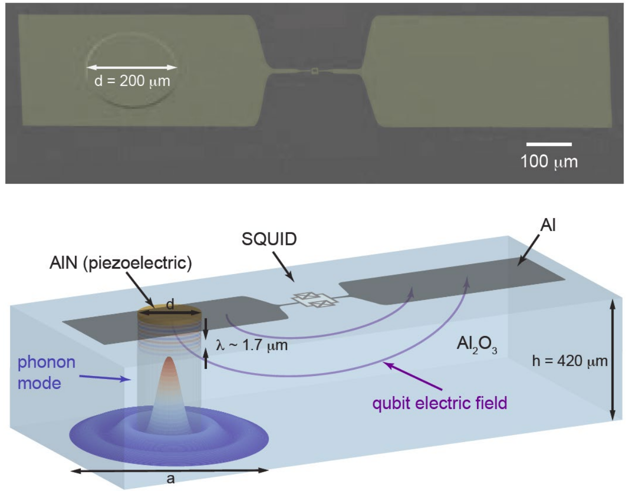

Y. Chu, R. Schoelkopf
Yale, 2017

surface waves

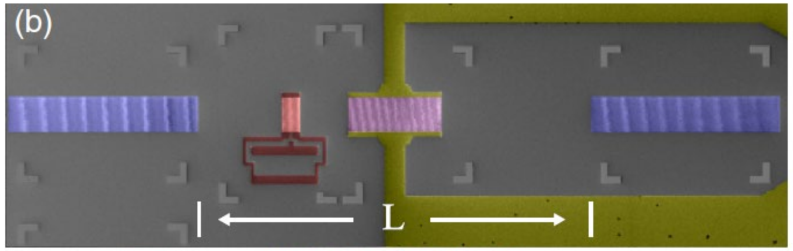

B. Moores, KWL,
JILA, 2018

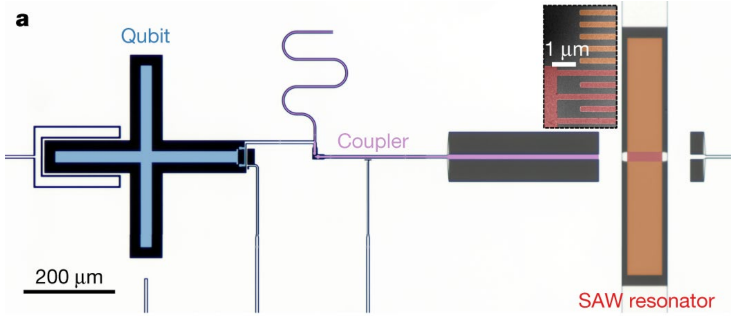

K. Satzinger, A. Cleland
Chicago, 2018

Count phonons in the dispersive limit of CQAD

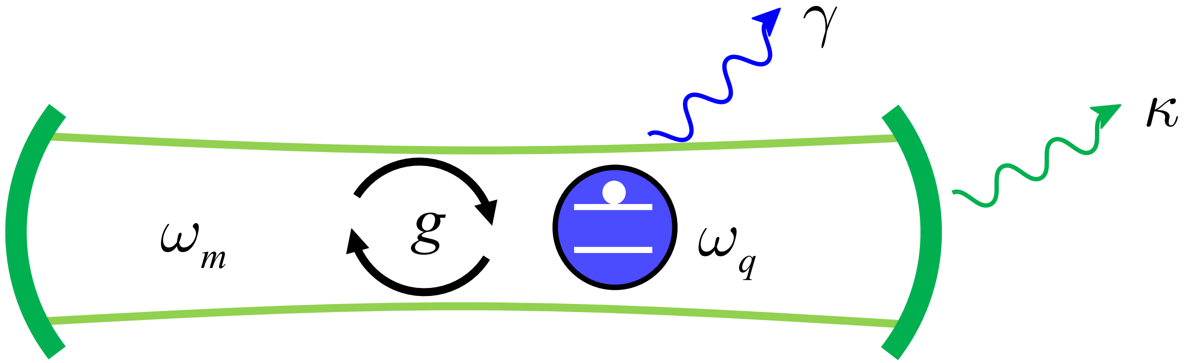

$$\hat{H}/\hbar \approx \frac{1}{2}\omega_q\hat{\sigma}_z + \omega_m\hat{b}^\dagger\hat{b} + g_0\hat{\sigma}_x\left(\hat{b}^\dagger + \hat{b}\right)$$

dispersive limit $\quad \omega_q - \omega_m = \Delta \gg g$

$$\hat{H}/\hbar \approx \frac{1}{2}\omega_q\hat{\sigma}_z + \omega_m\hat{b}^\dagger\hat{b} + \chi\hat{\sigma}_z\hat{b}^\dagger\hat{b} \qquad \chi = \frac{g^2}{\Delta}$$

resolve single phonon acoustical Stark shift

$$\chi > \max[\kappa, \gamma]$$

JILA
CU Boulder and NIST

SAW waves confined between mirrors form multimode cavities

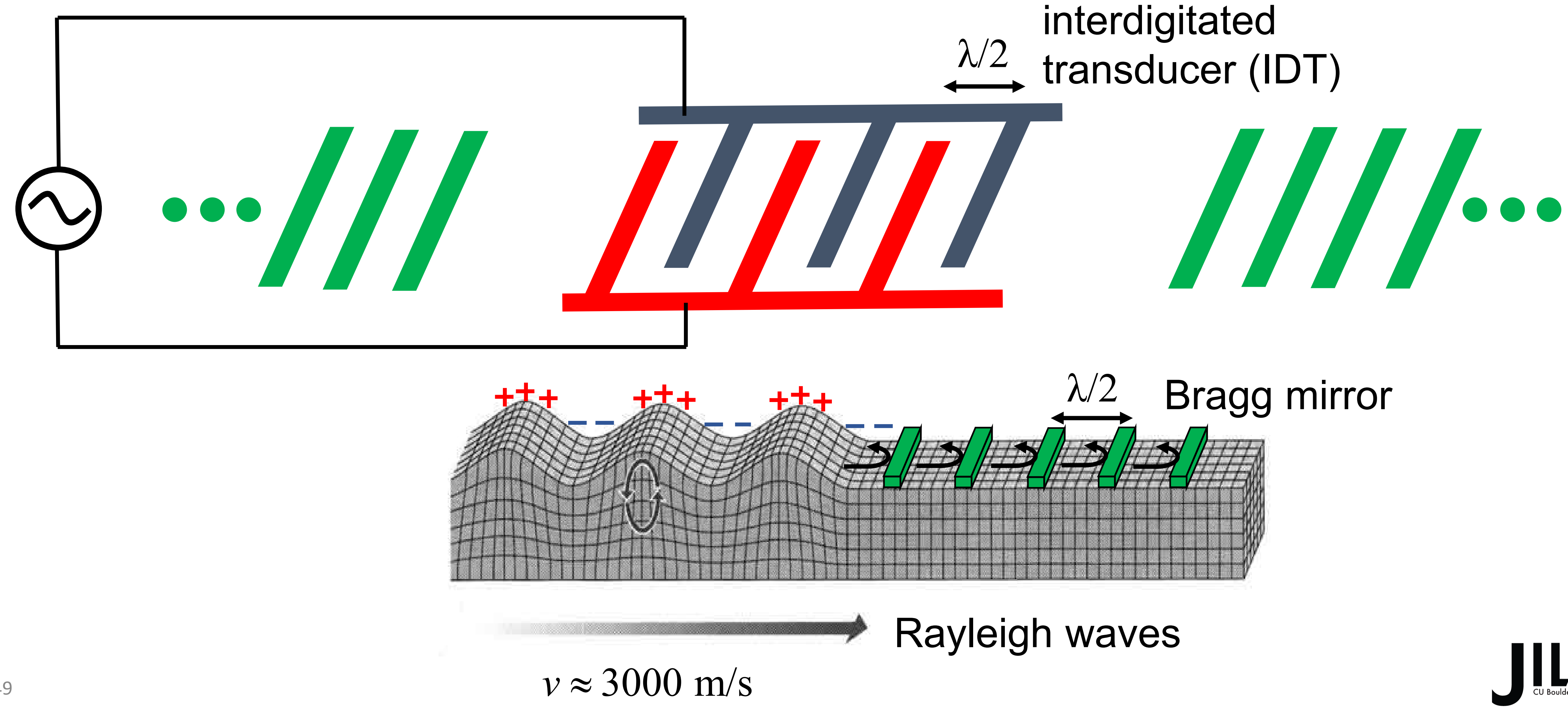

JILA
CU Boulder and NIST

Split finger transducers launch SAWs without reflecting them

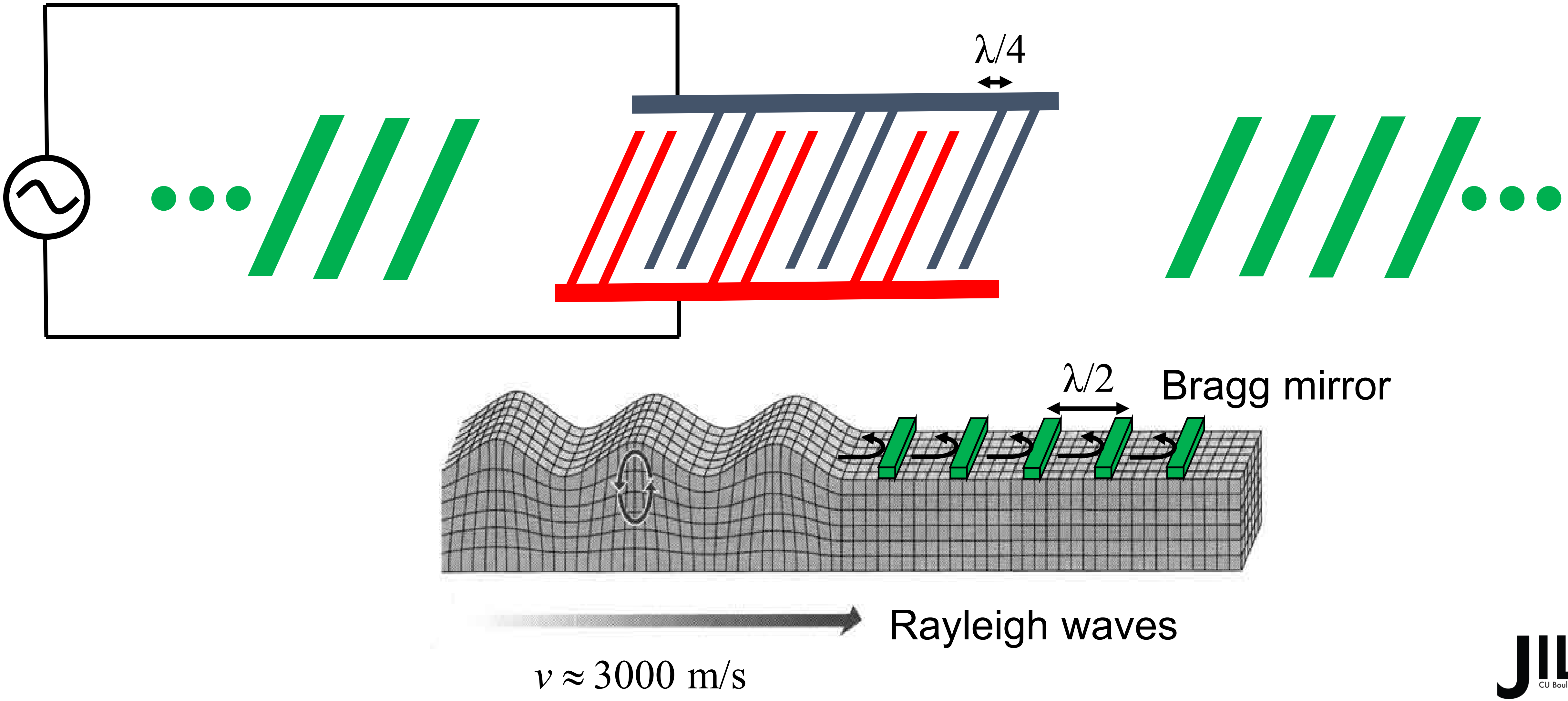

Transmon qubit coupled piezoelectrically to multimode SAW cavity in GaAs

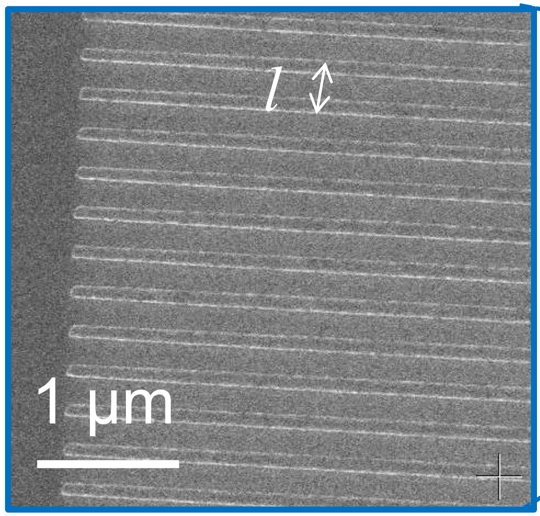

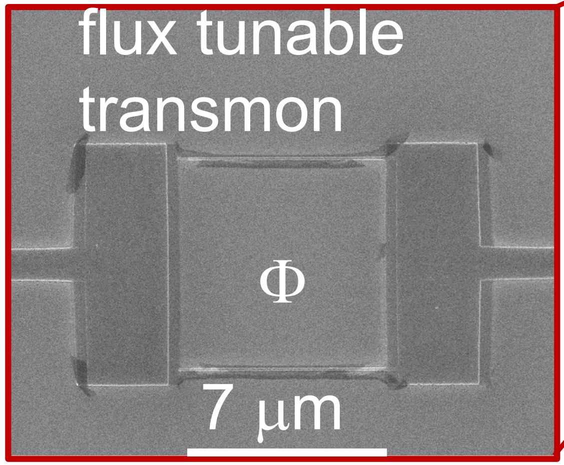

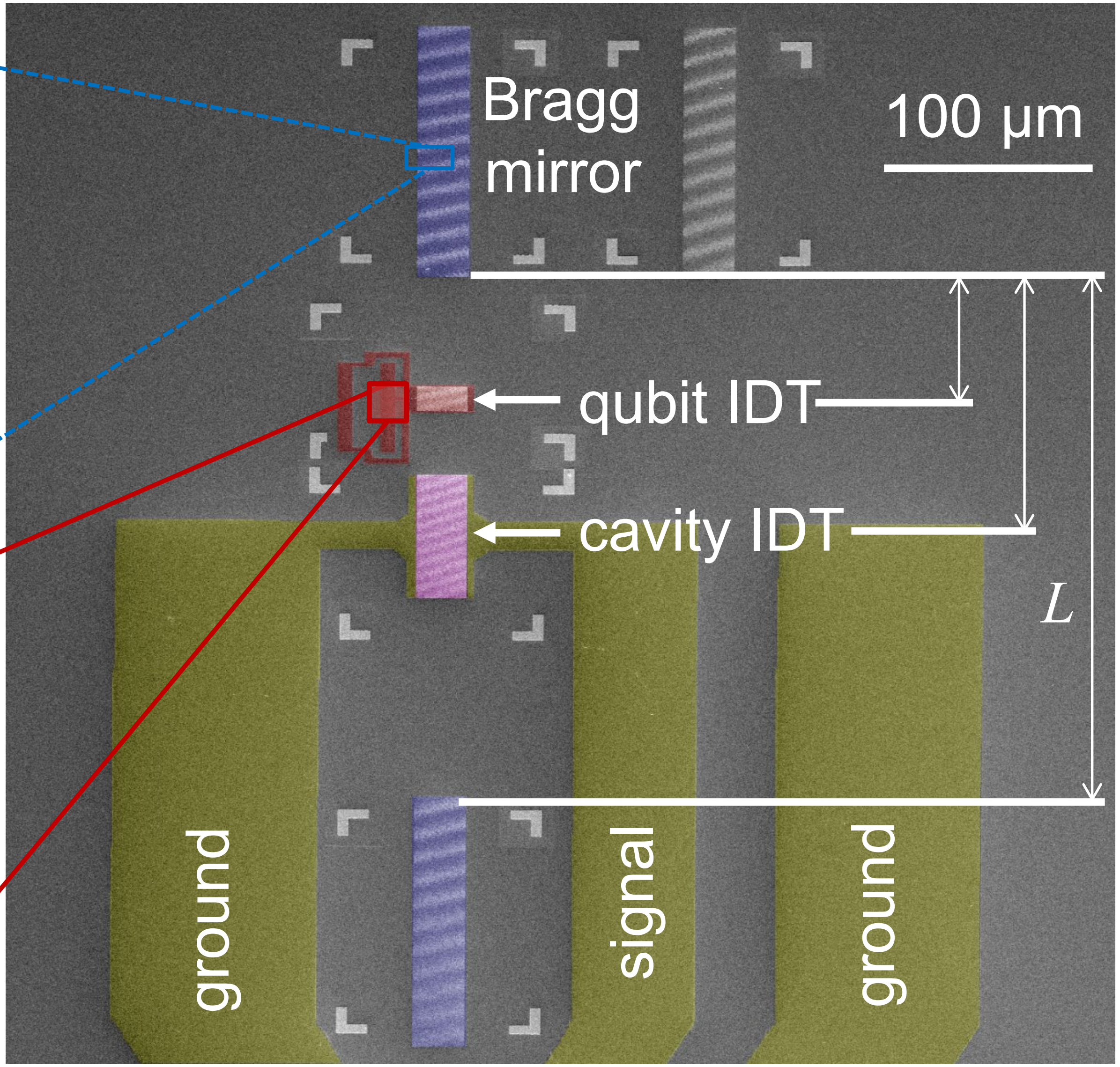

$L = 400\ \mu\mathrm{m}$

FSR: 4.8 MHz

$l = 380\ \mathrm{nm}$

$\omega_{cav} \approx 2\pi \times 4.25\ \mathrm{GHz}$

mirror bandwidth
50 MHz

JILA CU Boulder and NIST

All acoustical measurement and control of qubit

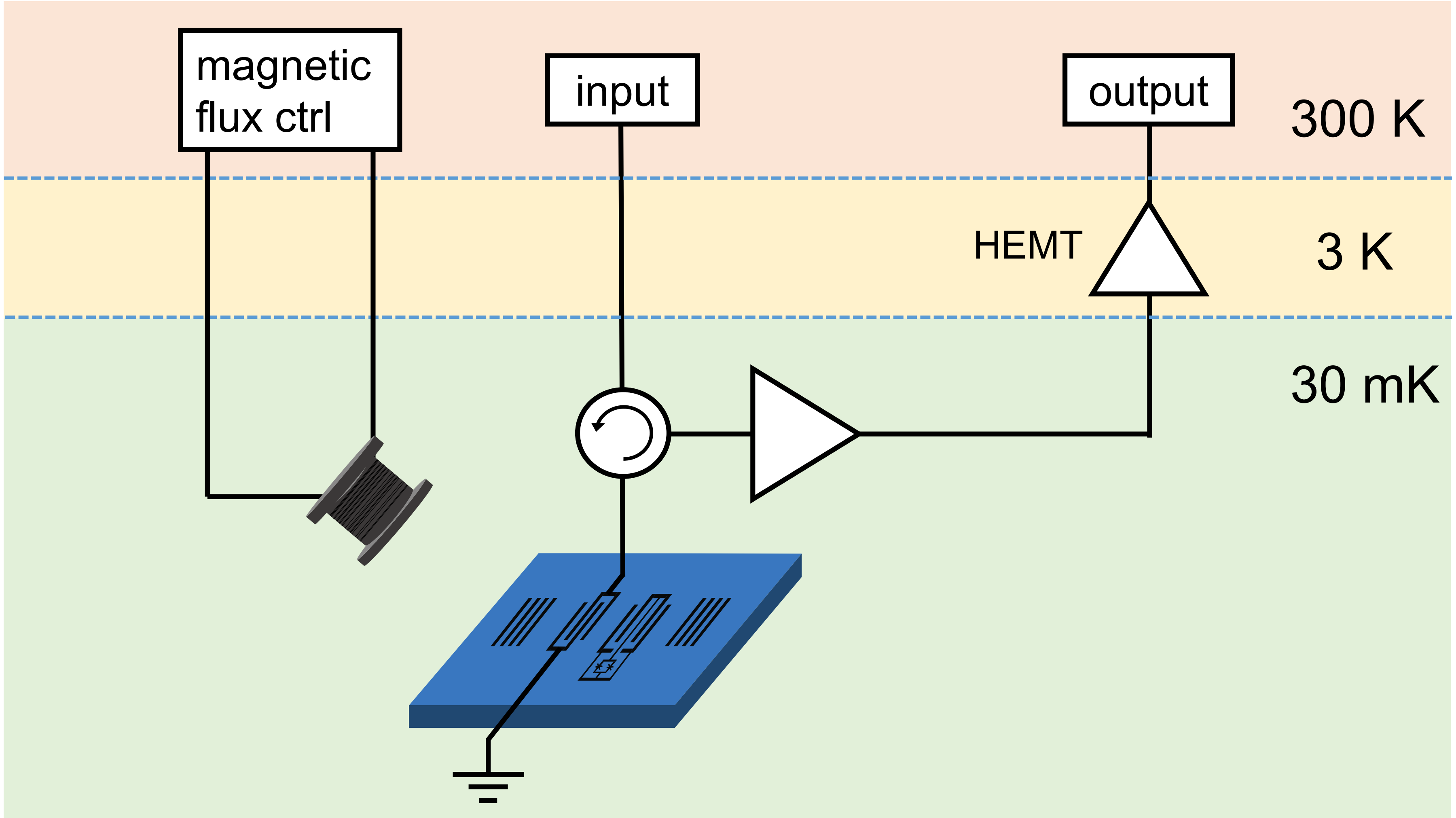

measure SAW cavity reflection

Cavity reflection reveals spectrum of high-Q longitudinal SAW mode

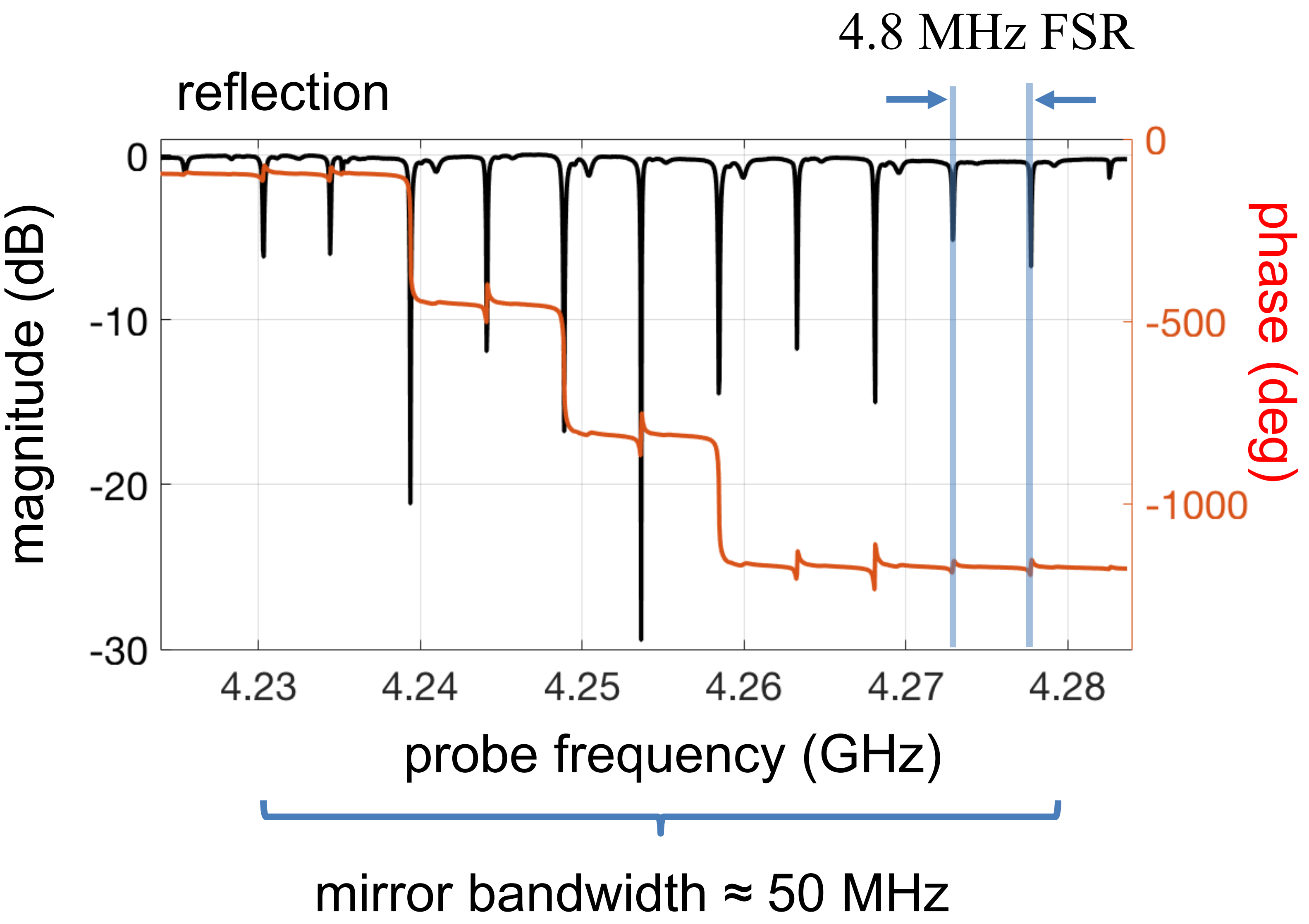

$\kappa \approx 2\pi \times 100$ kHz

CQAD system in the strong multimode regime

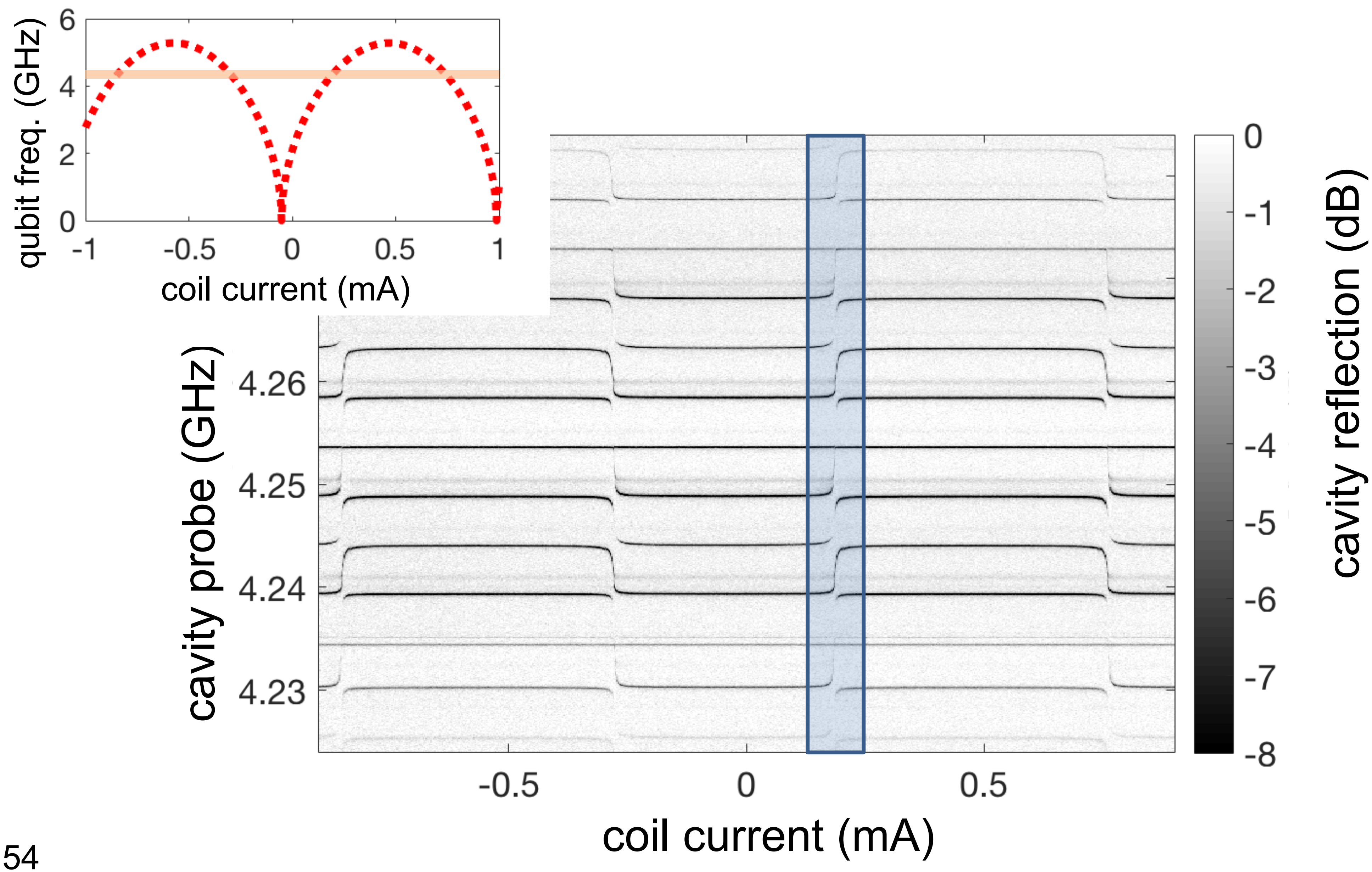

Qubit-cavity avoided crossing show coherent coupling

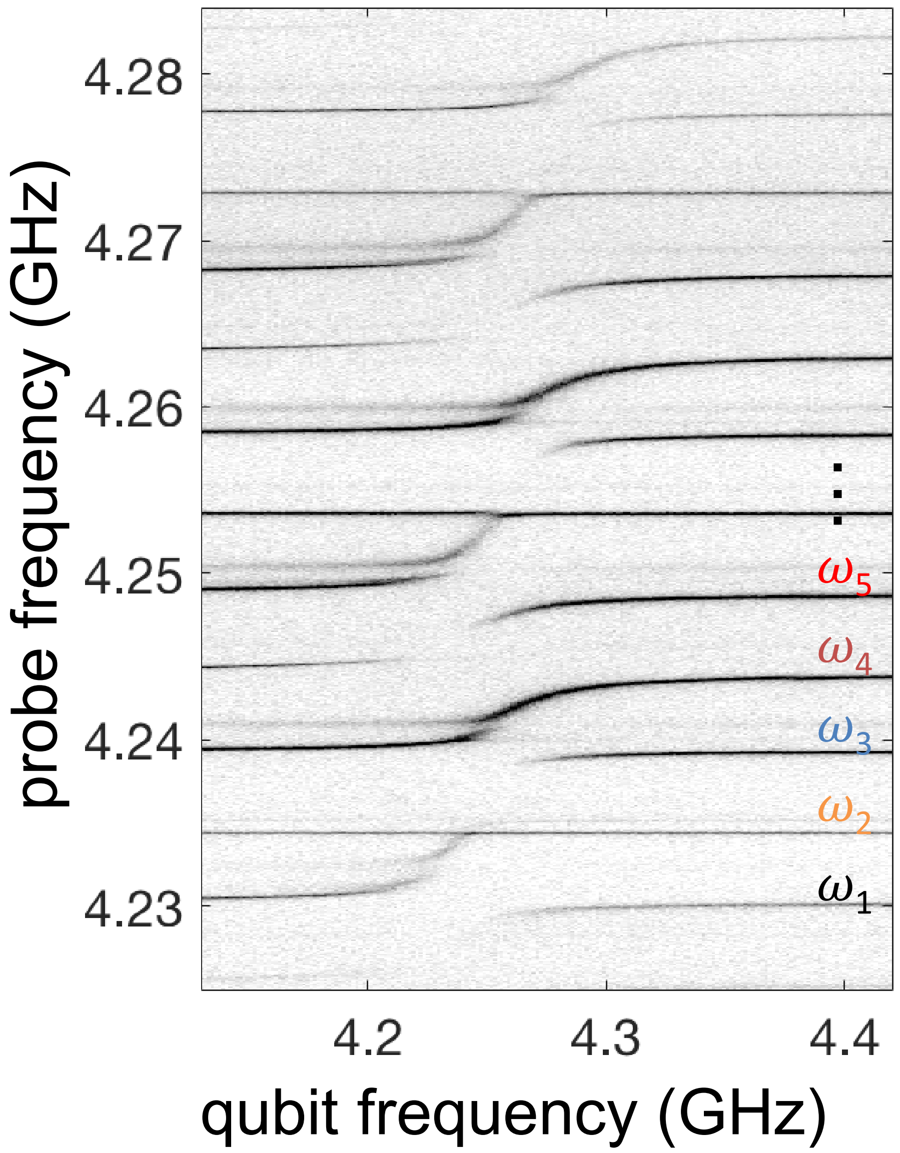

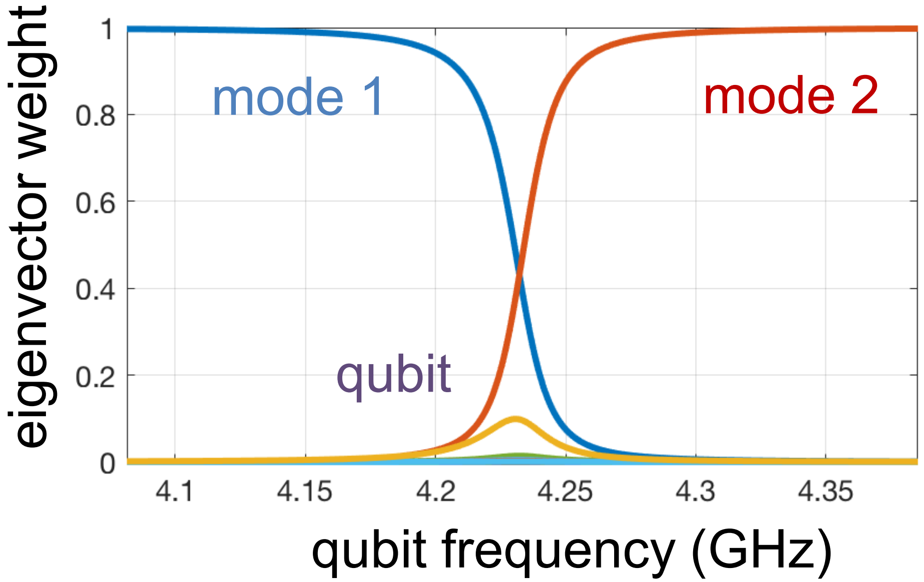

strong coupling limit:

$$g_0 \approx 2\pi \times 6.5\ \mathrm{MHz}$$

$$g_0 > \max(\kappa, \gamma)$$

multimode limit:

$$g_0 > \omega_{\mathrm{fsr}}$$

intrinsic qubit linewidth:

$$\frac{\gamma}{2\pi} = 1.1\ \mathrm{MHz}$$

B. A. Moores, L. R. Sletten, J. J. Viennot, KWL, *PRL* (2018)

JILA CU Boulder and NIST

Dense acoustical modes: too much of good thing?

strong dispersive limit

$$g_m \ll \Delta_m \qquad \chi_m = \frac{g_m{}^2}{\Delta_m} \gg \kappa_m$$

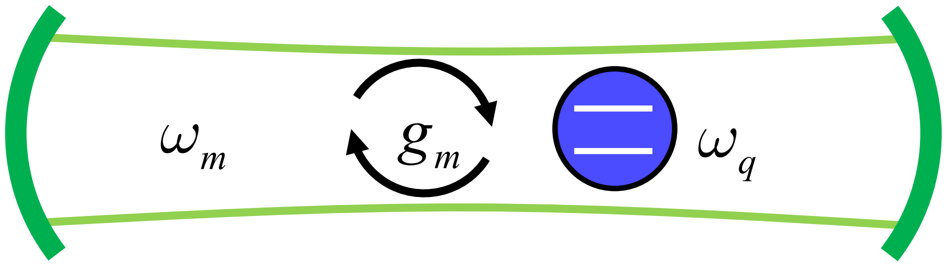

uniform coupling

$$g_m \ll \omega_{\text{fsr}}$$

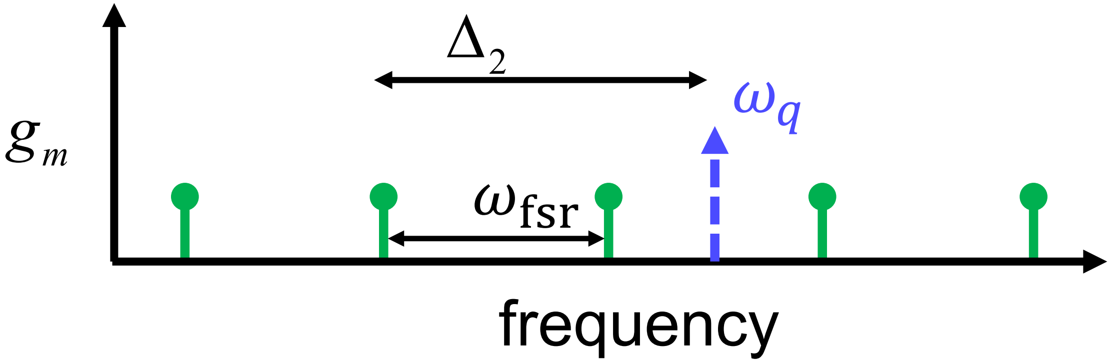

frequency-sensitive coupling

$$g_m = \frac{\Delta_m}{10}$$

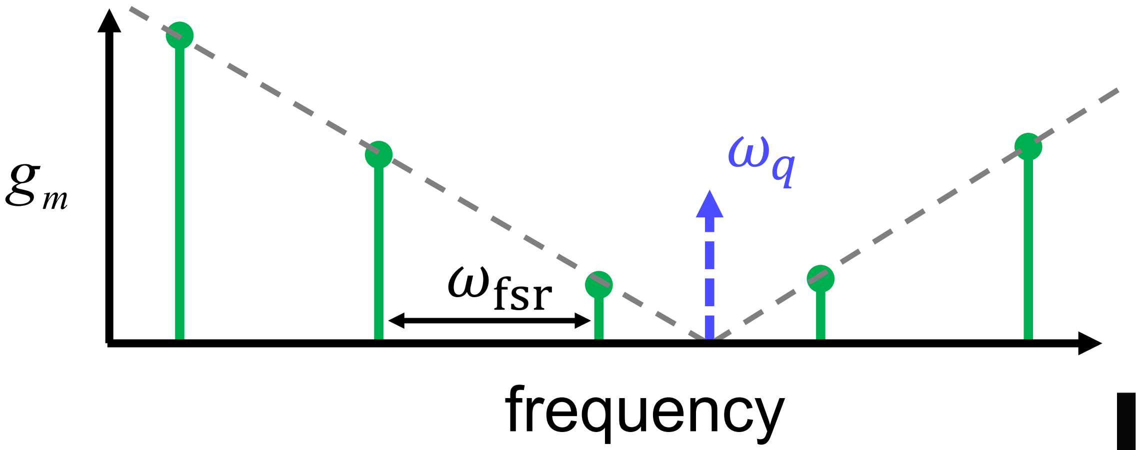

JILA
CU Boulder and NIST

Acoustical Ramsey interferometric coupling

space

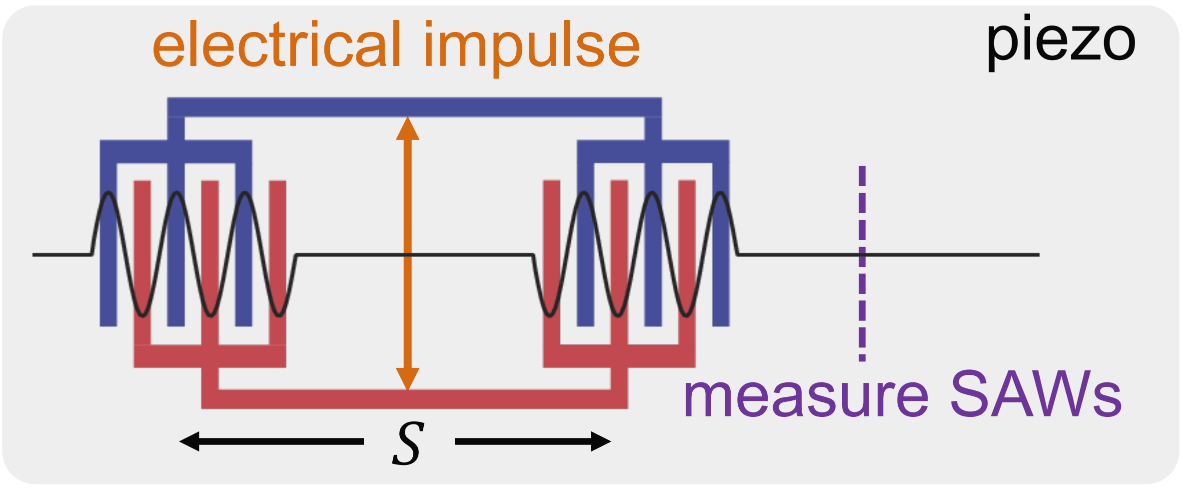

split IDT:
double-slit diffraction

frequency domain control
via IDT geometry

time

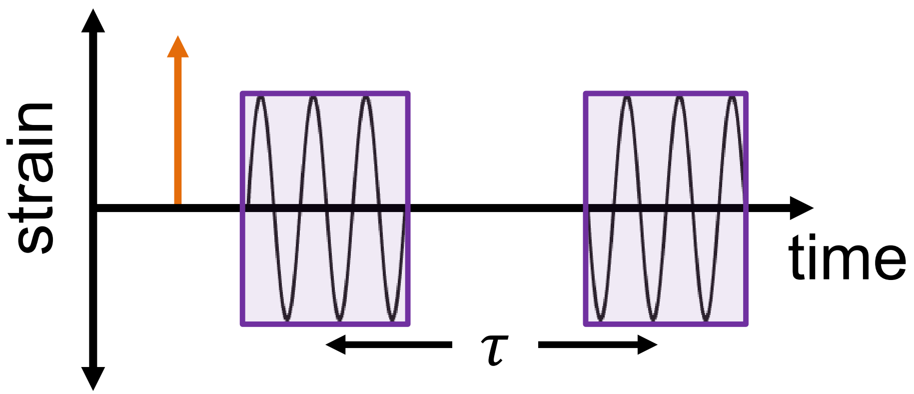

Fourier transform

frequency

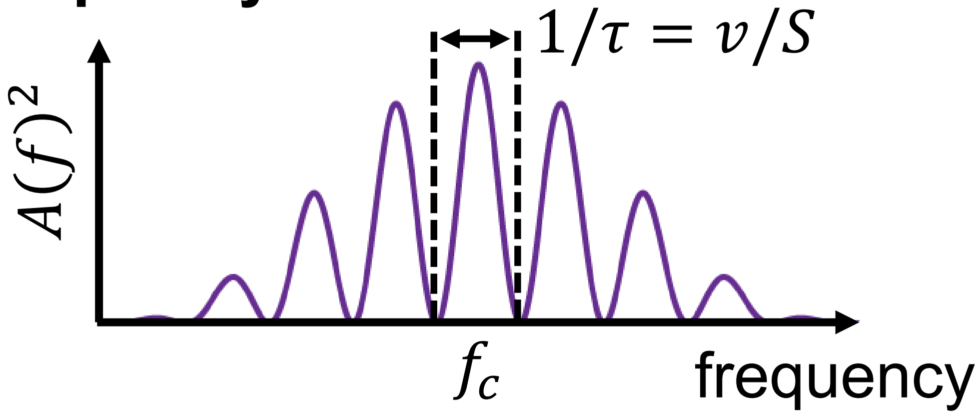

Anton Frisk Kockum, Per Delsing, Göran Johansson, *PRA* (2014)

JILA
CU Boulder and NIST

Ramsey qubit: realizing frequency sensitive couplings

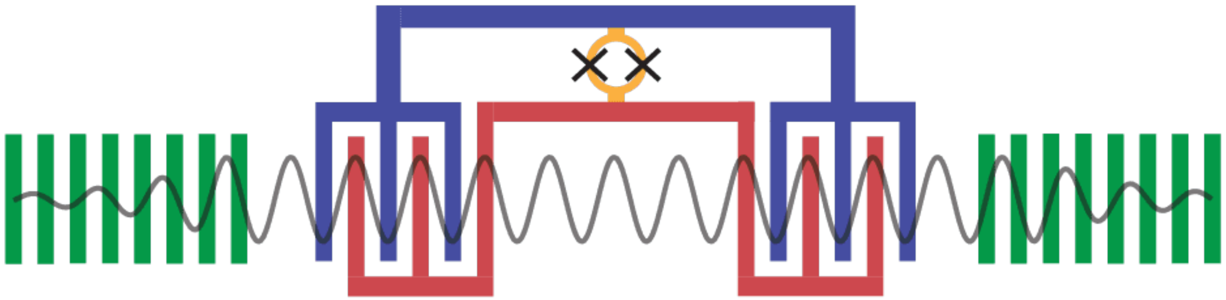

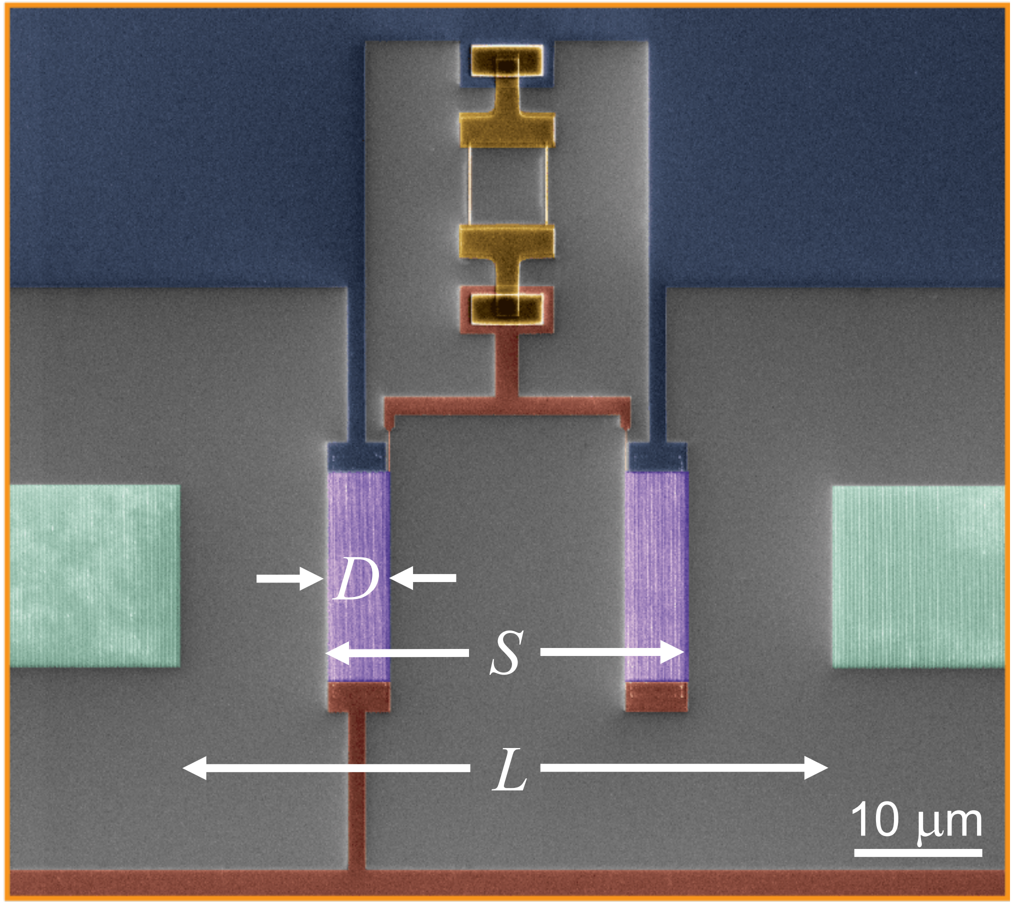

JILA
CU Boulder and NIST

Ramsey qubit: realizing frequency sensitive couplings

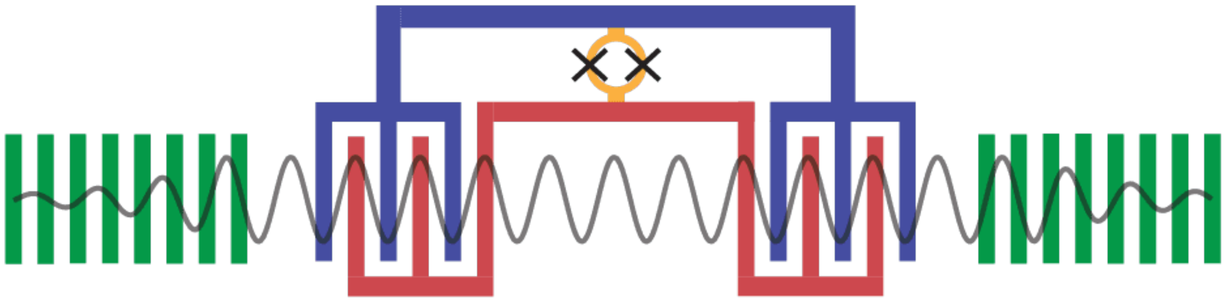

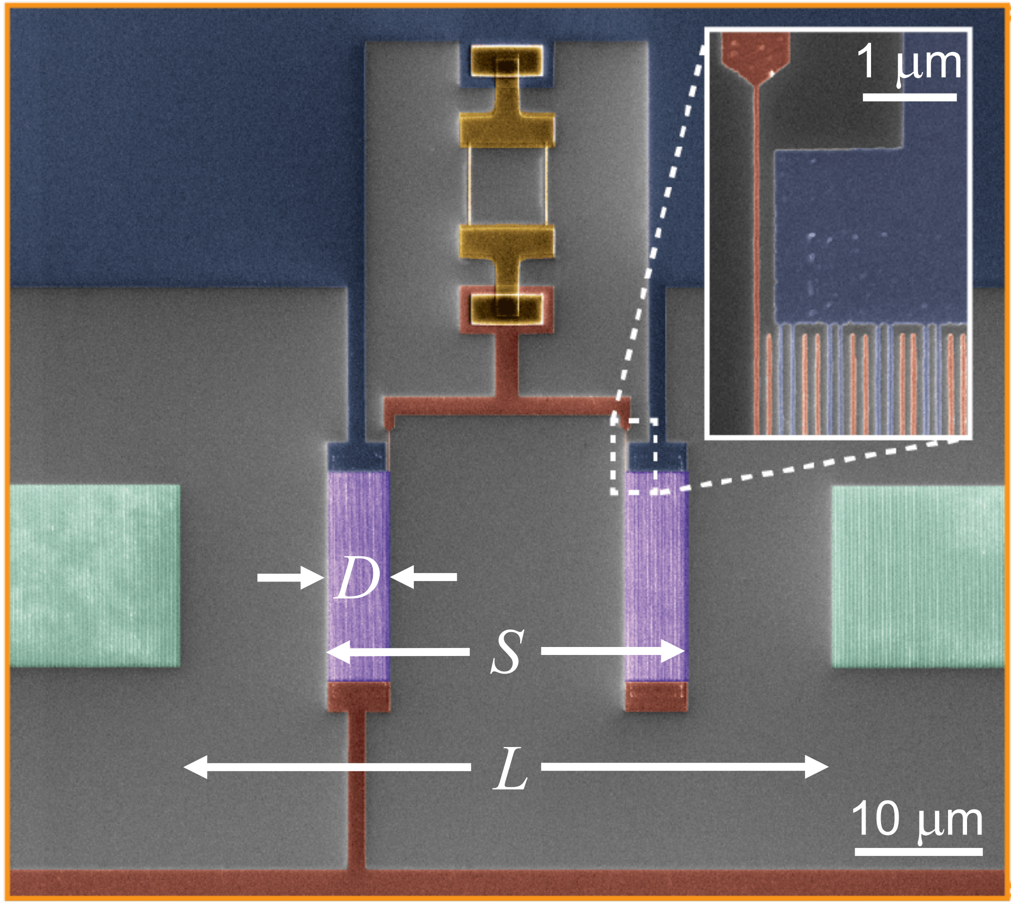

Ramsey qubit: realizing frequency sensitive couplings

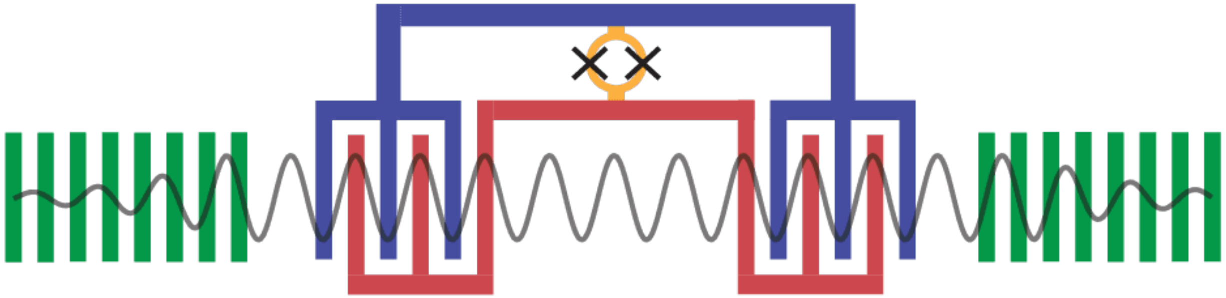

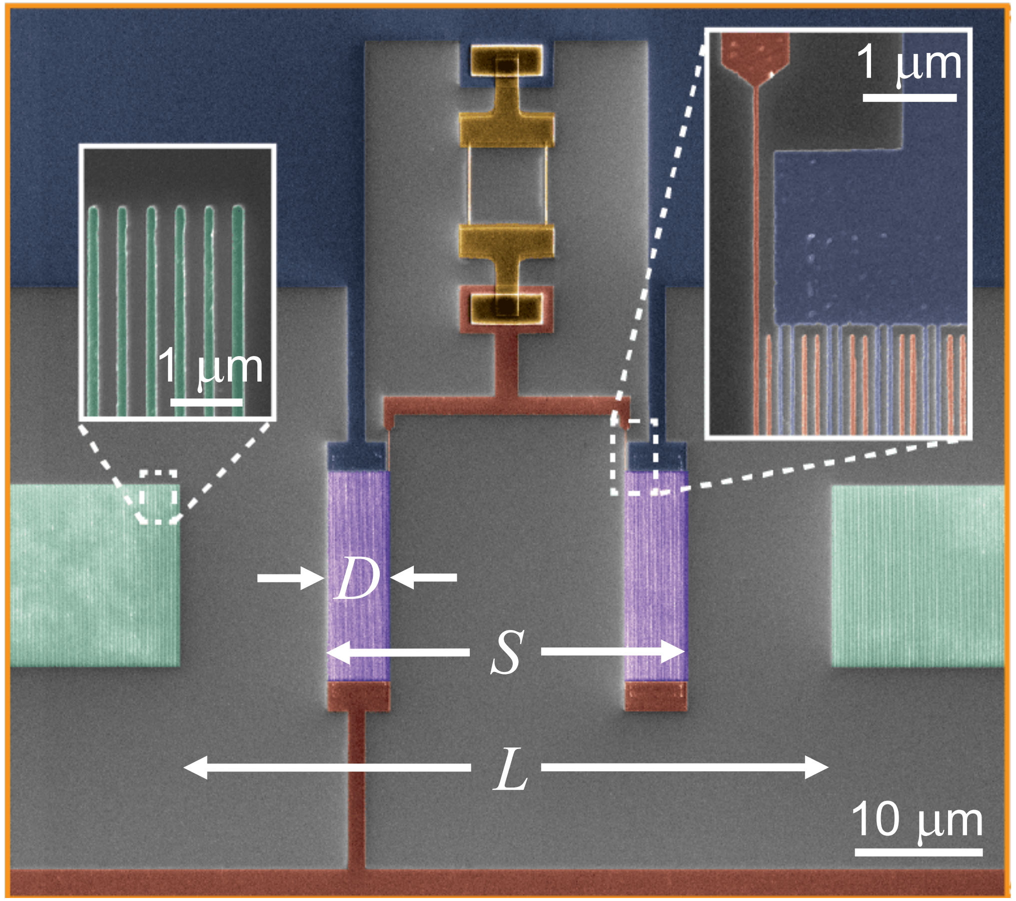

JILA
CU Boulder and NIST

Ramsey qubit: realizing frequency sensitive couplings

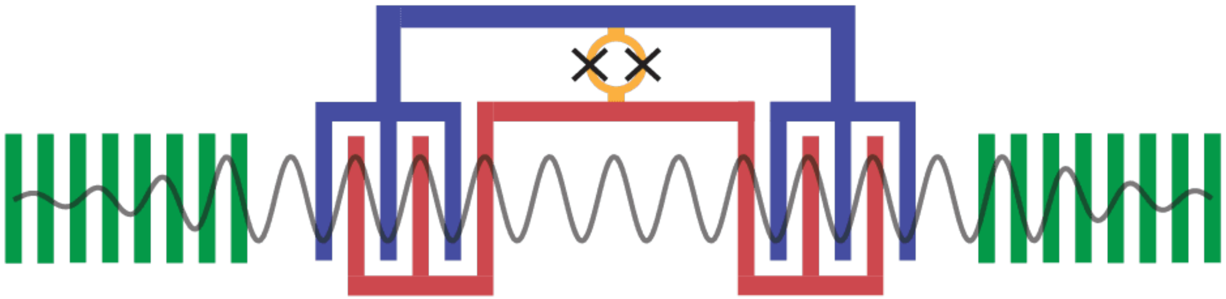

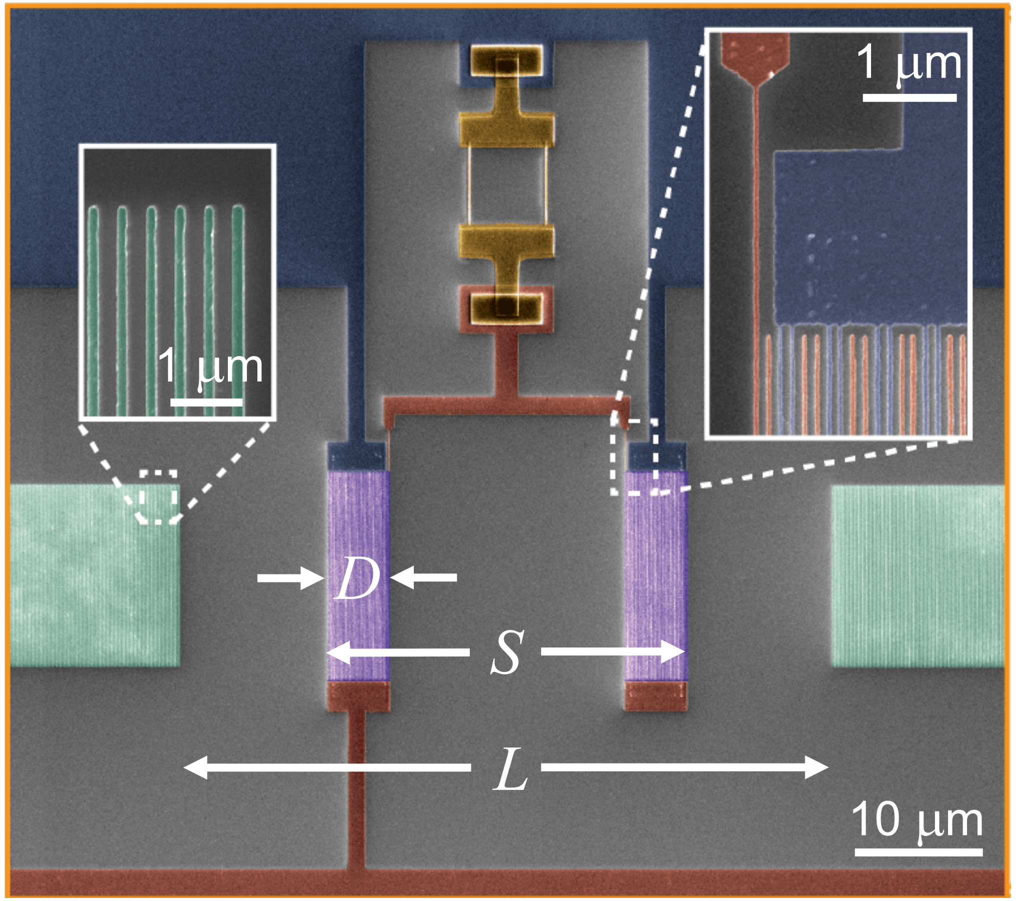

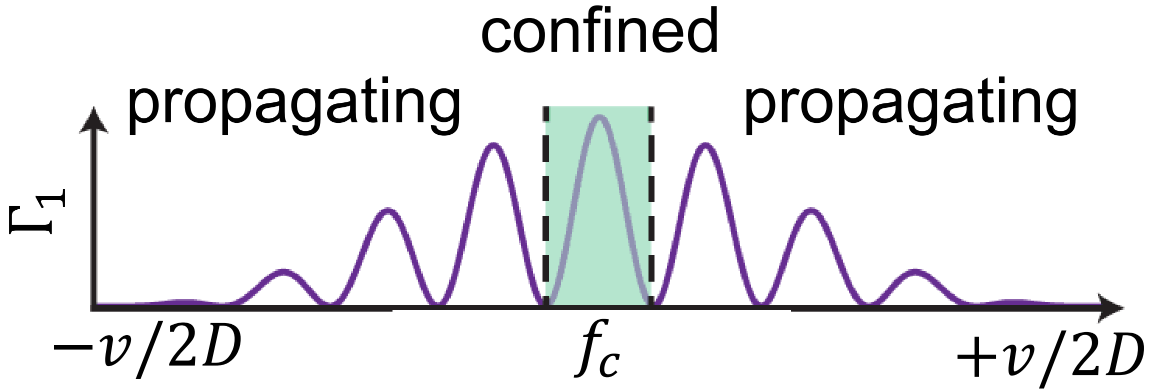

JILA
CU Boulder and NIST

Ramsey qubit: realizing frequency sensitive couplings

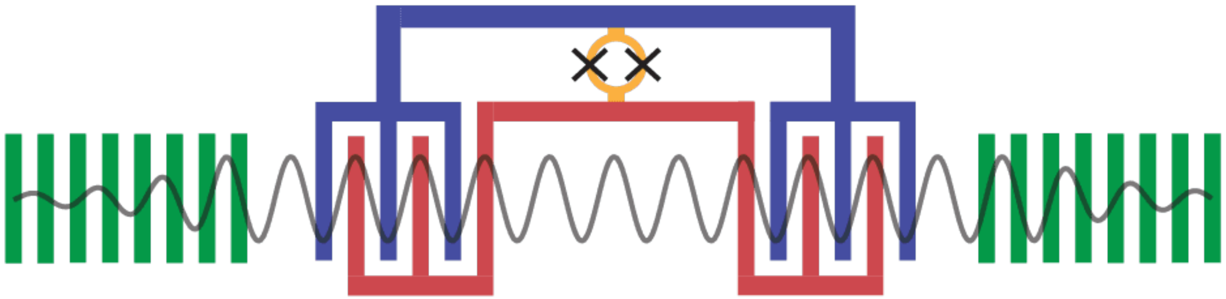

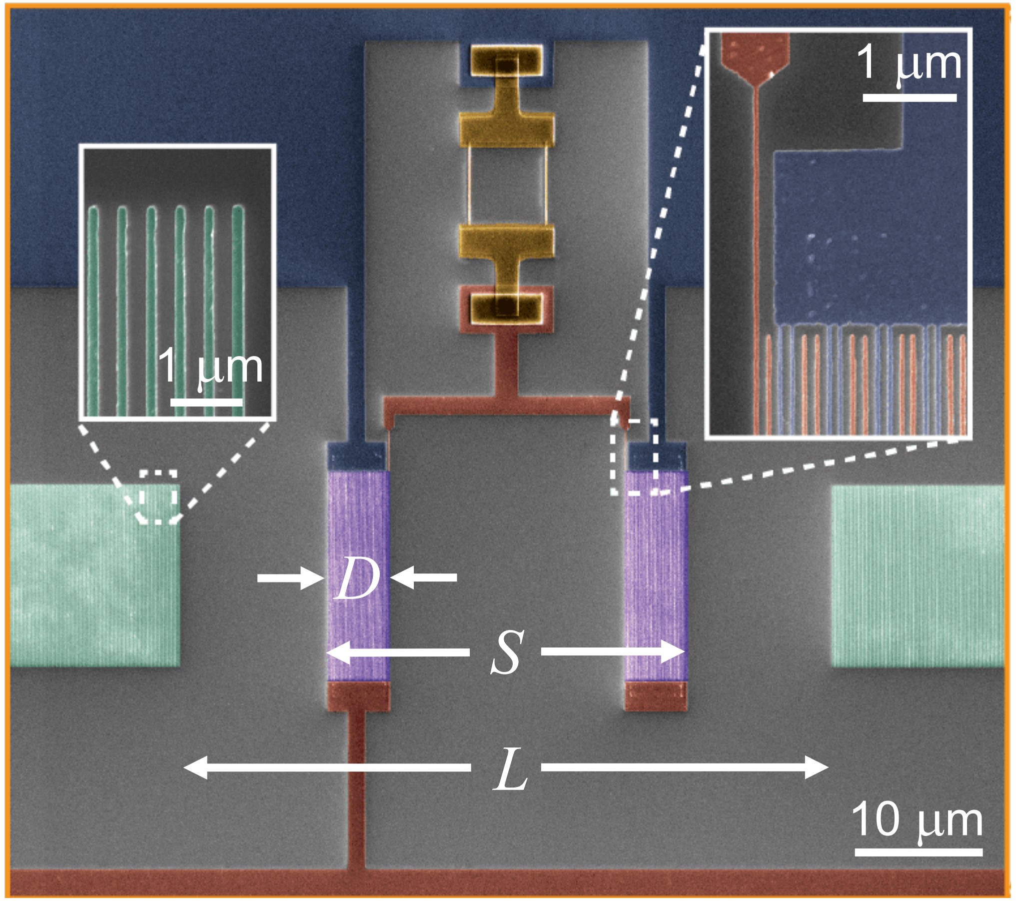

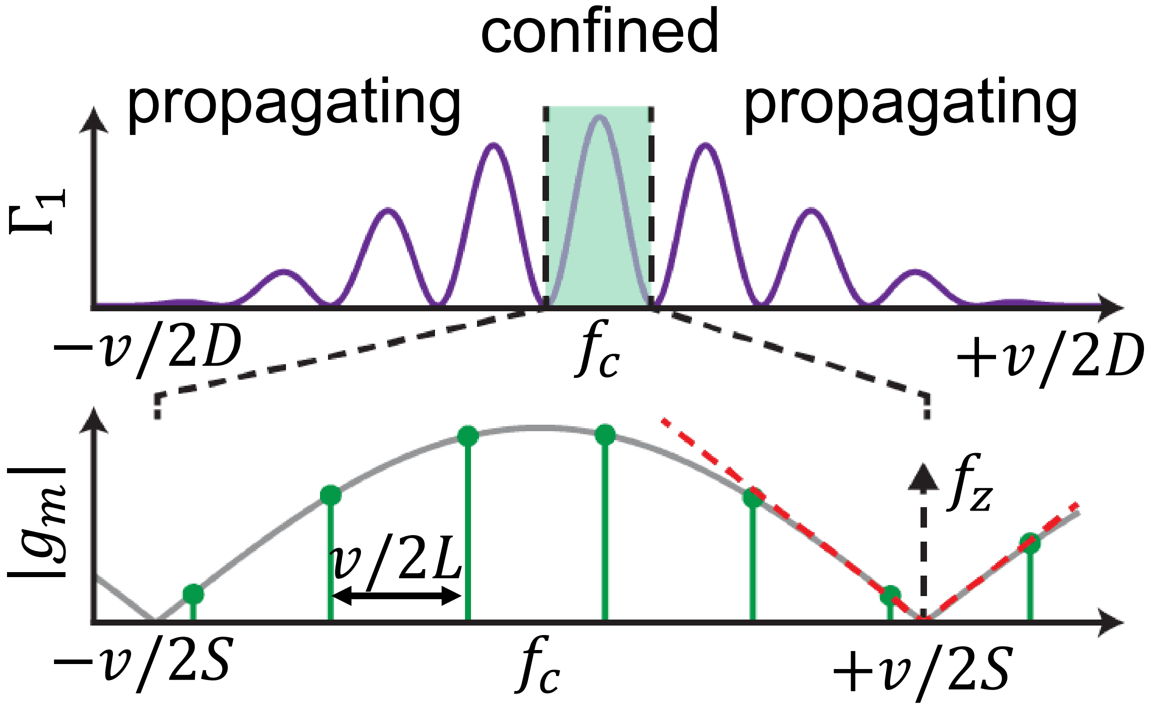

Tune qubit through acoustical cavity resonances

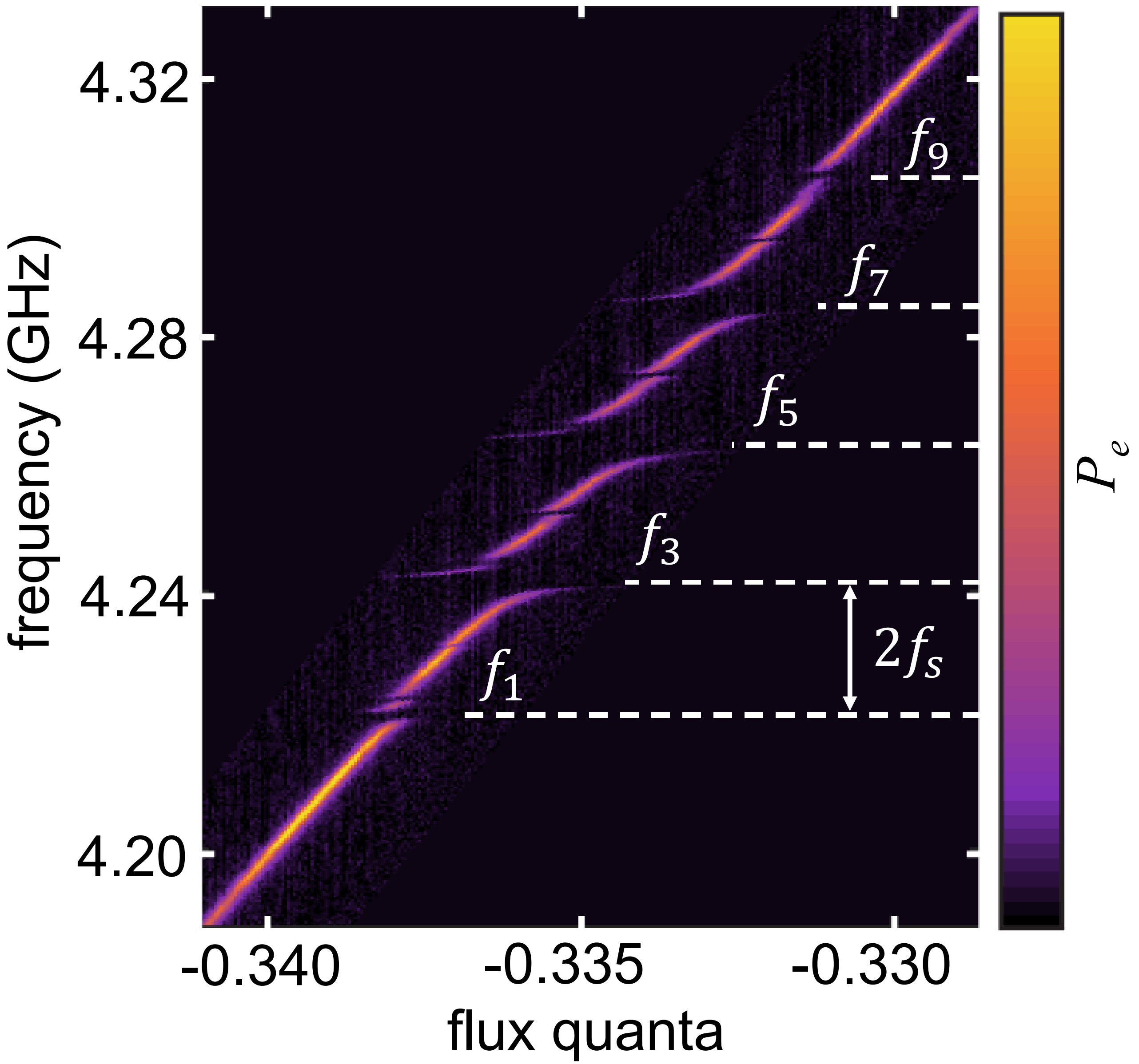

qubit spectroscopy

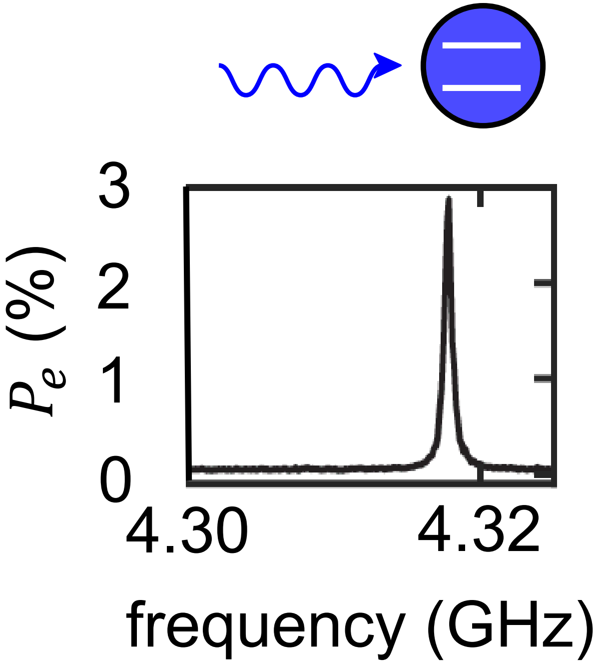

Measured coupling strengths depend on frequency

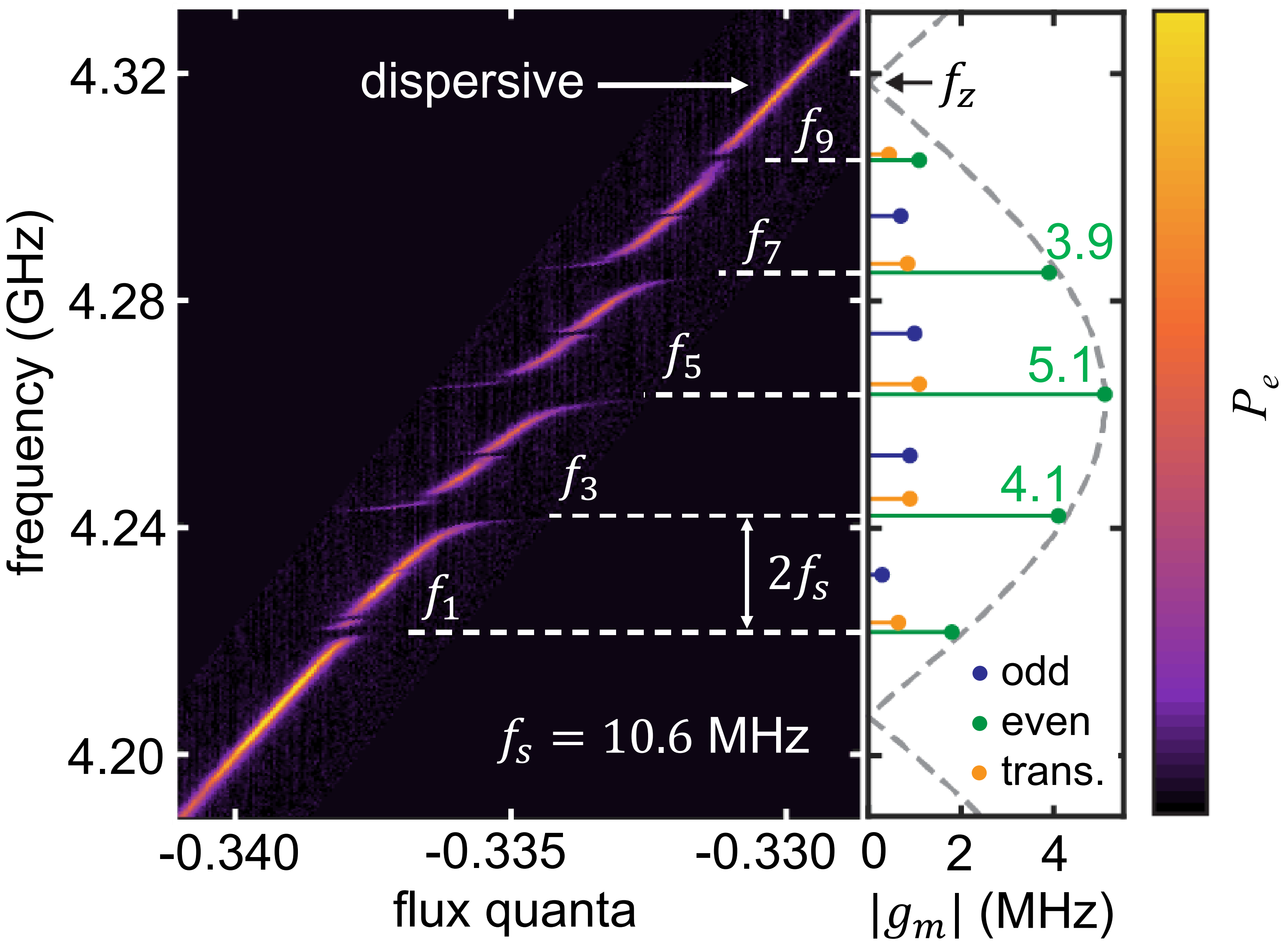

qubit tuned across mirror bandwidth (100 MHz)

three strongly coupled modes

mode-dependent coupling

dispersive "windows"

Characterizing the system with the qubit tuned to f_z

Qubit tuned to zero in coupling at f_z.

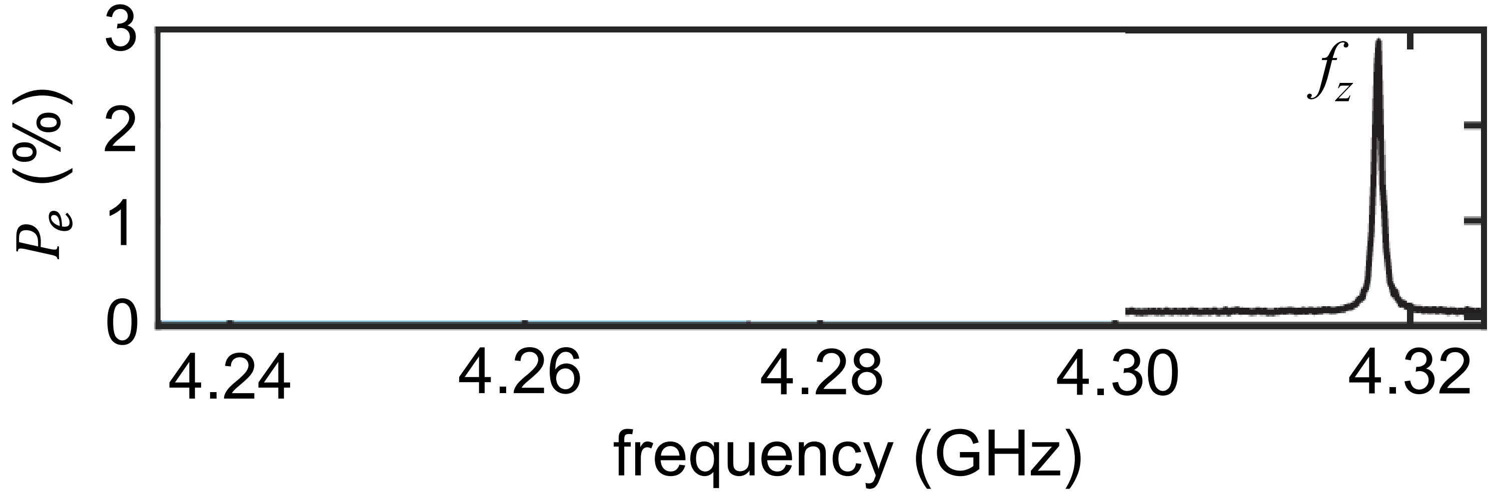

qubit linewidth

$\gamma = 550$ kHz

Characterizing the system with the qubit tuned to f_z

Qubit tuned to zero in coupling at f_z.

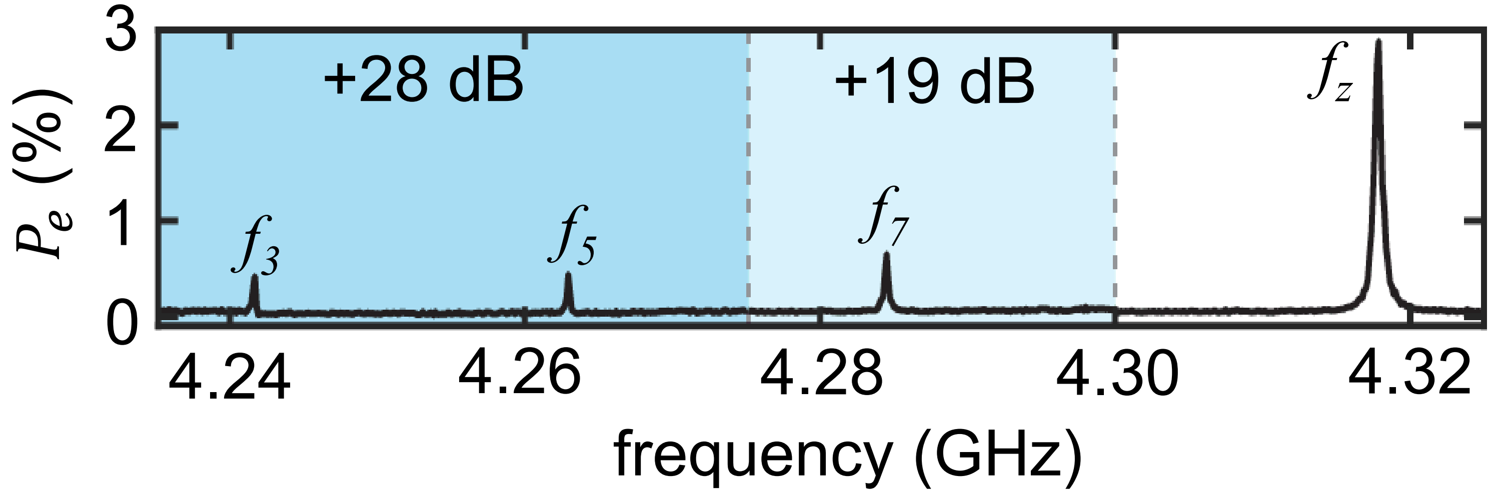

qubit linewidth

$\gamma = 550$ kHz

acoustic linewidths

$\kappa_{3,5,7} \approx 250$ kHz

dispersive with all acoustic modes

$\Delta_3/g_3 = 18$ $\Delta_5/g_5 = 11$ $\Delta_7/g_7 = 8.5$ $\Delta_9/g_9 = 12$

excite acoustic modes through qubit

JILA CU Boulder and NIST

Resolving the acoustical Stark shift of a single phonon!

excite acoustical mode, measure qubit spectrum

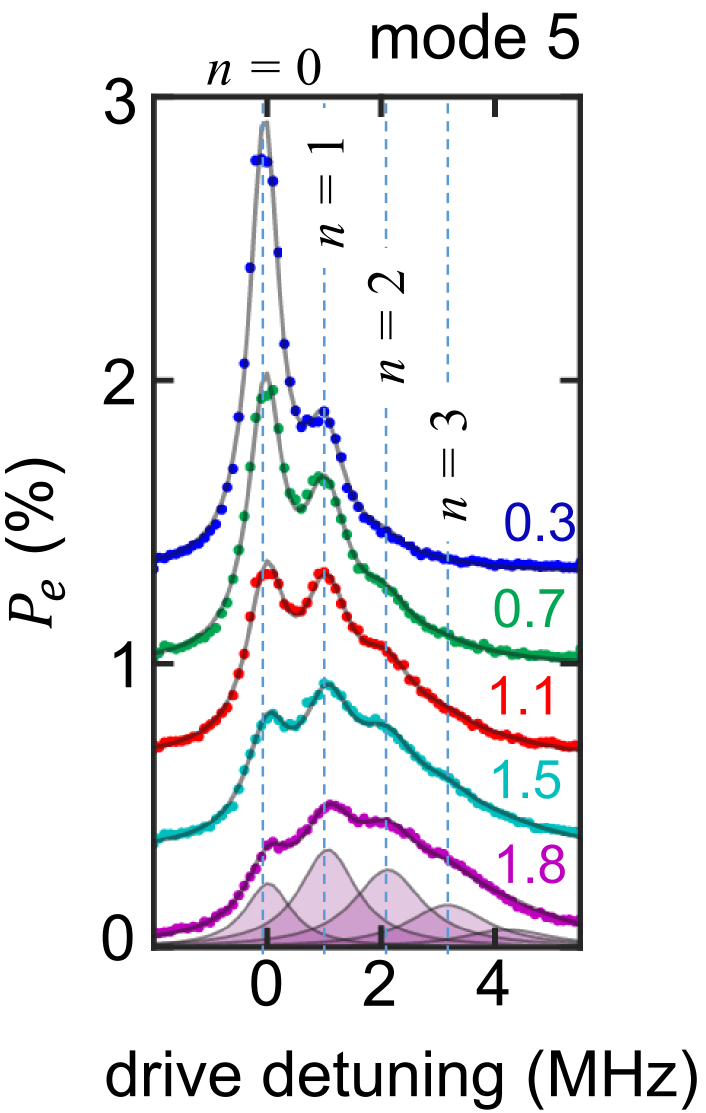

strong dispersive regime

$$\chi > \max[\kappa, \gamma]$$

JILA CU Boulder and NIST

Strong dispersive regime for two cavity modes

excite acoustical mode, measure qubit spectrum

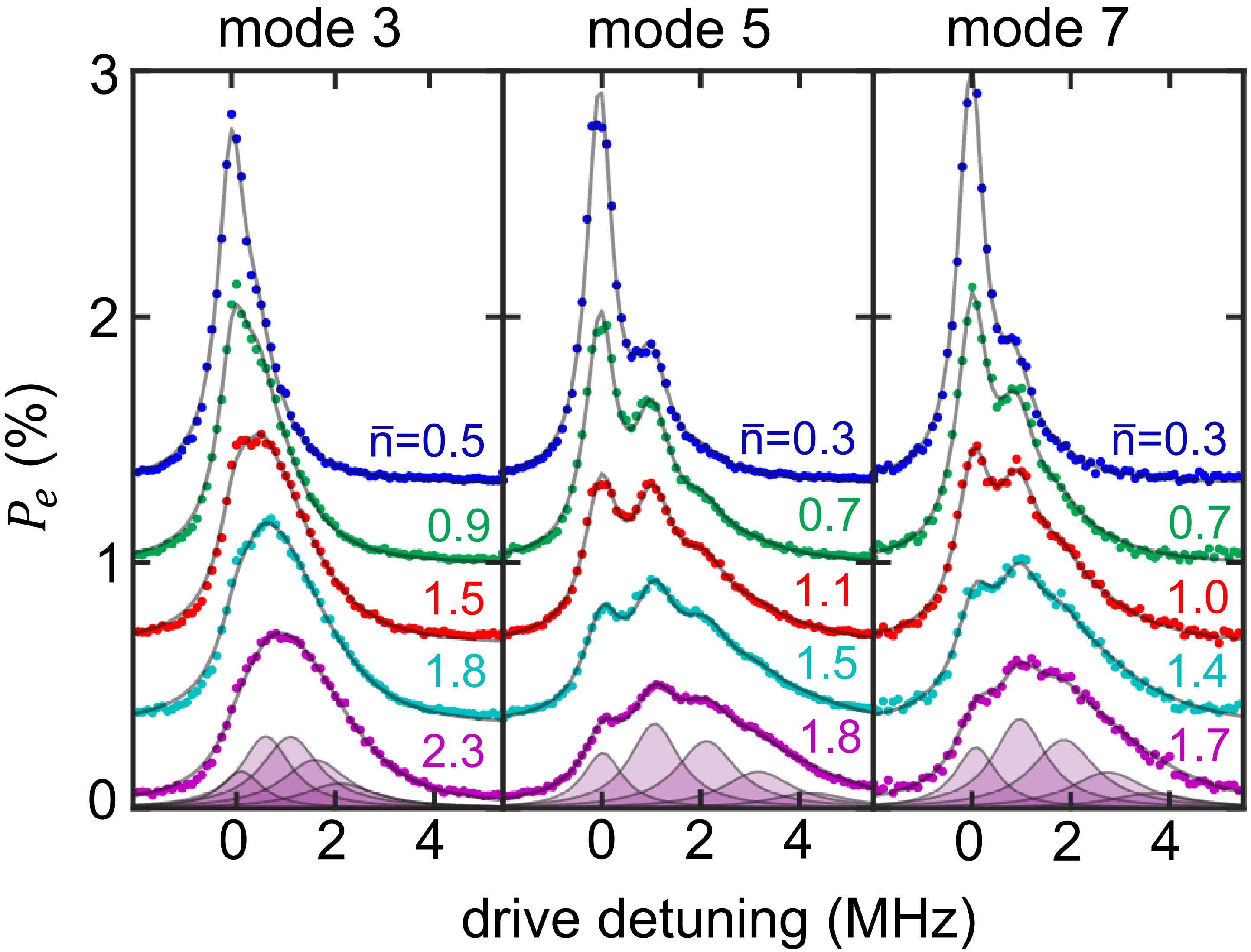

resolved peaks for modes 5, 7

qubit linewidth $\gamma = 550$ kHz

dispersive shifts

$2\chi_{3,5,7} = 500, 1050, 890$ kHz

JILA
CU Boulder and NIST

Single phonon self-interference!

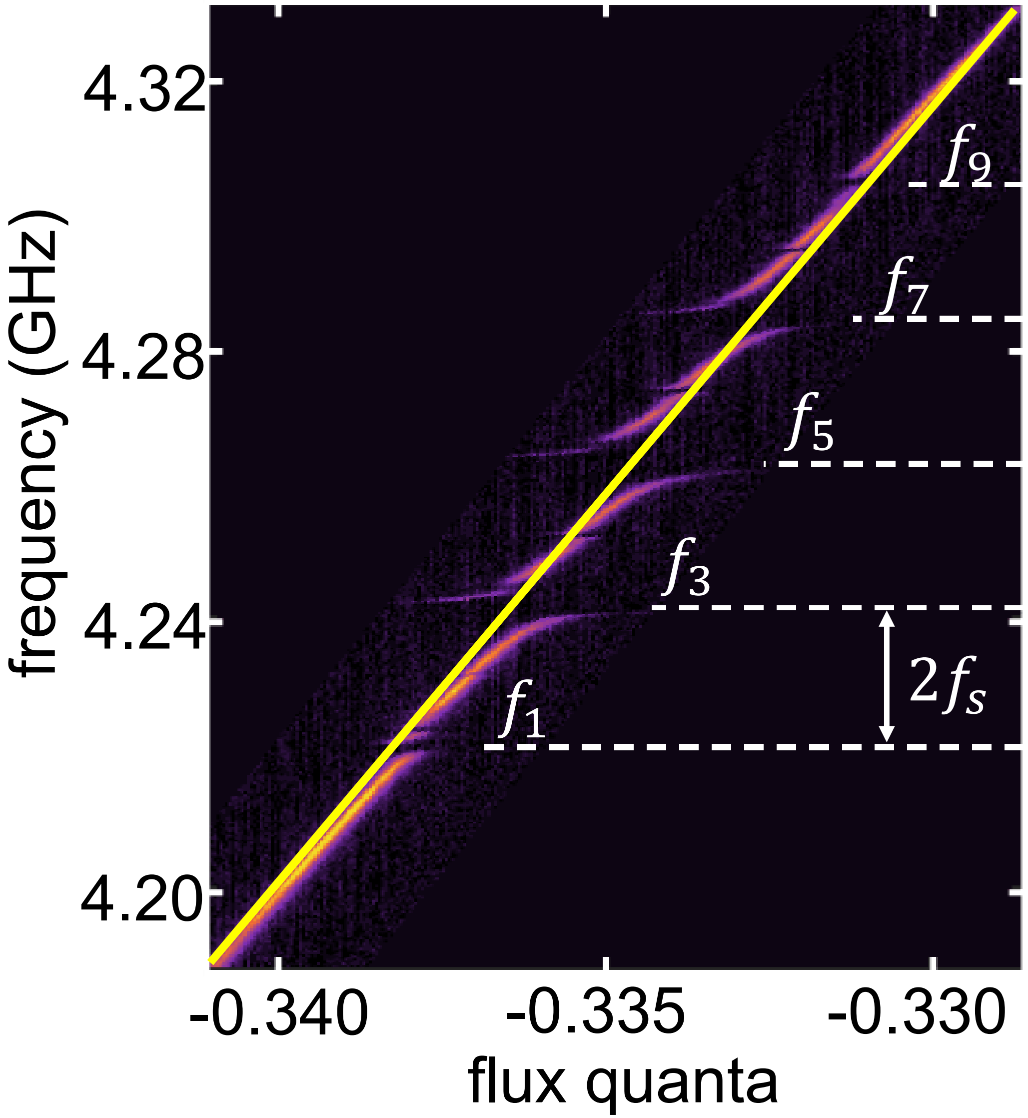

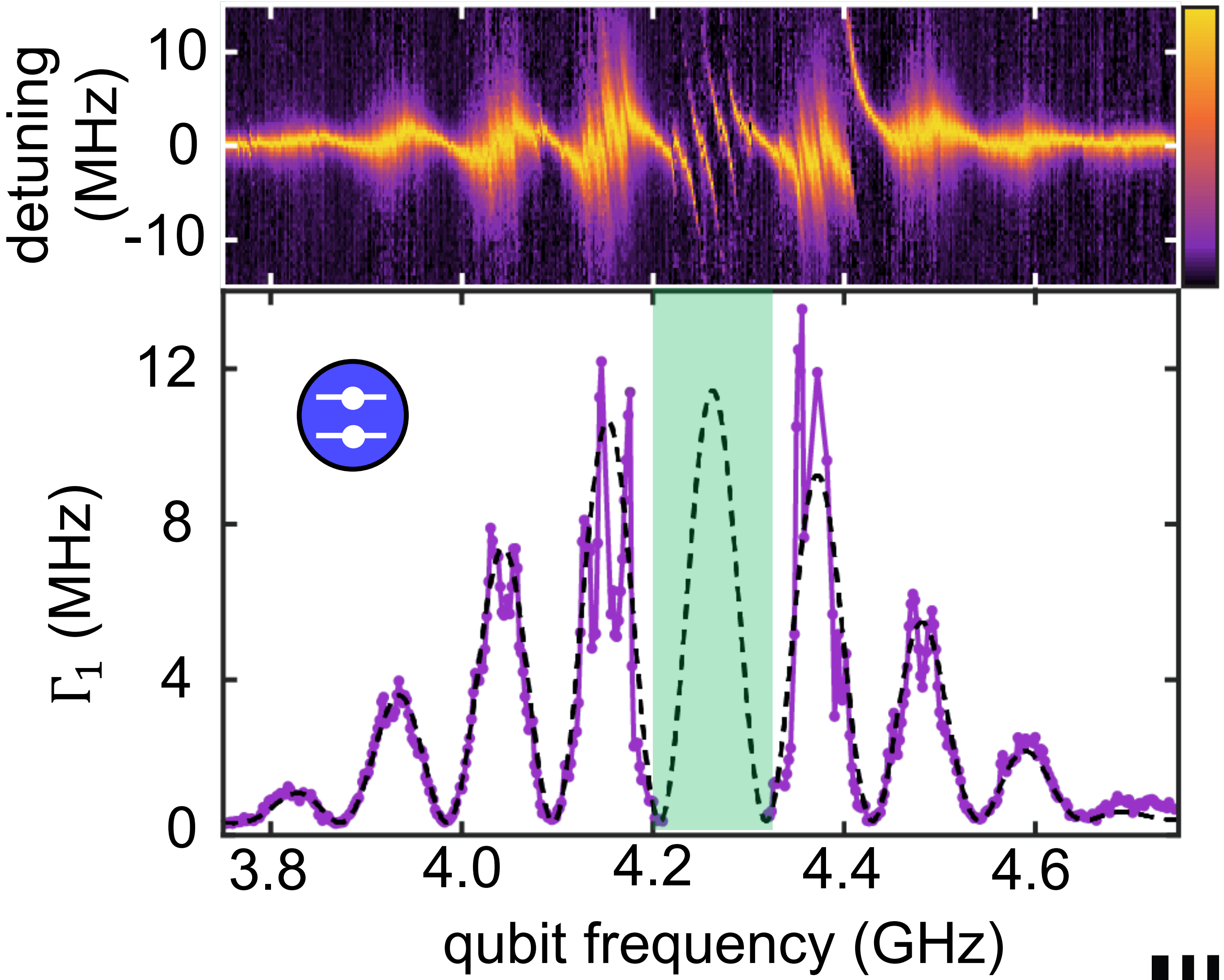

JILA
CU Boulder and NIST

Single phonon self-interference!

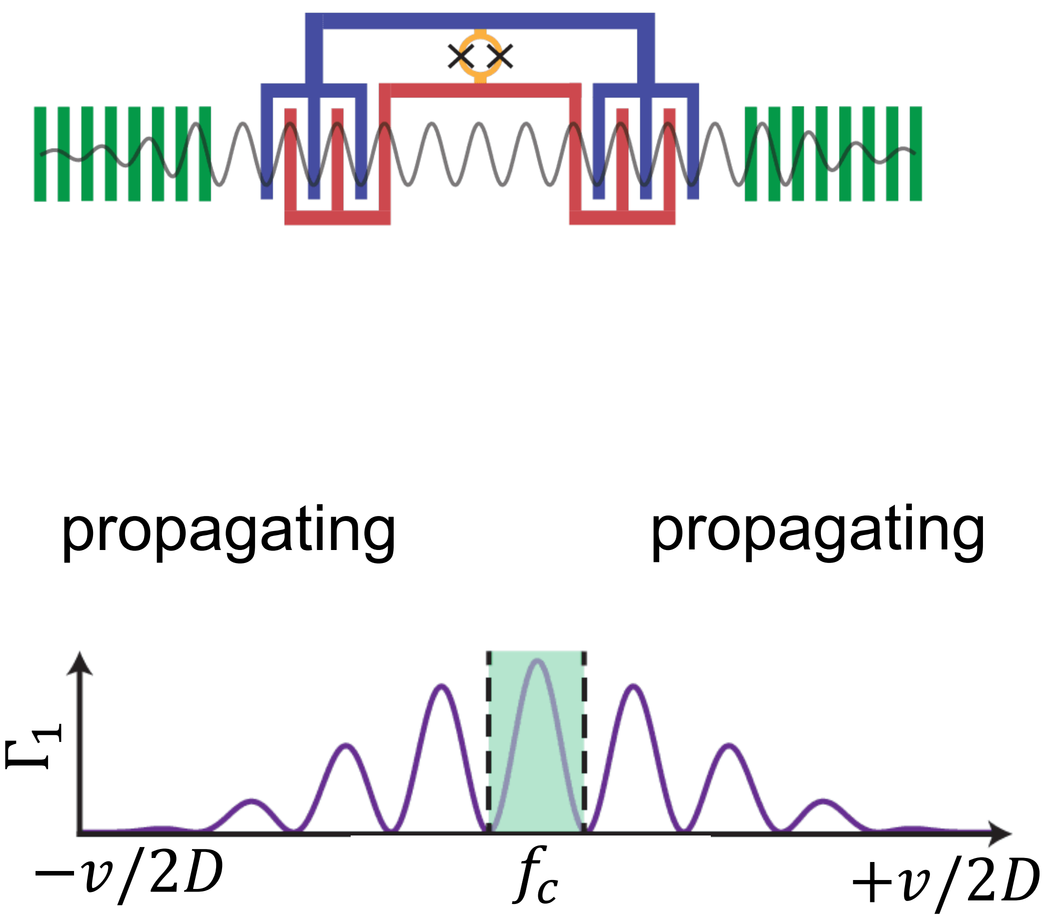

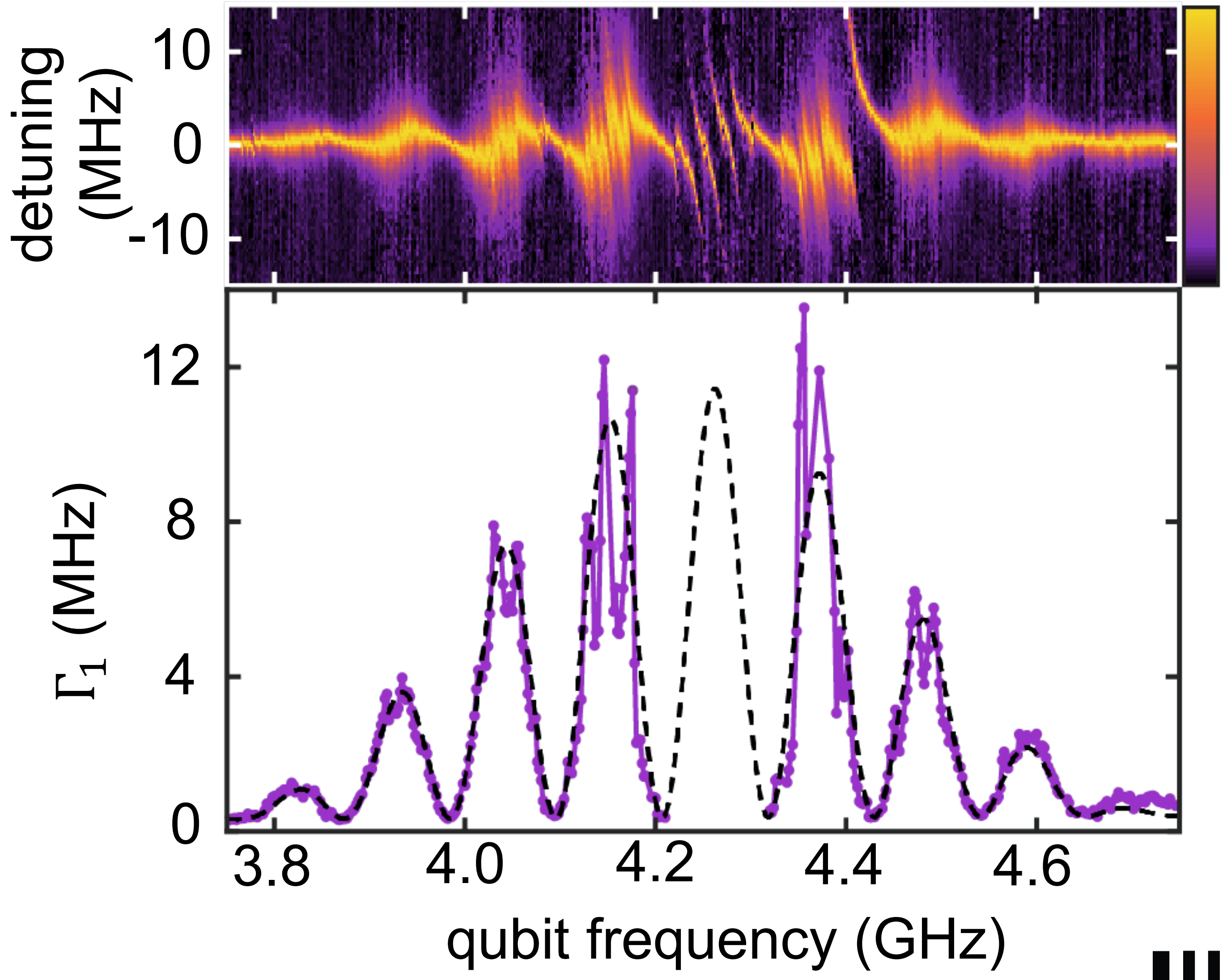

JILA CU Boulder and NIST

Acoustical Lamb shift

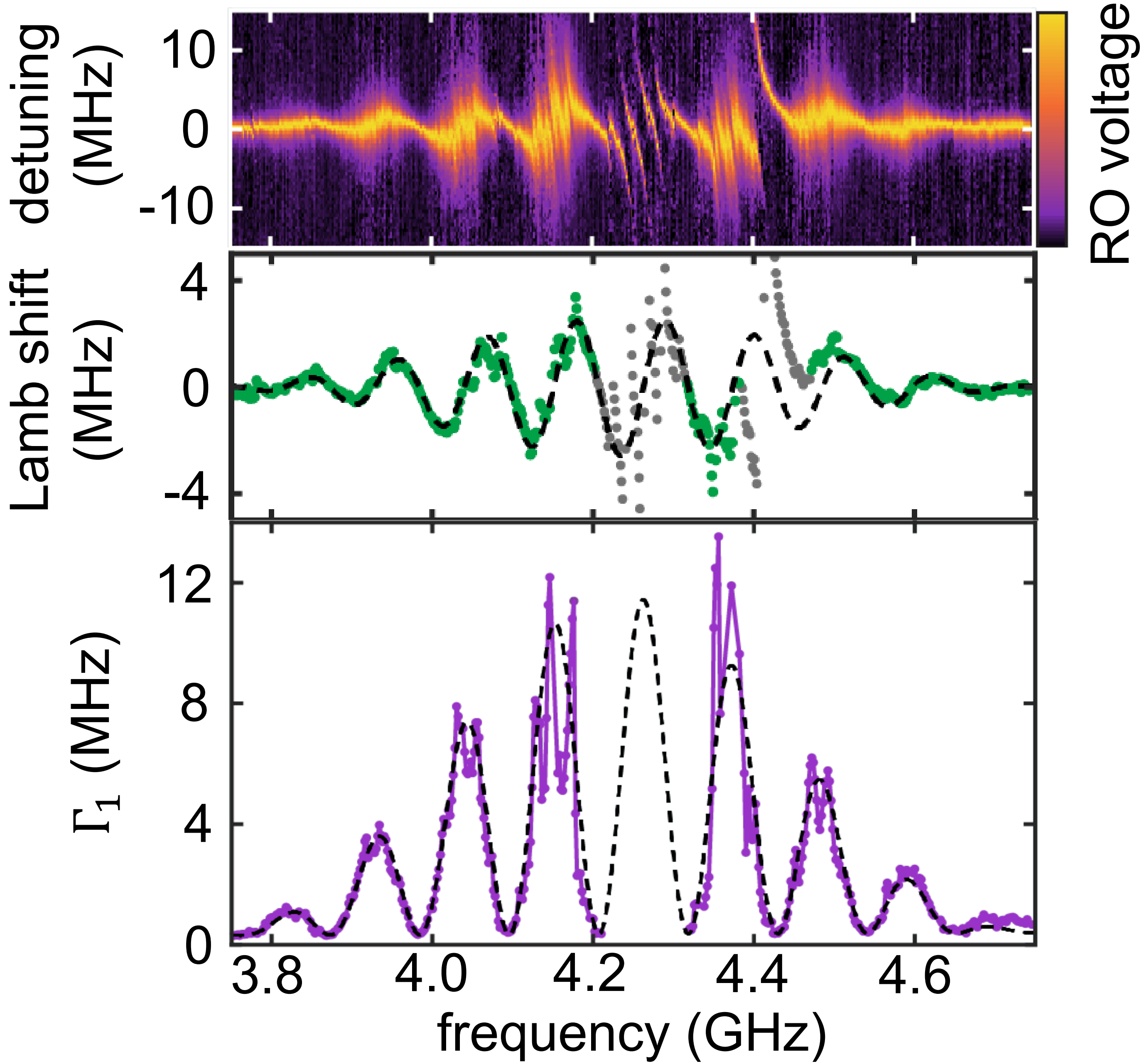

dissipation dispersion related by Kramers-Kronig

frequency shift

frequency dependent dissipation

Conclusion

linear quantum electromechanics

non-linear quantum electromechanics

resolving single acoustical phonons

acoustical qubits have designer couplings

observation of acoustic Purcell effect and Lamb shift

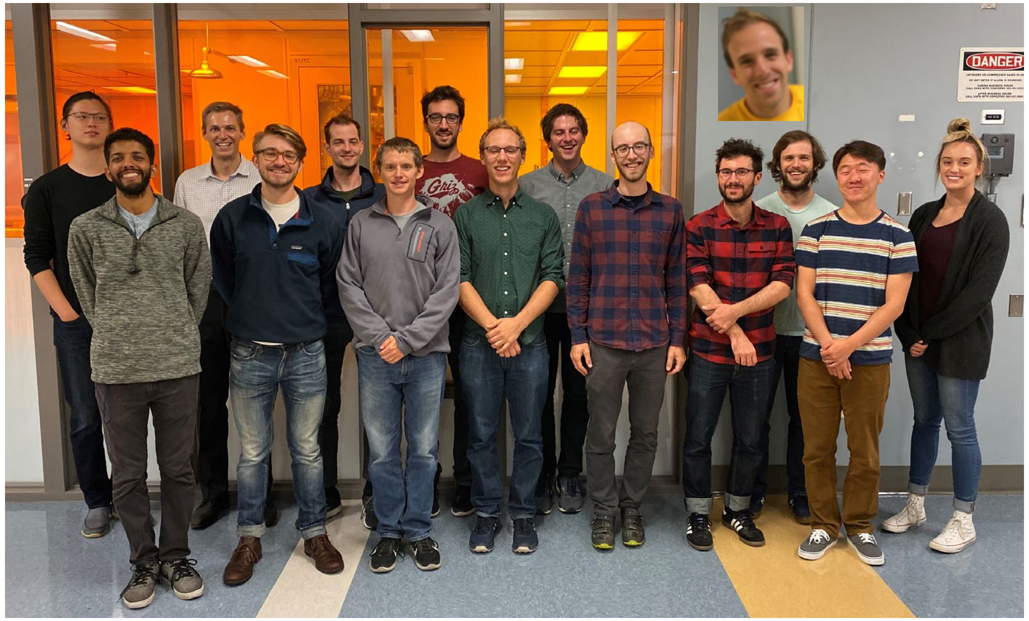

Collaborators
Cindy Regal
John Teufel
Kevin Silverman

Graduate students
Lucas Sletten
XiZheng Ma
Peter Burns
Max Urmey
Eric Rosenthal
Dan Palken
Kelly Wurtz
Sarang Mittal
Alec Emser
Rob Delaney
Ziyi Zhou

Post-docs
Brad Moores
Brendon Rose
Jeremie Viennot
Ben Brubaker
Jon Kindem

Undergraduates
Justin White
Adam Farmer